

2015

# Functional MRI and behavioral investigations of long-term memory-guided visuospatial attention

---

<https://hdl.handle.net/2144/16356>

*"Downloaded from OpenBU. Boston University's institutional repository."*

BOSTON UNIVERSITY  
GRADUATE SCHOOL OF ARTS AND SCIENCES

Dissertation

**FUNCTIONAL MRI AND BEHAVIORAL  
INVESTIGATIONS OF LONG-TERM MEMORY-GUIDED  
VISUOSPATIAL ATTENTION**

by

**MAYA L. ROSEN**

B.A., Skidmore College, 2007

M.A. Boston University, 2011

Submitted in partial fulfillment of the

requirements for the degree of

Doctor of Philosophy

2015

© 2015 by  
MAYA ROSEN  
All rights reserved,  
except Chapter 2, which is © 2014, Frontiers in Psychology  
and Chapter 3, which is © 2015, Cerebral Cortex

Approved by

First Reader

---

David C. Somers, Ph.D.  
Professor of Psychological and Brain Sciences

Second Reader

---

Chantal E. Stern, D. Phil.  
Professor of Psychological and Brain Sciences

Third Reader

---

Sam Ling, Ph.D.  
Assistant Professor of Psychological and Brain Sciences

## **Dedication**

To Dr. Adrienne Gordon,  
for your wisdom and support ,  
and for paving the way for women in science.

## **ACKNOWLEDGEMENTS**

I have been extremely lucky during the writing of this dissertation and owe a great deal of gratitude to the many people who contributed to my experience. First, I would like to thank my advisor, Dr. David Somers for teaching me so much about how to be a scientist. I would like to thank him for his support and kindness, for always listening to me, challenging me, and for helping me pursue my career goals. I would also like to thank my secondary advisor, Dr. Chantal Stern for her support and advice, and for helping David and I navigate the memory world. I would also like to thank my other committee members. Thank you to Dr. Sam Ling for his enthusiasm, frankness and passion for science. Thank you to Dr. Karin Schon for always asking interesting and rigorous questions. Finally, thank you to Dr. Jackie Liederman. My experience teaching with you for three years was invaluable. Your passion and enthusiasm are contagious. Your support has meant so much to me over the years.

I have been fortunate to spend my graduate school career in a collaborative lab surrounded by curious, encouraging, and intelligent people. I would also like to thank the other members of the Somers' lab. Thank you to alumni Dr. Summer Sheremata, Dr. Katie Bettencourt and Dr. Lingqiang Kong for your help, patience and training throughout my graduate career. I would also like to thank all of my current labmates for their feedback and collaboration. I would especially like to thank our lab manager, Emily Levin, for her incredible organization and making my life so much easier, and for being an awesome

office mate. Thank you to Kathryn Devaney for her generosity in knowledge, time, kindness and friendship. Most of all, I would like to thank Dr. Samantha Michalka, who was the absolute best partner through this journey that I could have asked for. You have taught me so much about balance, hard work, matrices, and friendship. Thank you for your encouraging words in times of struggle and constant faith in my ability to succeed.

I would also like to acknowledge the wonderful neuroscience and psychology community at BU. Thank you to everyone who helps run the department and BBC program, especially to Dr. Joanne Palfai and Denise Parisi of the Center for Memory and Brain. I would also like to thank the staff of the CBSN at Harvard. I have been fortunate to have made great friends and collaborators in graduate school and would like to thank you all for your friendship and support, especially Justine, Deepti, and Eric.

Arriving at this moment in my career would not have been possible without the encouragement and support of my undergraduate advisor and former professor, Dr. Hassan Lopez and Dr. Flip Phillips. I would also like to thank all the volunteers who participated in my sometimes long and grueling experiments. This research was largely supported by CELEST, a National Science Foundation Science of Learning Center (NSF SMA-0835976), the National Institutes of Health (NIH R01EY022229).

Most of all, I would like to thank my family and friends for their unwavering love and support throughout this sometimes arduous process. To my parents,

Emanuel and Daria, thank you for inspiring curiosity and a love of hard work in me, for listening to me, and for encouraging me throughout this process. Thank you to my siblings and friends for keeping me grounded and in tune to what is happening outside of graduate school, and for making me laugh. And finally, thank you to my loving husband, Alex. It is impossible to express the gratitude I feel that I have you as a partner. You have seen me through my roughest moments and always managed to make me smile. Thank you for enduring with me, challenging me, encouraging me to learn more, and always reminding me to backup my laptop.

**FUNCTIONAL MRI AND BEHAVIORAL  
INVESTIGATIONS OF LONG-TERM MEMORY-GUIDED  
VISUOSPATIAL ATTENTION**

(Order No.        )

**MAYA L. ROSEN**

Boston University Graduate School of Arts and Sciences, 2015

Major Professor: David Somers, Professor of Psychological and Brain Sciences

**ABSTRACT**

Real-world human visual perception is superb, despite pervasive attentional capacity limitations that can severely impact behavioral performance. Long-term memory (LTM) is suggested to play a key role in efficiently deploying attentional resources; however, the nature of LTM-attention interactions remains poorly understood. Here, I present a series of behavioral and functional magnetic resonance imaging (fMRI) investigations of the mechanisms of LTM-guided visual attention in 139 healthy participants (18-34 years).

In Experiment 1, I hypothesized that humans can use memory to guide spatial attention to multiple discrete locations that have been previously studied. Participants were able to simultaneously attend to more than one spatial location using an LTM cue in a novel change-detection behavioral paradigm also used in fMRI Experiments 2 and 4.

Cortical networks associated with LTM and attention often interact competitively. In Experiment 2, I hypothesized that the cognitive control network

supports *cooperation* between LTM and attention. Three posterior regions involved with cognitive control were more strongly recruited for LTM-guided attention than stimulus-guided attention: the posterior precuneus, posterior callosal sulcus, and lateral intraparietal sulcus.

In Experiment 3, I hypothesized that regions identified in Experiment 2 are specifically activated for LTM-guided attention, not for LTM retrieval or stimulus-guided attention alone. This hypothesis was supported. Taken together, the results of Experiments 2 and 3 identify a cognitive control subnetwork specifically recruited for LTM-guided attention.

Experiment 4 tested how LTM-guided attention affected spatial responsivity of maps within intraparietal sulcus. I hypothesized that left parietal maps would change their spatial responsivity due to the left lateralized effects of memory retrieval. During stimulus-guided attention, contralateral visuotopic maps in the right but not left intraparietal sulcus responded to the full visual field. In contrast, during LTM-guided attention, maps in both the left and right intraparietal sulcus responded to the full visual field, providing evidence for complementary forms of dynamic recruitment under different attentional conditions.

Together, these results demonstrate that LTM-guided attention is supported by a parietal subnetwork within the cognitive control network and that internal attentional states influence the spatial specificity of visuotopically mapped regions in parietal cortex.

## TABLE OF CONTENTS

|  |           |
|--|-----------|
| <b>CHAPTER 1: Introduction .....</b>                                       | <b>1</b>  |
| <b>1.1 Behavioral Evidence for Long-Term Memory Biasing Attention.....</b> | <b>2</b>  |
| <b>1.2 Divided Attention .....</b>   | <b>4</b>  |
| <b>1.3 Neural Mechanisms of Attention .....</b>                            | <b>4</b>  |
| <b>1.4 Neural Mechanisms supporting Long-Term Memory Retrieval.....</b>    | <b>5</b>  |
| <b>1.5 Competitive Interactions Between Memory and Attention .....</b>     | <b>6</b>  |
| <b>1.6 Neural Mechanisms of Long-Term Memory-Guided Attention .....</b>    | <b>7</b>  |
| <b>1.7 Hemispheric Asymmetries .....</b>                                   | <b>9</b>  |
| <b>1.8 Experiments in this Dissertation .....</b>                          | <b>11</b> |
| <br><b>CHAPTER 2: Long-term memory guidance of visuospatial attention</b>  |           |
| <b>in a change detection paradigm.....</b>                                 | <b>15</b> |
| <b>2.1 Introduction .....</b>  | <b>16</b> |
| <b>2.2 Experiment 1.....</b>   | <b>21</b> |
| 2.2.1 Materials and Methods.....   | 21        |
| 2.2.2 Results: Experiment 1 .....  | 25        |
| <b>2.3 Experiment 2.....</b>   | <b>28</b> |
| 2.3.1 Materials and Methods: Experiment 2.....                             | 29        |
| 2.3.2 Results and Discussion: Experiment 2.....                            | 31        |
| <b>2.4 General Discussion.....</b>   | <b>34</b> |
| <b>2.5 Chapter 2 Figures.....</b>  | <b>39</b> |
| <br><b>Chapter 3: Cognitive Control Network Contributions to</b>           |           |
| <b>Memory-Guided Visual Attention .....</b>                                | <b>45</b> |

|   |           |
|---|-----------|
| <b>3.1 Introduction</b> .....                         | <b>46</b> |
| <b>3.2 Materials and Methods</b> .....                | <b>49</b> |
| 3.2.2. Visual Stimuli and Experimental Paradigm. .... | 50        |
| 3.2.3. MR Data Acquisition.....                       | 55        |
| 3.2.3. MR Data Analysis:.....                         | 56        |
| <b>3.3 Results</b> .....                              | <b>63</b> |
| 3.3.1 Behavioral Results: .....                       | 63        |
| 3.3.2. fMRI Results:.....                             | 65        |
| <b>3.4 Discussion</b> .....                           | <b>74</b> |
| <b>3.5 Chapter 3 Figures</b> .....                    | <b>84</b> |
| <b>3.6 Chapter 3 Tables</b> .....                     | <b>94</b> |

**CHAPTER 4: Posterior Parietal Network is Recruited Specifically for**

|  |            |
|--|------------|
| <b>Long-Term Memory-Guided Attention</b> .....         | <b>102</b> |
| <b>4.1 Introduction</b> .....                          | <b>103</b> |
| <b>4.2 Methods</b> .....                               | <b>108</b> |
| 4.2.1 Participants: .....                              | 108        |
| 4.2.2. Visual Stimuli and Experimental Paradigm: ..... | 108        |
| 4.2.2. MR Data Acquisition:.....                       | 112        |
| 4.2.4. MR Data Analysis:.....                          | 112        |
| <b>4.3 Results</b> .....                               | <b>115</b> |
| <b>4.4. Discussion</b> .....                           | <b>119</b> |
| <b>4.5 Chapter 4 Figures</b> .....                     | <b>127</b> |
| <b>4.6 Chapter 4 Tables</b> .....                      | <b>130</b> |

|   |            |
|---|------------|
| <b>CHAPTER 5: Influences of Long-Term Memory-Guided Attention and Stimulus-Guided Attention on Visuospatial Representations .....</b> | <b>135</b> |
| <b>Within Human Intraparietal Sulcus .....</b>  | <b>135</b> |
| <b>5.1 Introduction .....</b>   | <b>136</b> |
| <b>5.2 Materials and Methods .....</b>  | <b>138</b> |
| 5.2.1 Participants: .....   | 138        |
| 5.2.2 Visual Stimuli and Experimental Paradigms: .....  | 138        |
| 5.2.3 MR Data Acquisition:.....   | 141        |
| <b>5.3 Results .....</b>  | <b>144</b> |
| 5.3.1 Behavioral Performance:.....  | 144        |
| 5.3.2 fMRI Analysis: .....  | 145        |
| <b>5.4 Discussion .....</b>   | <b>148</b> |
| <b>5.5 Chapter 5 Figures.....</b>   | <b>154</b> |
| <b>5.6 Chapter 5 Tables .....</b>   | <b>157</b> |
| <b>Chapter 6: Summary and Discussion.....</b>   | <b>158</b> |
| <b>6.1 Summary of Results .....</b>   | <b>159</b> |
| 6.1.1 Restatement of Original Goals .....   | 159        |
| 6.1.2 Summary of Results from Experiment 1 .....  | 159        |
| 6.1.3 Summary of Results from Experiment 2 .....  | 161        |
| 6.1.4 Summary of Results from Experiment 3 .....  | 162        |
| 6.1.5 Summary of Results from Experiment 4 .....  | 162        |
| <b>6.2 Discussion .....</b>   | <b>164</b> |
| 6.2.1 Long-Term Memory Guided Divided Attention.....  | 165        |

|   |            |
|---|------------|
| 6.2.2 Cortical Mechanisms Supporting Long-Term Memory-Guided Attention.....   | 165        |
| 6.2.3 The long-term memory-guided attention subnetwork is specifically recruited<br>for LTM-guided attention and not memory retrieval ..... | 167        |
| 6.2.4 Visuotopic maps in parietal cortex change their spatial specificity depending<br>on attentional cue type .....                        | 168        |
| <b>6.3 Conclusions.....</b>   | <b>170</b> |
| <b>References .....</b>   | <b>172</b> |
| <b>CURRICULUM VITAE.....</b>  | <b>189</b> |

## LIST OF TABLES

|                  |  |     |
|------------------|--|-----|
| <b>Table 3.1</b> | Significant areas of activation in the contrast of LTM-Guided vs. STIM-Guided conditions   | 94  |
| <b>Table 3.2</b> | Percent signal change in regions of interest of the Cognitive Control, Dorsal Attention and Default Mode Networks  | 96  |
| <b>Table 3.3</b> | Post-hoc Alternative Network Region of Interest Analysis   | 98  |
| <b>Table 3.4</b> | Within-Hemisphere Intrinsic Connectivity   | 99  |
| <b>Table 4.1</b> | Significant areas of activation in the contrast of LTM-Guided Attention vs. Stimulus-guided attention, LTM-Guided Attention vs. LTM retrieval, and LTM retrieval vs. Stimulus-guided attention | 130 |
| <b>Table 4.2</b> | Region of Interest Analysis of posterior Cognitive Control Network (PrC-p, latIPS, CaS-p)  | 134 |
| <b>Table 5.1</b> | Region of Interest Analysis in IPS0-IPS4 for LTM-Guided and STIM-Guided Attention in Contralateral and Ipsilateral Visual Fields   | 157 |

## LIST OF FIGURES

|                   |   |    |
|-------------------|---|----|
| <b>Figure 2.1</b> | Change Detection Task   | 39 |
| <b>Figure 2.2</b> | Capacity for Remembered Changes in<br>Experiment 1A   | 41 |
| <b>Figure 2.3</b> | Experiment 1B Study Phase Results   | 42 |
| <b>Figure 2.4</b> | Experiment 1B Test Phase Results  | 44 |
| <b>Figure 3.1</b> | One-Shot Change Detection Paradigm  | 84 |
| <b>Figure 3.2</b> | Long-Term Memory-Guided Attention vs.<br>Stimulus-Guided Attention Surface-Based<br>GLM Analysis            | 86 |
| <b>Figure 3.3</b> | Region of Interest Analysis for Cognitive<br>Control Network  | 87 |
| <b>Figure 3.4</b> | Region of Interest Analysis for Dorsal<br>Attention and Default Mode Networks                               | 89 |
| <b>Figure 3.5</b> | Posterior Precuneus Seed-Based Intrinsic<br>Connectivity Analysis   | 91 |
| <b>Figure 3.6</b> | Post-hoc Analysis Using Alternative Region<br>of Interest Definitions                                       | 92 |
| <b>Figure 3.7</b> | Posterior Callosal Sulcus and Lateral<br>Intraparietal Sulcus Seed-Based Intrinsic<br>Connectivity Analysis | 93 |

|                   |   |     |
|-------------------|---|-----|
| <b>Figure 4.1</b> | Experiment 3 Target Detection Task Paradigm   | 127 |
| <b>Figure 4.2</b> | Whole Cortex and Region of Interest Analysis<br>for latIPS, PrC-p and CaS-p in LTM-Guided<br>Attention, LTM retrieval, and Attention<br>Control | 128 |
| <b>Figure 5.1</b> | One-Shot Change Detection Paradigm  | 154 |
| <b>Figure 5.2</b> | Activation maps for Retinotopic Mapping,<br>Stimulus-Guided Attention and LTM-Guided<br>Attention   | 155 |
| <b>Figure 5.3</b> | Comparison of Contralateral Bias during<br>Retinotopic Mapping, STIM-guided and<br>LTM-guided Attention   | 156 |

## LIST OF ABBREVIATIONS

|               |                                       |
|---------------|---------------------------------------|
| <b>ACC</b>    | anterior cingulate cortex             |
| <b>AnG</b>    | angular gyrus                         |
| <b>BOLD</b>   | Blood Oxygen Level Dependent          |
| <b>CaS-p</b>  | posterior callosal sulcus             |
| <b>CCN</b>    | cognitive control network             |
| <b>DAN</b>    | dorsal attention network              |
| <b>DMN</b>    | default mode network                  |
| <b>dmPFC</b>  | dorsomedial prefrontal cortex         |
| <b>ERP</b>    | event-related potential               |
| <b>FAR</b>    | false alarm rate                      |
| <b>fMRI</b>   | functional Magnetic Resonance Imaging |
| <b>IFS</b>    | inferior frontal sulcus               |
| <b>IPS</b>    | intraparietal sulcus                  |
| <b>GLM</b>    | general linear model                  |
| <b>HR</b>     | hit rate                              |
| <b>HC</b>     | hippocampus                           |
| <b>iPCS</b>   | inferior precentral sulcus            |
| <b>latIPS</b> | lateral intraparietal sulcus          |
| <b>LH</b>     | left hemisphere                       |
| <b>LTC</b>    | lateral temporal cortex               |
| <b>LTM</b>    | long-term memory                      |

|              |                                 |
|--------------|---------------------------------|
| <b>LOC</b>   | lateral occipital complex       |
| <b>LVF</b>   | left visual field               |
| <b>MR</b>    | magnetic resonance              |
| <b>MNI</b>   | Montreal Neurological Institute |
| <b>OFC</b>   | orbitofrontal cortex            |
| <b>PCC</b>   | posterior cingulate cortex      |
| <b>PHC</b>   | parahippocampal cortex          |
| <b>ROI</b>   | region of interest              |
| <b>RVF</b>   | right visual field              |
| <b>RH</b>    | right hemisphere                |
| <b>RT</b>    | reaction time                   |
| <b>SEM</b>   | standard error of the mean      |
| <b>SS</b>    | set size                        |
| <b>STS</b>   | superior temporal sulcus        |
| <b>sPCS</b>  | superior precentral sulcus      |
| <b>SPL</b>   | superior parietal lobule        |
| <b>vIPFC</b> | ventrolateral prefrontal cortex |

## **CHAPTER 1: Introduction**

Human attentional capacity is severely limited. Previous experience with an environment ameliorates this attentional bottleneck because long-term memory can be used to guide attention to relevant information. Historically, however, attention and memory have been studied by distinct groups of scientists and much of the focus of their interactions has been on competition between these systems. Thus, the mechanisms that underlie long-term memory-guided visuospatial attention are poorly understood and are the focus of this dissertation.

### **1.1 Behavioral Evidence for Long-Term Memory Biasing Attention**

Human attentional capacity is limited to approximately four objects (Pylyshyn and Storm, 1988; Cowan, 2001). The remarkably high performance of real-world human vision can be accounted for in part by considering the role that long-term memory plays in guiding visual attention. Several studies have shown a behavioral advantage in attentionally demanding tasks when a subject has previous experience with a stimulus. Most notably, Chun and Jiang (1998) found that in a visual search paradigm that the latency to detect a target decreases when targets appear in consistent spatial locations, even when subjects are not explicitly aware of this consistency. This phenomenon, known as contextual cueing, indicates prior experience implicitly directs attention to relevant information to aid performance (Brockmole and Henderson, 2006; Chun and Turk-Browne, 2007). Expertise in a particular area can also help guide attention more efficiently. Soccer players detect changes in soccer scenes faster than do

soccer novices (Werner and Thies, 2000). This finding provides evidence that humans can generalize knowledge from previous experience to direct spatial attention.

Depending on the task demands, long-term memory may bias attention and hurt rather than help performance. Olivers (2011) presented subjects with a target detection task using street signs and subjects were asked to detect a gray scale sign in an array of distractor signs. Every trial contained one distractor presented in color. The color of that distractor either matched the color of the target in the real world (e.g. target is stop sign and distractor is a red do not enter sign, relevant distractor), or did not match (irrelevant distractor). Reaction time to detect targets was significantly longer in the presence of a relevant distractor compared to an irrelevant distractor. This finding indicates that the color of the distractor captured subjects' attention when it matched their long-term memory of the color feature of the target providing further evidence for long-term memory biasing attention.

Furthermore, explicit long-term memories can guide attention more efficiently than visual cues. Summerfield and colleagues (2006) tracked eye movements of subjects as they searched for a target in visual scenes. Subjects had either studied the scenes previously and used their memory to guide their attention to the location of the target or were presented with a box around the location where the target would appear. Subjects were faster and more efficient in their eye movements to the location of the target when they used their memory

to guide their attention than when they used a visual stimulus.

## **1.2 Divided Attention**

Another mechanism that supports processing in complex visual environments is divided spatial attention. Numerous lines of evidence indicate that humans and non-human primates are able to divide visual attention into multiple discrete spotlights (Shaw and Shaw, 1977; Awh and Pashler, 2000; Müller *et al.*, 2003; McMains and Somers, 2004; Cavanagh and Alvarez, 2005; McMains and Somers, 2005; Alvarez and Franconeri, 2007; Adamo *et al.*, 2008; Cave *et al.*, 2010; Niebergall *et al.*, 2011). Several studies have indicated that dividing attention and processing stimuli in parallel can improve performance (Awh and Pashler, 2000; Cavanagh and Alvarez, 2005; McMains and Somers, 2005; Bettencourt *et al.*, 2009). Experiment 1, presented in Chapter 2, was designed to test the hypothesis that humans can divide spatial attention to multiple discrete locations simultaneously using long-term memory to guide attention.

## **1.3 Neural Mechanisms of Attention**

Top-down, goal directed attention is supported by the dorsal attention network (DAN; Corbetta and Shulman, 2002), which consists of the intraparietal sulcus (IPS), the superior precentral sulcus (sPCS), and the inferior precentral sulcus (iPCS). These regions are recruited in a broad range of visual attention, visual short-term memory, visual working memory tasks and overlap with visuotopically mapped regions (e.g. Hagler and Sereno, 2006; Szczepanski *et al.*, 2010; Sheremata *et al.*, 2010). Activation within the dorsal attention network tracks

behavioral performance, plateauing when subjects reach attentional or working memory capacity (Cohen et al., 1997; Todd and Marois, 2004; Sheremata et al., 2010).

#### **1.4 Neural Mechanisms supporting Long-Term Memory Retrieval**

Long-term memory retrieval is correlated with activation in medial temporal lobe structures including the hippocampus, and cortically, with the default mode network (DMN) (Andrews-Hanna et al., 2010; Spreng and Grady, 2010). The hippocampus and default mode network exhibit strong functional and structural connections in humans (Vincent et al., 2006; Buckner et al., 2008; Kahn et al., 2008). Regions within DMN have been linked to different aspects of memory retrieval. The dorsal medial prefrontal cortex and posterior cingulate cortex are thought to play an important role in autobiographical memory retrieval (Summerfield et al., 2009; Maddock et al., 2001). The contributions of the lateral parietal cortex to memory retrieval are the most hotly debated.

Activation in the lateral posterior parietal cortex especially in the left hemisphere have been repeatedly found in long-term recognition or episodic memory retrieval (reviewed in Hutchinson, Uncapher and Wagner, 2009; Schooler et al., 2011). There is a dissociation between strong episodic memories recruiting ventral parietal cortex (including the angular gyrus) and effortful memories recruiting dorsal parietal cortex (including the IPS; Cabeza et al., 2008; Vilberg and Rugg, 2007). A large body of literature in recent years has focused on the interpretation of this dissociation. Some hypotheses state that this activity

indicates a true episodic contribution of the parietal lobe to long-term memory retrieval. One such hypothesis has arisen from more extensive neuropsychological data that suggests that the parietal lobe is critical for one's subjective recollective experience (Ally *et al.*, 2008; Berryhill *et al.*, 2011). Another hypothesis suggests that inferior parietal cortex is a site of Baddeley's proposed episodic buffer, such that it holds retrieved information in working memory until a decision can be made about that information (Vilberg and Rugg, 2007; Vilberg and Rugg, 2008; Vilberg and Rugg 2009). Conversely, other hypotheses rely on known functional roles of the parietal lobes, such as attentional, default mode and semantic processes. The dual attention to memory hypothesis posits that the dissociation between retrieval of vivid and weak memories in the parietal cortex reflects an established dissociation between bottom-up and top-down attention respectively (Cabeza *et al.*, 2008; Cabeza, 2008; Ciaramelli *et al.*, 2010). Recent work has suggested that these hypotheses are not necessarily mutually exclusive, but rather that the parietal cortex is made up of multiple distinct regions with different contributions to long-term memory retrieval (Hutchinson *et al.*, 2014).

### **1.5 Competitive Interactions Between Memory and Attention**

The DMN was originally defined as the task-negative network because researchers consistently saw this network of brain regions deactivated during an attentionally demanding task (Raichle *et al.*, 2001). Activation within the dorsal attention network is correlated with greater deactivation in the default mode

network (Fox et al., 2005; Buckner et al., 2008; Todd et al., 2005). A recent study focused on parietal lobe structures directly contrasted a visual search paradigm with an episodic memory retrieval paradigm in the same subjects (Sestieri et al., 2010, 2011). Activation within the angular gyrus of the DMN was high during the memory retrieval task, while deactivation was reported in the intraparietal sulcus. Conversely, during the visual search task, activation was high in the intraparietal sulcus while the angular gyrus was strongly deactivated. These findings suggest that the DAN and DMN are anti-correlated and that attending to the visual world and retrieving memories are supported by different structures that may actively repress one another. Furthermore, there has been little evidence for direct communication between the DMN and DAN and it has been suggested that the cognitive control network (CCN) supports switching between these two networks (Spreng et al., 2013).

### **1.6 Neural Mechanisms of Long-Term Memory-Guided Attention**

The competition seen between the DMN and the DAN stands in direct contrast with the known behavioral findings of memory biasing attention (Chun and Jiang, 1998; Soto et al., 2009; Werner and Thies, 2000; Olivers, 2011). The behavioral evidence suggests that there are situations in which attention and long-term memory cooperate rather than compete. Yet, the majority of studies investigating the neural substrates of attention and memory have focused on their competition rather than their cooperation. However, four studies have investigated their cooperation. Summerfield and colleagues (2006) provided the

first fMRI experiment to contrast memory-guided attention with stimulus-guided attention. Summerfield and colleagues report largely overlapping mechanisms for both memory-guided and stimulus-guided attention within the intraparietal sulcus, the frontal eye fields and the inferior precentral sulcus, all nodes of the dorsal attention network. The main difference noted in this paper is in the left hippocampus, which is more strongly recruited for memory-guided attention than stimulus-guided attention. While this study made important strides to bridge the gap between attention and memory, the volume based group-averaging techniques may have blurred any cortical differences seen between memory-guided and stimulus-guided attention.

Summerfield et al. (2011) followed up on their previous experiment in an event-related potential (ERP) study. Previous studies have shown that when attending to a particular area in space, alpha band power is reduced in the hemisphere contralateral to the attended area of space, reflecting desynchronization of alpha band oscillations. Summerfield and colleagues directly contrasted activation in the brain during the cue period when participants used memory to guide attention compared to when they had no cue and found that during the cue period, alpha band power was reduced for contralateral targets, indicating that long term memory biases spatial perception. This was further expanded in an fMRI study that found that this alpha desynchronization was localized to the contralateral visual cortex. Patai and colleagues (2012) found that LTM cues improved sensitivity to detect targets in familiar

environments. Explicit visual cues enhance the N2pc ERP, a component linked to selective attention. However, LTM cues were found to attenuate the N2pc ERP response, suggesting that LTM-guided attention biases perception using a different mechanism than explicit cues (Patai et al., 2012).

Recent advancements in fMRI techniques including surface based region of interest analysis were used here to investigate the neural mechanisms of LTM-guided attention. I hypothesized that LTM-guided attention is supported by a distinct set of cortical regions, from those that support memory retrieval and stimulus-guided attention alone. This work improved on past fMRI studies of cooperation between long-term memory and attention and these experiments will be discussed in Chapters 3 and 4.

### **1.7 Hemispheric Asymmetries**

There are at least five contralateral hemifield maps in intraparietal sulcus (IPS) in both hemispheres in humans and these representations are highly symmetric between the hemispheres (Silver *et al.*, 2005; Wandell et al., 2007; Swisher *et al.*, 2007). However, in the neuropsychological disorder hemispatial neglect, damage to the right ventral lateral parietal cortex, among other regions, can result in inattention to the left half of space (Corbetta et al., 2005; Corbetta and Shulman, 2011, Verdon et al., 2010; He et al., 2007). Interestingly, while left neglect is common, right neglect is quite rare. To explain this hemispheric asymmetry, representational models of hemispatial neglect suggested that the right hemisphere contains representational maps of the visual world that

encompass both the left and right hemifields whereas the left hemisphere only contains a map of the right visual field (Heilman and Van Den Abell, 1980). Thus, if the left hemisphere is damaged, neglect does not occur because the right hemisphere contains maps of the right visual field. However, if the right hemisphere is damaged, the left hemisphere does not contain maps of the left visual field and the patient exhibits left neglect symptoms.

Previous work from our laboratory and others has shown that a hemispheric asymmetry in the intraparietal sulcus (IPS) emerges at high load in visual short-term memory (Sheremata *et al.*, 2010) and attention (Szczepanski, *et al.*, 2010). Under high load the left IPS retains its contralateral field bias; activation is high when attending to the contralateral (right) visual field but not when attending to the ipsilateral (left) visual field. In contrast, at high load, the right IPS switches to a full-field representation; equal levels of activation were observed when attending to the contralateral or to the ipsilateral visual fields. These findings indicate that right hemisphere IPS maps are flexible under different cognitive demands and provides a possible mechanism to explain why attentional deficits of hemispatial neglect syndrome are highly asymmetric and associated with right hemisphere damage.

Memory effects in the lateral parietal cortex are largely lateralized to the left hemisphere (for review see Hutchinson *et al.*, 2014). Here, I investigated how LTM guidance affects this hemispheric asymmetry. I predicted that when subjects use a visual cue to guide spatial attention, a hemispheric asymmetry

would be evident, where the left IPS codes for only contralateral (right) targets whereas the right IPS codes for bilateral targets. In contrast, I hypothesized that under LTM-guided attention conditions, both the left and right visuotopic IPS would code for bilateral targets.

### **1.8 Experiments in this Dissertation**

The experiments described in Chapters 2-5 used behavioral and functional MRI methods to examine the mechanisms that underlie long-term memory guidance of visual attention. This dissertation used novel tasks to probe whether humans can use LTM to guide attention to multiple discrete locations, determine the neural mechanisms underlying LTM-guided attention, and characterize the influence that LTM and visual cues have on recruitment of spatially mapped parietal cortex.

Experiment 1, described in Chapter 2, was designed to test the hypothesis that humans can divide spatial attention to multiple discrete locations using LTM to guide attention. While several studies have investigated divided spatial attention using either exogenous (at the target locations) or endogenous cues (at fixation), no studies have investigated whether subjects can use long-term memory to guide spatial attention to multiple discrete locations. In Experiment 1A, I developed a novel paradigm to investigate LTM guidance of visual spatial attention to multiple locations in which participants learned the locations of 0, 1, 2, or 3 changes in complex visual scenes. They were subsequently tested using a one-shot change detection task while fixating. Results indicate that sensitivity

to detect changes increased in conditions where there were studied changes compared to when no change was previously studied. Furthermore, capacity significantly increased in the multiple-change conditions (2 or 3 studied changes) compared with the single change condition. However, capacity did not increase significantly above 1. In Experiment 1B, I increased the number of study exposures to each image with 3 changes and recorded the reaction time to find each change during study. Results indicated that after one exposure, subjects did not remember the location of all three changes, perhaps explaining why participants' capacity was not higher than 1 in Experiment 1A. After 3 exposures, participants remembered nearly all changes in all images. In a one-shot change-detection task capacity was significantly higher than 1. Furthermore, capacity did not increase with longer probe durations suggesting that participants did not use the extra time to move their attentional spotlight serially between locations. Taken together, these results indicate if humans have robust memory for locations, they can use this memory to guide attention to multiple discrete locations simultaneously.

To contrast the cortical networks underlying LTM-guided attention with those underlying visual stimulus-guided attention, in Experiment 2 I adapted a change-detection paradigm (Rensink *et al.*, 1997; Rosen *et al.*, 2014); subjects use LTM (LTM-guided) or an exogenous visual cue (STIM-guided) to guide spatial attention in order to detect scene changes. I performed both whole-brain and region-of-interest (ROI) analysis of fMRI activation patterns during task

performance. I utilized a cortical-surface brain atlas compiled from intrinsic functional connectivity analysis of 1000 brains (Yeo, Krienen *et al.*, 2011) to define the three brain networks and their constituent ROIs. In Experiment 3, I used a novel paradigm to compare neural mechanisms of LTM-guided attention, memory retrieval, and visually cued attention, in the same subjects and session. This allowed me to expand on the findings from Experiment 2 and further explore the regions of the CCN that are recruited in LTM-guided attention.

Because numerous studies of the parietal lobe have shown a right hemisphere bias for attention, and a left hemisphere bias for memory retrieval, Experiment 4, described in Chapter 5, I investigated hemispheric asymmetries in the parietal cortex, because the open question remains what happens to these hemispheric asymmetries when long-term memory guides attention. In Experiment 4, I used the same data presented from the change-detection task presented in Chapter 3, but now focused on both cue type (LTM or stimulus) and visual field. Furthermore, I performed retinotopic mapping on each of the participants in order to identify the contralateral maps IPS0-IPS4 in the parietal cortex. Previous studies have shown that under high attentional or visual short term memory load (Sheremata *et al.*, 2010; Szczepanski *et al.*, 2010), the retinotopically mapped regions of left IPS respond to targets in the right (contralateral) visual field, whereas the retinotopically mapped regions of right visuotopic IPS respond to targets in both the left (contralateral) and right (ipsilateral) visual field; these results suggest that the spatial representations of

the right hemisphere IPS regions dynamically shift between stimulus driven and attention/STM conditions. Results from the current stimulus-guided condition replicated this prior hemispheric asymmetry using complex real world scenes. In the LTM-guided condition, both the right and left retinotopic IPS exhibited strong bilateral responses. Thus hemispheric symmetry is observed in IPS in the LTM-guided condition, but the responses exhibit much less contralateral specificity than observed for retinotopic mapping. These findings suggest that attentional demands drive right IPS, while long-term memory retrieval demands drive left IPS.

Memory-guided attention is an important and understudied component of how humans direct attention. The work presented in this dissertation discusses novel results regarding the behavioral and cortical mechanisms underlying this cooperation between attention and memory.

**CHAPTER 2: Long-term memory guidance of visuospatial attention  
in a change detection paradigm**

## 2.1 Introduction<sup>1</sup>

In our every day life, we are bombarded with visual information and we typically experience the world as if we have a complete picture. Yet, it is well documented that our visual working memory and attentional capacity is severely limited. Numerous experiments have observed an attentional capacity of approximately  $4 \pm 1$  objects (e.g. Pylyshyn and Storm, 1988; Yantis, 1992; reviewed in Cowan, 2001). How can we reconcile our rich visual experience with the evidence of limited processing? While attention and short-term memory are limited resources, human long-term memory has a much higher capacity (e.g., Hollingworth, 2005; Brady, *et al.*, 2008). Therefore, it is reasonable to infer that humans exploit the massive capacity of long-term memory to aid visuospatial attention. Visual working memory is thought to act as the interface between long-term memory and attention such that items from long-term memory are called up into working memory and particular items can be held within the focus of attention as needed (Oberauer, 2002; Lewis-Peacock and Postle, 2012). Consider the experience of driving on an unfamiliar busy highway. It can be overwhelming. Even when road signs indicate that a lane is merging or an exit is approaching, it is easy to make mistakes due to the volume of new information. Once one has driven on this busy highway a few times, the task of maneuvering

---

<sup>1</sup> This work has been previously published as Rosen ML, Stern CE and Somers DC. (2014). Long-term memory guidance of visuospatial attention in a change-detection paradigm. *Frontiers in Psychology: Cognitive Science*

through the complex environment becomes much simpler. It is likely that part of this behavioral advantage is due to learning where to direct one's attention.

Long-term memory guided attention is an important and understudied form of visual working memory. A recent review (Hutchinson and Turk-Browne, 2012) has highlighted this issue and suggested that memory-guided attention should be added to the existing taxonomy of attention, which has historically solely focused on the division between exogenous, stimulus-guided attention and endogenous, goal-directed attention. There are many forms of memory-guided attention that have been studied in recent years. For instance, Soto *et al.* (2007) found that attention was drawn to a stimulus that was the same color as an item held in working memory. Subjects performed a target discrimination task within a working memory delayed match-to-sample paradigm for colored shapes. Reaction time was fastest when the target was embedded in the same colored shape that was held in working memory and slowest when the distractor was embedded in the colored shaped that was held in working memory. This finding provides evidence for the contents of working memory biasing attention. However, other studies (Downing and Dodds, 2004; Woodman and Luck, 2007) have found that when a distractor matches an item held in working memory, it speeds up reaction time. Woodman and Luck (2007) conclude that subjects are making voluntary shifts of attention away from a memory-matching stimulus based on the knowledge that the stimulus is a distractor. These findings suggest that holding information in working memory is not in and of itself sufficient to

guide attention (Woodman and Luck, 2007; Olivers, 2009). It has been argued that after only moderate amounts of exposure, long-term memory takes over for working-memory in guiding attention (Woodman *et al.*, 2013). Here, I further argue that long-term memory can bias attention by bringing relevant items into visual working memory.

Several studies have shown a behavioral advantage of attention when a subject has previous experience with a stimulus. Most notably, Chun and Jiang (1998) found in a visual search paradigm that the latency to detect a target decreases when targets appear in consistent spatial locations, even when subjects are unaware of this consistency. This effect, which they named “contextual cueing,” provides evidence that the human brain implicitly uses prior experience to direct attention (Brockmole and Henderson, 2006; Chun and Turk-Browne, 2007). Furthermore, Werner and Thies (2000) used a change-detection flicker paradigm in soccer experts and novices and found that change detection in novel soccer scenes was more rapid in experts than novices. This finding provides evidence that humans can also generalize knowledge from previous experience to direct spatial attention.

Another mechanism that supports processing in complex visual environments is divided spatial attention. Numerous lines of evidence indicate that humans and non-human primates are able to divide visual attention into multiple discrete spotlights (Shaw and Shaw, 1977; Awh and Pashler, 2000; Müller *et al.*, 2003; McMains and Somers, 2004; Cavanagh and Alvarez, 2005;

McMains and Somers, 2005; Alvarez and Franconeri, 2007; Adamo *et al.*, 2008; Cave *et al.*, 2010; Niebergall *et al.*, 2011). Although some have questioned whether multiple object selection reflects parallel or very rapid serial processing (e.g., Tsal, 1983; Jans *et al.*, 2010), there is clear evidence that such selection can provide behavioral advantages in the presence of many distracting stimuli (Awh and Pashler, 2000; Cavanagh and Alvarez, 2005; McMains and Somers, 2005; Bettencourt and Somers, 2009). Prior studies have investigated multifocal attention using explicit cues either at the locations of interest (exogenous) or at central location (endogenous), but none have explicitly investigated long-term memory-driven orienting of spatial attention.

It has been proposed that working memory, the ability to hold information in mind and manipulate it in some way, is an emergent property of interactions between attention and long-term memory (Oberauer, 2002) and that working memory consists of two components, those items that are in the focus of attention which has a limited capacity, and those items that are outside the focus of attention, but in an active state of long-term memory and thus more easily accessible (Cowan, 1988). It has been debated whether more than one object can simultaneously be within the focus of attention (Gilchrist and Cowan, 2011; Oberauer and Bialkova 2009). In a recent review of the literature, Oberauer (2013) reanalyzed data from several studies to try to determine whether more than one item can be held simultaneously in the focus of attention. He concluded

that humans are able to simultaneously attend to distinct objects held in working memory.

Here, I developed a novel paradigm to investigate long-term memory guidance of visual spatial attention. My goals were to tightly control the time window in which attention must be deployed and to investigate the deployment of LTM-guided attention to multiple locations. To this end, I adapted a popular change detection / change blindness paradigm. Change blindness, the tendency of subjects not to detect differences between stimuli, occurs even when subjects are actively searching for a change (Levin and Simons, 1997; Rensink, O'Regan and Clark, 1997; Simons and Levin, 1997; Simons, 2000). However, when participants find a change, it becomes very obvious to them. To exploit this phenomenon, I designed a paradigm in which participants studied the location of changes in complex outdoor scenes in a standard change detection flicker paradigm (Rensink, O'Regan and Clark, 1997). Then, subjects were tested in a one-shot change detection task on the images that they studied previously. In this adapted change-detection paradigm, subjects view a scene and must retrieve from long-term memory the location(s) of the potential change(s), they must then hold those location(s) in visual working memory until the image disappears and the probe image appears and they may compare the location(s) in the probe image to what is being held in working memory. Additionally, the brief target scene presentation of this paradigm permits investigation of the ability

to simultaneously deploy attention to multiple discrete remembered locations in complex real-world scenes.

## **2.2 Experiment 1**

In the first experiment, I presented subjects with images of scenes in a change detection task. I manipulated the number of studied changes in each scene (0, 1, 2, or 3). At test, subjects were required to covertly attend to the remembered location(s) in order to determine capacity in this task. The experiment consisted of a study phase, in which subjects viewed the image changes repeating in a flicker-paradigm loop, and a one-shot test phase, in which subjects had to detect a change that occurred on 50% of trials. I hypothesized that studying changes would increase subjects' sensitivity to detect changes. Additionally, I hypothesized that subjects' capacity would be higher in the multiple studied change conditions (2- and 3-studied changes) than in the single studied change condition.

### *2.2.1 Materials and Methods*

#### *2.2.1.1 Subjects*

Subjects were recruited from the Boston University community and received course credit or \$10 compensation for their participation. This research was approved by Boston University Charles River Campus Institutional Review Board and all subjects gave written informed consent. Thirty healthy subjects participated in Experiment 1 (mean age 18.8 years, 8 male). The data from 6

subjects (2 male) were excluded from analyses because subjects failed to hold fixation during the testing period.

#### 2.2.1.2 Study Period

Subjects freely viewed scenes in the change detection flicker paradigm. Scenes had been used in a previous experiment (Schon *et al.* 2004) and were edited in Adobe Photoshop to create multiple versions of the scene with spatially discrete changes (e.g. a car changing color, a building disappearing). Subjects viewed 80 scenes in total with 0, 1, 2, or 3 changes (20 per condition). Twenty unique scenes were used in each condition and were not counterbalanced across subjects (*i.e.* all subjects viewed the same 20 scenes as all other subjects in the 3-change condition). This is a limitation of the study design because the differences seen between the responses to each condition could be due to differences in the scenes themselves. However, note that in many cases, the images with more scene changes (2- and 3-studied change images) had subtler and smaller changes than in the 1- and 0-studied change conditions. This fact may have in fact reduced the ability to find differences between the different conditions rather than rather than falsely inflating the differences. Note that subjects were given equal exposure to scenes with and without changes. Subjects were instructed to visually search the image until they found the change(s). Once they detected a change, they were instructed to click on it with the mouse. If they determined that no change occurred between the scenes they were instructed to click anywhere outside of the image. Trials were presented in

blocks of 0- and 1-change images and blocks of 2- and 3-change images. A cue appeared at the beginning of the block that indicated how many changes the subject should be looking for (i.e. “0 or 1 changes” or “2 or 3 changes”). Subjects were also informed that the goal was to learn the changes because they would be tested on them. On a given trial, a picture of a scene (Scene A) flashed on the screen for 1000 ms, then a blank screen appeared for 250 ms and then a potentially altered scene (Scene A') appeared for 1000 ms, and was then replaced with a blank screen for another 250 ms. This cycle continued for 16 seconds after which a 10 second reveal period occurred. During the reveal period, Scene A appeared for 1000 ms followed immediately by Scene A' for 1000 ms and so on. Because no blank screen occurred between the presentation of Scene A and Scene A', any changes that were present became very apparent. Subjects were instructed to click on the changes at any point during the 26-second presentation (during the initial flicker period or the reveal period) (Figure 2.1A). Images subtended approximately  $12^{\circ} \times 8^{\circ}$  of visual angle. Visual stimuli were presented on a Mac Pro using the Vision Egg software package (Straw, 2008).

#### 2.2.1.3 Test period

A given image appeared on screen for 4000 ms. Subjects were instructed to use this time to covertly direct their attention to all possible location(s) of the changes, in preparation for a one-shot change detection. Eye position was manually monitored by the experimenter throughout the task using an eye camera to

ensure that subjects maintained fixation throughout the test period. Subjects were excluded if they did not hold adequate fixation for at least 95% of trials. If they had not previously studied a change in that scene (0-change condition), they were instructed to attempt to diffusely direct their attention to the entire scene. The image then disappeared for 250 ms and appeared (possibly changed) for 500 ms. There was a 50% chance that a single change occurred and a 50% chance of no change occurring in the second image presentation. For images where subjects studied 1, 2, or 3 changes, if a change occurred, it was always a studied change. In the images that subjects saw no changes during the study period, test phase changes were always unstudied changes. Subjects were given 3000 ms to make a two-alternative forced choice whether or not a change occurred (Figure 2.1B).

Sensitivity to detect changes was calculated using  $d'$ :

$$(1) \quad d' = z(HR) - z(FAR)$$

where  $z(HR)$  is the normalized hit rate and  $z(FAR)$  is the normalized false alarm rate.

In order to evaluate whether subjects were able to hold more than one location in visual working memory in the 2- and 3-studied change conditions, it is critical to take into account set size when assessing performance on task that requires divided attention. Cowan's  $k$  is a well-established method for estimating

capacity in change-detection paradigms (Pashler, 1988; Cowan 2001; Todd and Marois, 2004; Xu and Chun, 2006).  $k$  was calculated:

$$(2) \quad k = (HR - FAR) \times SS,$$

where HR is the hit rate, FAR is the false alarm rate and SS is the set size.  $k$  provides an estimate of the number of locations to which the subject is effectively holding in the focus of attention.

### 2.2.2 Results: Experiment 1

Although subjects had equal exposure to all images, exposure to image changes during the study phase significantly improved their change detection performance during the test phase. The mean sensitivity ( $d'$ ) to detect the changes for the 0-, 1-, 2-, and 3-studied change conditions was  $0.60 \pm 0.12$ ,  $1.89 \pm 0.15$ ,  $1.47 \pm 0.17$  and  $0.89 \pm 0.15$ , respectively. A one-sample *t*-test revealed that subjects performed this task significantly better than chance ( $d' = 0$ ) in the 0-studied change condition ( $t(23) = 4.78$ ,  $p = 0.0002$ ). Exposure to changes in images prior to the test period significantly modulated subsequent sensitivity to detect these changes. The sensitivity to detect changes in each of the (1-,2-,3-) studied change conditions was significantly higher than the 0-studied condition ( $t(23) = 8.14$ ,  $p < 0.0001$ ,  $t(23) = 5.43$ ,  $p < 0.0001$ ,  $t(23) = 2.16$ ,  $p = 0.041$ , for 1-, 2-, and 3-changes respectively, all  $p$ -values are Holm-Bonferroni corrected for three one-sample comparisons). These results indicate

that prior exposure to the location of changes helps to support visual working memory to guide visuospatial attention. Subjects are able to rapidly remember the studied location(s) and deploy their attention to those locations to monitor whether a change occurs. It should be noted that as the number of locations to which the subject needed to attend increased, the sensitivity to detect those changes decreased. The  $d'$  for the 1-studied change condition was significantly higher than for the 2- and 3-studied change conditions ( $t(23) = 2.25$ ,  $p = 0.034$ ,  $t(23) = 7.27$ ,  $p < 0.0001$ , respectively) and the  $d'$  for the 2-studied change condition was significantly higher than the  $d'$  for the 3-studied change condition ( $t(23) = 2.73$ ,  $p = 0.024$ , all  $p$ -values are Holm-Bonferroni corrected for 3 between-condition comparisons). Clearly, as subjects had more trained locations to which to direct their attention, sensitivity declined. The hit rate was significantly higher for all studied change conditions (1-, 2-, and 3-change conditions) compared to the no-studied change condition (Mean(1-change) =  $0.77 \pm 0.03$ , Mean(2-change) =  $0.69 \pm 0.04$ , Mean(3-change) =  $0.55 \pm 0.07$ , compared to Mean(0-studied change) =  $0.24 \pm 0.04$ , all  $p < 0.05$ , Holm-Bonferroni corrected). Additionally, the false alarm rate was also significantly higher in all the studied change conditions compared to the 0-studied change condition (Mean(1-change) =  $0.17 \pm 0.032$ , Mean(2-change) =  $0.22 \pm 0.04$ , Mean(3-change) =  $0.27 \pm 0.07$ , compared to Mean (0-studied change) =  $0.09 \pm 0.01$ , all  $p < 0.05$ , Holm-Bonferroni corrected).

In order to evaluate whether subjects were able to hold more than one location in visual working memory in the 2- and 3-studied change conditions, it is critical to take into account set size when assessing performance on a task that requires divided attention. Cowan's  $k$  is a well-established method for estimating capacity in change-detection paradigms (Pashler, 1988; Cowan 2001; Todd and Marois, 2004; Xu and Chun, 2006).  $k$  for each condition was  $0.16 \pm 0.03$ ,  $0.60 \pm 0.04$ ,  $0.94 \pm 0.10$ , and  $0.84 \pm 0.13$  for the 0-, 1-, 2- and 3-studied change conditions, respectively.  $k$  in 2-studied change condition was significantly higher than the 1-studied change condition ( $t(23) = 3.45$ ,  $p = 0.0066$ , Holm- Bonferroni corrected) and there was a trend toward a higher  $k$ -score in the 3-change condition compared to the 1-change condition ( $t(23) = 2.09$ ,  $p = 0.095$ , corrected). There was no significant difference in  $k$  for the 2-studied change condition compared to the 3-studied change condition ( $t(23) = 0.617$ ,  $p = 0.543$ , corrected) (Figure 2.2).

These findings suggest that subjects were able to attend to more locations when they studied 2 or 3 changes compared to when they studied 1 location. However, since  $k$  did not exceed 1 in any condition, this leaves doubt about the ability to simultaneously attend to multiple target locations in this paradigm. One possible explanation for the low capacity in Experiment 1 is that subjects did not remember the location of the changes in some images. Given the large number of images studied (80), it is likely that one exposure during the study phase is not adequate to strongly encode multiple image change locations. A second concern

is that the 500ms probe image presentation time might be sufficiently long to permit subjects to rapidly switch the focus of attention from one spatial location to another (e.g., Tsal, 1983; Sperling and Weichselgartner, 1995). I address these issues in Experiment 2 by increasing the number of study exposures for each image during the training phase and by parametrically varying the probe presentation time during the test phase.

### **2.3 Experiment 2**

In Experiment 2, subjects studied each scene three times. I measured latency to find each change during the study periods. I used these latencies to determine whether subjects successfully learned the locations of each change. Subjects then underwent two test phases with different probe presentation times (150, 250 and 500 ms). I expected that subjects would learn more change locations with each viewing of the scenes. Furthermore, I hypothesized that the increased exposure to the images would result in increased capacity compared to that of the subjects' in Experiment 1. Finally, I explored whether subjects exhibit similarly high capacities with shorter probe presentation times (150 and 250 ms probes) compared to the longer probe presentation times (500 ms probe). The motivation for varying the probe presentation time was to investigate possible effects of a rapidly moving attentional spotlight (e.g., Tsal, 1983). Volitional moves of attention are generally believed to take a relatively fixed amount of time, regardless of the distance between the attended and to-be attended locations (Yantis, 1988; Sperling and Weichselgartner, 1995; Cave and

Bichot, 1999), and thus suggests that the attention does not need to pass through the space between an attended location and a to-be attended location. Rather, attentional shifts can be made in a quantal fashion. These volitional shifts are generally believed to take approximately 200 ms (Wolfe et al., 2000).

### *2.3.1 Materials and Methods: Experiment 2*

#### 2.3.1.1 Subjects:

Sixty-two healthy subjects (mean age 22.8 years, 22 male) participated in Experiment 2. Data from 15 subjects (4 male) were excluded due to inadequate fixation during the test period.

#### 2.3.1.2 Study period:

Subjects viewed 20 scenes using the same flicker paradigm described in Experiment 1. During the study phase, all 20 scenes contained 3 changes. Reaction time to find and click on the location of each of the 3 changes was recorded. Subjects viewed all 20 scenes in the flicker paradigm three times to ensure that they learned each of the locations of the changes.

In order to estimate the number of changes remembered after each exposure, I created a simple linear model which assumes that the average reaction times reflect a weighted average of the time to respond to a remembered change and the time to search for, find and respond to an unremembered (new or forgotten) change:

$$(3) \quad Avg\Delta RT(x) = P_M(x) \times RT_M + (1 - P_M(x)) \times RT_S,$$

where,  $P_M$  is the proportion of changes remembered.  $RT_M$  is the reaction time for remembered changes, which I assume to be the group average fastest recorded reaction time (difference between detecting one change and detecting the next change, 1.65 seconds).  $RT_S$  is the reaction time for visual search trials, which I assume to be the average difference in reaction times for all detected changes during the first exposure to the images (*i.e.* the average difference in RT between locating the 1<sup>st</sup> and 2<sup>nd</sup> change and the RT difference between locating the 2<sup>nd</sup> and 3<sup>rd</sup> change, 6.52 seconds). The 1<sup>st</sup>, 2<sup>nd</sup> and 3<sup>rd</sup> changes were defined simply by the order in which subjects clicked on each change, not predefined by the experimenter. On the first exposure the subjects cannot be using memory and thus must be searching. I then rearrange the terms of this equation to estimate the proportion of locations remembered after each exposure,  $P_M(x)$ :

$$(4) \quad P_M(x) = \frac{RT_S - Avg\Delta RT(x)}{RT_S - RT_M},$$

$P_M$  was calculated separately for each of the 1<sup>st</sup>, 2<sup>nd</sup> and 3<sup>rd</sup> changes. I can then estimate how many changes each subject remembers at each exposure by adding the proportion of trials in which subjects are relying on their memory for the 1<sup>st</sup>, 2<sup>nd</sup> and 3<sup>rd</sup> change using the following equation:

$$(5) \quad C = P_M(1^{st}) + P_M(2^{nd}) + P_M(3^{rd}),$$

where C is the estimated number of learned changes.

### 2.3.1.3 Test period:

The test period paradigm was similar to that of Experiment 1 with two major differences. As in the first experiment, the original scene was presented for 4000 ms. After a 250 ms blank screen, the second image was presented for one of three pseudo randomly chosen durations (150 ms, 250 ms, or 500 ms). Additionally in Experiment 2, subjects were given one practice test, followed by two test phases with all 20 images appearing twice and the probe durations intermixed. I collapse results of the two test phases because performance did not differ on these two tests.

## 2.3.2 Results and Discussion: Experiment 2

### 2.3.2.1 Study phase:

With each study exposure, latency to find the changes decreased (Figure 2.3A). On the first exposure, the latency to find the 1<sup>st</sup>, 2<sup>nd</sup> and 3<sup>rd</sup> changes were  $7.00 \pm 0.42$  s,  $13.07 \pm 0.46$  s,  $19.57 \pm 0.42$  s, respectively. On the second exposure, latency to find the changes was faster ( $3.44 \pm 0.19$  s,  $6.59 \pm 0.36$  s, and  $11.35 \pm 0.55$  s for the 1<sup>st</sup>, 2<sup>nd</sup> and 3<sup>rd</sup> changes, respectively.) In the third and final study phase, latency was even faster ( $2.64 \pm 0.12$  s,  $4.55 \pm 0.25$  s, and  $7.08 \pm 0.44$  s, for the 1<sup>st</sup>, 2<sup>nd</sup>, and 3<sup>rd</sup> changes, respectively). During the first exposure, subjects found some of the changes after the reveal period, but during the

second and third exposures, subjects were able to find all changes before the reveal period.

Using the above formula to estimate  $C$  (the number of learned changes), I estimate that after the 1<sup>st</sup> exposure, subjects had learned approximately 1.9 changes and after the second exposure, subjects had learned approximately 2.8 changes (Figure 2.3B). These data demonstrate that subjects did not remember the location and identity of all 3 changes after just one exposure. This fact likely contributed to the low  $k$ -score found in the 3-change condition in Experiment 1.

#### 2.3.2.2 Test Period:

$K$ -score was calculated at each probe presentation time. The mean  $k$  was  $1.36 \pm 0.11$ ,  $1.25 \pm 0.12$ , and  $1.23 \pm 0.11$  for the 500 ms, 250 ms, and 150 ms probe conditions, respectively. I performed a two-sample  $t$ -test comparing the  $k$ -score for the 500 ms probe in Experiment 2 (20 scenes each with 3 changes) to the 3-change condition (20 scenes) in Experiment 1. The  $k$  in Experiment 2 was significantly higher than that of Experiment 1 ( $t(69) = 2.84$ ,  $p = 0.0076$ ). This confirms the finding from model analysis of the study phase that increased study exposures improved capacity. I performed a one-sample  $t$ -test to compare the average  $k$  in the test period in Experiment 2 to hypothetical mean of 1 in order to determine whether subjects could effectively deploy their attention to more than one location. At all three probe durations, the  $k$ -score was significantly higher than 1 ( $t(46) = 3.10$ ,  $t(46) = 2.10$ ,  $t(46) = 2.25$ , all  $p < 0.05$  for the 500, 250 and 150 ms probe durations respectively). There were no significant differences in  $k$

at the three different probe presentation durations (Figure 2.4). The mean hit rates were  $0.66 \pm 0.3$ ,  $0.62 \pm 0.3$ , and  $0.56 \pm 0.3$  for the 500 ms, 250 ms and 150 ms probe durations. The mean false alarm rates were  $0.21 \pm 0.03$ ,  $0.21 \pm 0.03$  and  $0.15 \pm 0.03$  for the 500 ms, 250 ms, and 150 ms probe durations, respectively.

These findings indicate that subjects were able to successfully detect more than one change at all probe durations. However, the number of successfully detected changes in this paradigm (Figure 2.4) is lower than the number of change locations that subjects learned in the study phase (Figure 2.3B). In the study phase analysis I estimated that subjects required 1.65 seconds per change location to identify changes, while in the test phase, subjects had only 150-500 ms to identify changes. Moreover, subjects freely viewed images in the study phase, but were required to maintain central fixation and detect peripheral changes in the test phase. Given these large temporal and spatial advantages, it is not surprising that performance in the study phase exceeded that in the test phase.

There has been a long debate in the literature about the speed at which attention may move (e.g., Reeves and Sperling, 1986; Sperling and Weichselgartner, 1995; Wolfe *et al.*, 2000; Jans *et al.*, 2010; Cave and Bichot, 1999; Cave *et al.*, 2010). Volitional moves of attention are widely accepted to take 200 ms or longer (Wolfe *et al.*, 2000; Cave *et al.*, 2010), regardless of distance between the locations, note that I failed to observe any significant difference in capacity as the probe time varied between 150 ms and 500 ms and

thus the results across all probe times are not consistent with a rapidly moving spotlight interpretation for this paradigm. Rather, these results provide evidence that subjects can divide attention based on a memory associated with a particular image. However, I note that this finding is a null result and therefore should be interpreted with caution.

## **2.4 General Discussion**

In a series of two experiments, I used a modified change detection paradigm to explore how memory helps to guide spatial attention. In Experiment 1, participants were trained on a change-detection flicker paradigm with complex visual scenes that contained 0, 1, 2, or 3 changes at different spatial locations. During the test phase, a previously studied scene was presented statically and subjects were instructed to covertly direct their attention to all the possible locations in which a change had occurred during the study phase. The scene would disappear and then reappear after a short blank period, and participants responded with a two-alternative forced choice whether or not they detected a change (Change, No change). Results indicate that the number of successfully attended items significantly increased in the multiple-change conditions (2- or 3-studied changes) compared with the single change condition. In Experiment 2, I increased the number of study exposures and found that subjects were faster at finding the changes with every study exposure. Change detection performance increased to significantly above 1 with increased study exposures. These findings suggest that humans can covertly attend to more than one remembered

location. Moreover, this work introduces a new paradigm for investigating interactions between long-term memory for visual scenes and visual working memory deployment of visuospatial attention.

Our findings also provide additional evidence that humans can simultaneously hold more than one location in the focus of attention. The results indicate that in order to successfully divide attention in this task, the memories must be sufficiently robust, which was accomplished by exposing subjects to the changes multiple times. In contrast, a rapidly shifting attentional spotlight model would predict more items would be attended with the longer probe duration; however, I failed to observe an effect of probe duration in the range of 150 ms to 500 ms in Experiment 2. This indicates that rapid shifts of attention likely did not play a role in these results. I note that this finding is a null result and should be interpreted with caution. Only in the free-viewing conditions of the long-duration study phase trials did I observe an effect of probe duration; it is not surprising that the opportunity to move ones eyes to a potential target location enhanced performance. However, in the critical test phase, eye movement controls insured that subjects did not move their eyes; under these conditions, I observed no evidence for rapid shifts of covert attention. The results also indicate that even inexperienced observers can divide spatial attention based on memory cues. It is possible that minimal training using another covert attention task would further improve subjects' ability to perform this task. Another possibility is that a single focus of attention is more broadly distributed in the multiple target conditions,

selecting targets and intervening distractors. These data cannot rule out this possibility and future studies should attempt to further tease apart this idea.

The contextual cueing paradigm (e.g., Chun and Jiang, 1998) has provided firm evidence that humans can use a familiar context to direct their attention to a particular spatial location. More recently, Conci and Müller (2012) showed that subjects could be contextually cued to multiple locations in the same context. This recent paper provides additional support for this finding that subjects can rapidly update attention to multiple locations based on a particular remembered stimulus. Conci and Müller used standard contextual cueing stimuli wherein subjects had to find a target letter (T) among several distractor letters (L). They found a reliable contextual cueing effect to multiple locations using these stimuli. Brockmole and Henderson (2006) showed the contextual cueing effect holds in real-world scenes. The present study demonstrates that humans are able to simultaneously attend to more than one remembered location using visually complex, real-world scenes. Contextual cueing effects are often attributed to implicit memory mechanisms (Chun and Jiang, 1998). Here, subjects report explicitly remembering the location of the change(s) and directing their attention based on that explicit memory. While the current study did not contain a test of explicit memory and my assumption that subjects were using explicit memory to guide their attention is based on anecdotal evidence, the type of stimuli used (complex visual scenes), the number of exposures, and the depth of encoding required by repeated visual search, encourage the formation of

explicit memories. Unlike in the visual search paradigm of contextual cueing, in this paradigm subjects have only one chance to detect a change in this task and therefore must effectively deploy their attention to the remembered locations rapidly. Therefore, this paradigm provides a unique method by which to probe questions regarding guidance of spatial attention by using explicit, declarative memory.

It is also noteworthy that I adapted the flicker paradigm (Rensink, O'Regan and Clark, 1997) to develop a new paradigm that provides tight control over the duration of attentional selection. The short exposure of the (potentially changed) probe stimulus limits the movement of attention. A one-shot change detection paradigm also has been used in visual short-term memory (VSTM) paradigms (e.g., Luck and Vogel, 1997). Many studies of visual working memory have focused solely on the contributions of short-term memory. Here, I explicitly investigated the interactions between long-term memory, short-term memory and attention. Subjects must retrieve the location(s) of the change(s) from long-term memory and hold them in the focus of attention in visual working memory until the probe image appears and they can make a decision about whether a change occurred. Notably, the tight timing control afforded by this paradigm may prove useful in fMRI experiments, a methodology that has only coarse temporal control.

In a prior study of contextual cueing using functional MRI, Summerfield and colleagues (2006) found that memory-guided attention recruits largely the same brain networks – notably the intraparietal sulcus and frontal eye fields –

recruited by visually guided attention; however, memory-guided attention also recruited the left hippocampus while visually-guided attention did not. Orbitofrontal cortex has also been implicated along with the hippocampus in context-dependent retrieval tasks (Brown *et al.*, 2012; Ross *et al.*, 2011). The present study lays the foundation for future investigations of the neural mechanisms by which memory guides spatial attention.

## 2.5 Chapter 2 Figures

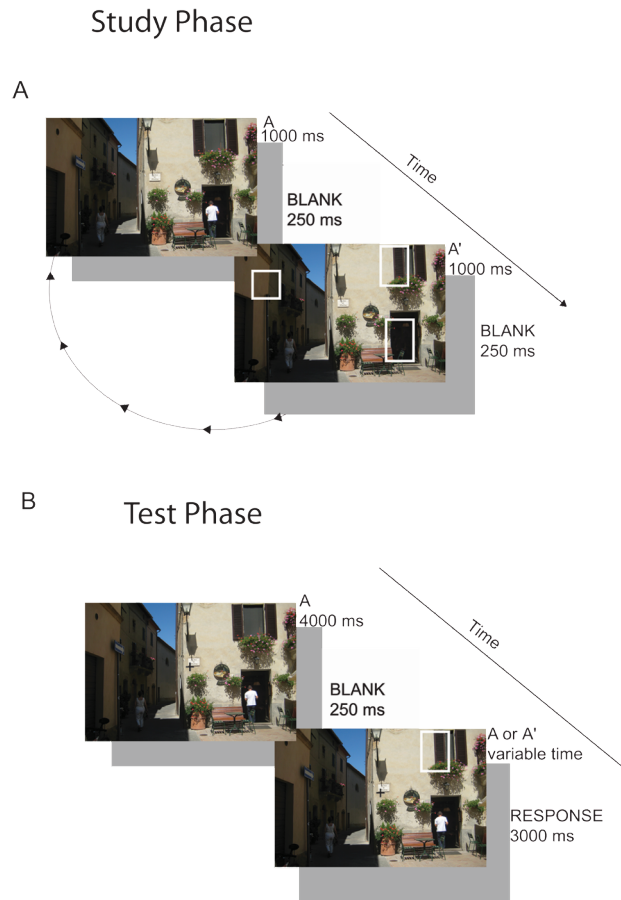


**Figure 2.1** Change detection task. Cycling Study Phase: during the study phase, subjects freely viewed images in a flicker paradigm. They were instructed to click on the changes as they found them. In Experiment 1, subjects viewed 80 scenes with 0, 1, 2, or 3 changes. In Experiment 2, subjects viewed 20 scenes with 3 changes and studied these three times. **(B)** One-shot Test Phase: subjects held central fixation while a novel or familiar scene image appeared. They were instructed to covertly attend to where they thought a change might occur. The

image disappeared and then flashed briefly with 0 or 1 change and then disappeared again. The subject had to determine whether a change occurred.

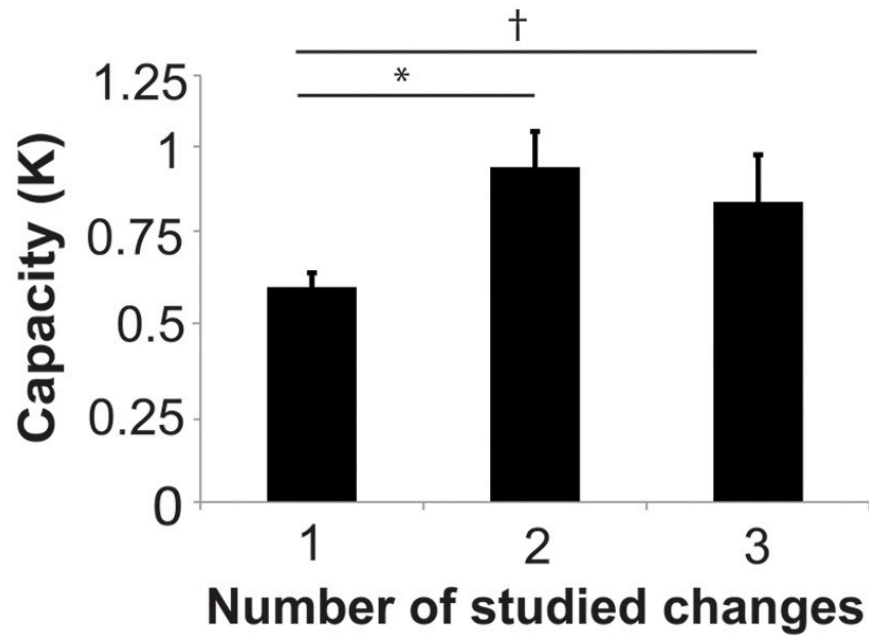


**Figure 2.2** Capacity (K) for remembered changes in studied images (1, 2, and 3-change conditions) contrasted with the same metric applied to images that were studied without changes (0-change condition).

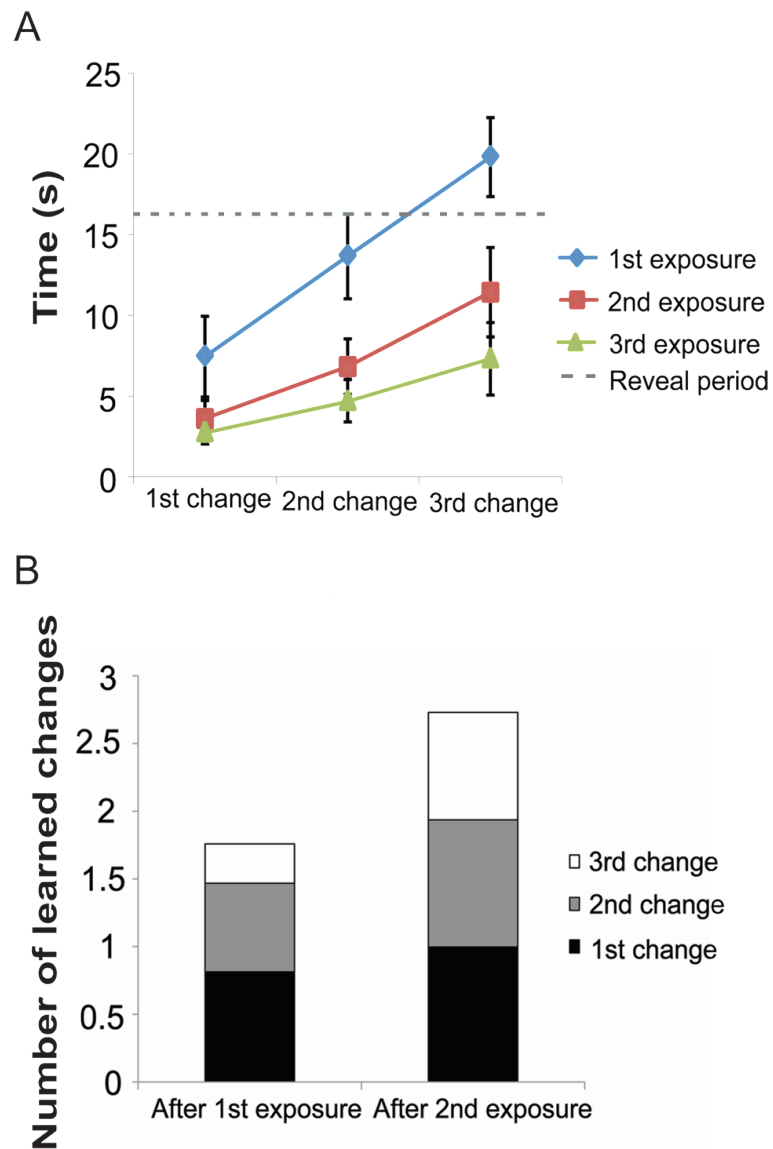


**Figure 2.3.** Experiment 1B Study Phase. A) Latency to find changes decreased with each exposure in the study phase. Note that all three changes were presented simultaneously (see Figure 2.1A) and thus subjects responded to each change as they noticed it. B) Using this model, (Equation 4), I estimated that after the second exposure subjects remember almost all three changes. These data

are taken from the time to detect the each change after each exposure. The first bar labeled "After 1<sup>st</sup> Exposure" was taken from latency to find each change during the second exposure and the second bar labeled "After 2<sup>nd</sup> Exposure" was taken from the latency to find each change during the third exposure. Subjects were not exposed to the images a fourth time and therefore the latency to estimate each change after the 3<sup>rd</sup> exposure was not available.

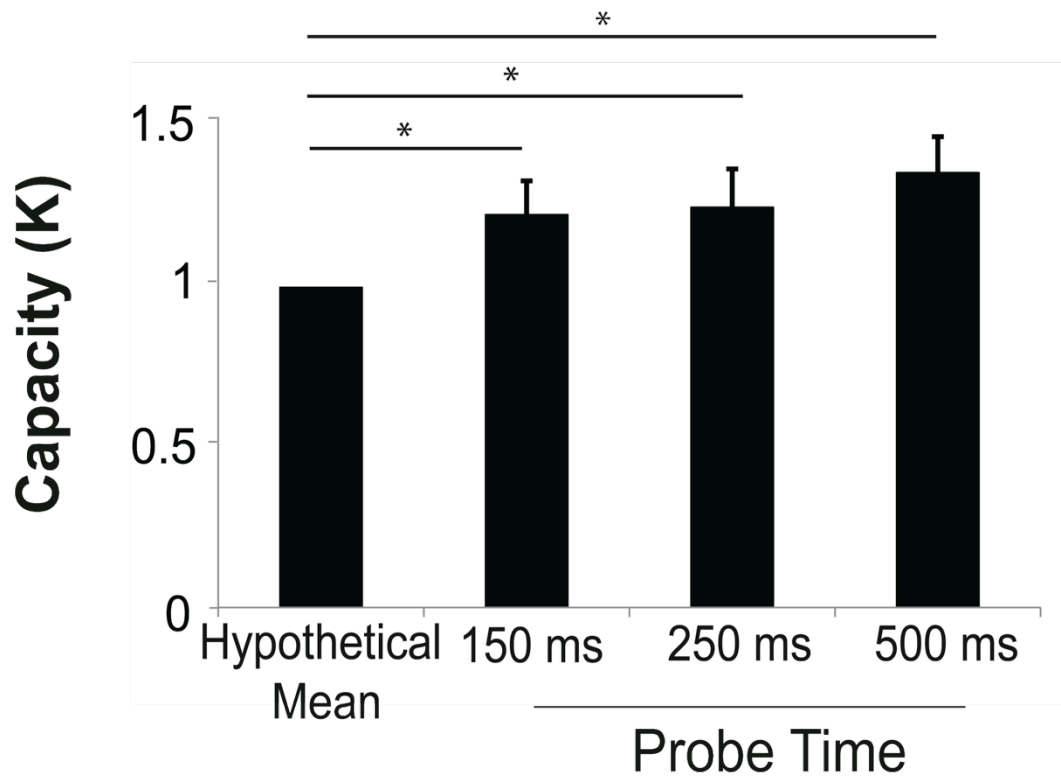


**Figure 2.4.** Capacity increased significantly above a hypothetical mean of 1 at all probe durations, suggesting that subjects could successfully deploy their attention to more than one remembered location. Error bars are *SEM*. \* indicates  $p < 0.05$ .

**Chapter 3: Cognitive Control Network Contributions to  
Memory-Guided Visual Attention**

### 3.1 Introduction<sup>2</sup>

Human visual abilities exceed those of powerful supercomputers, yet our visual performance is profoundly limited by our attentional capacity (e.g., Simons and Chabris, 1999). Although humans can attend to multiple objects (e.g., Awh and Pashler, 2000; McMains and Somers, 2004, 2005; Cave *et al.*, 2010), attentional capacity is limited to approximately four objects (Pylyshyn and Storm, 1988; Cowan, 2001). The paradox of high real-world performance and limited capacity can be reconciled by considering the important role that long-term memory (LTM) plays in guiding visual attention. Prior experience, via either explicit or implicit memory, can accurately direct visual attention and enhance performance (Chun and Jiang, 1998, 2003; Henderson and Hollingworth, 1999; Moores, *et al.*, 2003; Hollingworth, 2004, 2005; Summerfield *et al.*, 2006, 2011; Patai *et al.*, 2012; Chun and Turk-Browne, 2007; Olivers, 2011; Stokes *et al.*, 2012). Despite the functional importance of visual memory-guided attention, its neural mechanisms are understudied compared to other forms of visual attention (for review, see Hutchinson and Turk-Browne, 2012) and are the focus of the current study.

Long-term memory-guided visual attention should rely on memory retrieval mechanisms and on visual orienting and selection mechanisms. Additionally, I

---

<sup>2</sup> This work has previously been published as Rosen ML, Stern CE, Michalka SW, Devaney KJ, & Somers DC. (2015). Cognitive Control Network Contributions to Memory-Guided Visual Attention. *Cerebral Cortex*, bhv028.

hypothesized that cognitive control mechanisms help to mediate interactions between the attention and memory systems. To investigate this hypothesis, I contrasted long-term memory-guided visual spatial attention with stimulus-guided visual spatial attention in a set of fMRI experiments. Both forms of attention require spatial orienting and selection mechanisms, but differ in memory processing and stimulus processing demands. Prior work has contrasted endogenous or top-down visual attention with exogenous or bottom-up visual attention (e.g., Corbetta and Shulman, 2002), focusing on top-down effects driven by the presence of an explicit spatial cue. In contrast, long-term memory-guided visual attention places different demands on the top-down attentional system and/or may recruit additional brain structures. One prior fMRI study directly contrasted LTM-guided spatial attention with stimulus-guided attention (Summerfield *et al.*, 2006); this study reported greater left hippocampal activation in the memory-guided condition, but failed to observe differential activation in attentional and control structures. Another LTM-guided attention fMRI study focused on the preparatory activity in spatiotopic parietal cortex and did not include a comparison to stimulus-guided attention (Stokes *et al.*, 2012).

Here, I re-investigated the neural substrates of attentional processes supporting LTM-guided visual spatial attention and focused on three prominent brain networks, the *cognitive control network* (CCN), the fronto-parietal *dorsal attention network* (DAN), and the *default mode network* (DMN), including the hippocampus. The DAN, including the intraparietal sulcus / superior parietal

lobule / lateral occipital complex (IPS/SPL/LOC), the superior pre-central sulcus (sPCS), and the inferior pre-central sulcus (iPCS), is typically activated in a broad range of visual attention tasks (e.g., Hagler and Sereno, 2006; Konen and Kastner, 2008). The DMN, which includes important memory structures such as the hippocampus, parahippocampal cortex, and posterior cingulate cortex, is strongly deactivated or suppressed during attentionally demanding tasks (e.g. Raichle *et al.*, 2001). These strongly competitive interactions between attention and memory systems (Buckner *et al.*, 2008; Sestieri *et al.*, 2011) contrast with the cooperative interactions apparently required for LTM-guided attention (Hutchinson and Turk-Browne, 2012). I hypothesized that a third network, the CCN (e.g., Vincent *et al.*, 2008), supports cooperative interactions between explicit long-term memory and visual spatial attention. This hypothesis is supported by previous work demonstrating that the CCN is positively correlated with both the DAN and DMN at rest while the correlations between the DAN and DMN are largely negative (Spreng *et al.*, 2013). The CCN supports switching between different mental representations and is a strong candidate to mediate attention-memory interactions (Chiu and Yantis, 2009; Cole and Schneider, 2007, Spreng *et al.*, 2013). Specifically, medial superior parietal lobe / posterior precuneus has been implicated in attention switching functions (Shomstein and Yantis, 2004, 2006; Chiu and Yantis, 2009). Additionally, lateral parietal cortex has been implicated in long-term memory retrieval processes related to attention (e.g., Wagner *et al.*, 2005; Cabeza, 2008) and several recent studies have

sought to functionally parcellate this brain region into different memory and attention subregions (Vilberg and Rugg, 2009; Nelson *et al.*, 2010; Sestieri *et al.*, 2010; Hutchinson *et al.*, 2014).

To contrast the cortical networks underlying long-term memory-guided attention with those underlying visual stimulus-guided attention, I adapted a change-detection paradigm (Rensink *et al.*, 1997; Rosen *et al.*, 2014); participants used long-term memory (LTM-guided) or an exogenous visual cue (STIM-guided) to guide spatial attention in order to detect scene changes. I performed both whole-brain and region-of-interest (ROI) analysis of fMRI activation patterns during task performance. In a planned analysis, I utilized a cortical-surface brain atlas compiled from intrinsic functional connectivity analysis of 1000 brains (Yeo *et al.*, 2011) to define the three brain networks and their constituent ROIs. The results showed three regions located within the posterior CCN were more strongly recruited during LTM-guided attention than STIM-guided attention. This finding was also confirmed in a *post-hoc* analysis suggested by an anonymous reviewer. This *post-hoc* analysis used ROI coordinates derived from two alternative network definitions derived from Power *et al.* (2011) and Yeo *et al.* (2011). Intrinsic functional connectivity analysis indicated that these three regions form a posterior subnetwork within the CCN.

### **3.2 Materials and Methods**

*3.2.1. Participants:* Twenty-three healthy human participants (13 male, 10 female) with normal or corrected-to-normal vision were recruited from Boston

University and the greater Boston community. All participants were compensated and gave written informed consent to participate in the study, which was approved by the Institutional Review Board of Boston University. All participants were right-handed and between the ages of 23 and 33.

### *3.2.2. Visual Stimuli and Experimental Paradigm.*

Change detection experiments were conducted over two sessions: a behavioral training session followed by an fMRI test session. A separate version of the change detection paradigm, with the same images, was used for each session. For training, an extended-exposure, looped version was used to facilitate learning of the scene changes; for the fMRI test session, a brief-presentation single-shot version was used in order to strongly encourage pre-deployment of spatial attention prior to the appearance of the probe stimulus.

Day 1, Training: The initial training session was designed to allow participants to learn a single change in each of 24 scenes (change detection encoding task) that would be used in the long-term memory-guided attention (LTM-guided) condition on Day 2. Additionally, participants viewed 192 scenes with no changes (man-made/natural judgment task) that would be used in the stimulus-guided attention (STIM-guided) condition during the scan session. Scene stimuli were presented on a Macintosh Macbook Pro laptop computer using the Vision Egg software package (Straw, 2008).

Change-detection Encoding Task: Participants were shown 24 scene images in a change-detection flicker paradigm (Rensink *et al.*, 1997; Rosen *et al.*, 2014).

Each scene was an outdoor scene obtained from Google Images that was altered using Adobe Photoshop (e.g., removed tree, added window, changed color of car, etc.), thus creating two versions of each scene (original and altered). On a given trial, a scene appeared on the screen for 1000 ms, followed by a blank screen for 250 ms, and the same scene, containing one change, for another 1000 ms. The original scene and altered scene flickered on and off for 15 s, and participants were instructed to visually search for the change. Detecting changes in novel scenes is attentionally demanding and typically requires several flicker cycles (Rensink *et al.*, 1997). Participants were instructed to click on the scene change using the computer mouse when they detected the change. Following the flicker period was a “reveal period” in which the original and the altered scene alternated without a blank screen for 10 s. In this phase, the altered part of the scene appeared to flicker on and off to attract the participant’s attention. The purpose of the reveal period was to ensure that all participants saw all changes and to reinforce the location and identity of the change.

Man-made/Natural Judgment Encoding Task: Participants also viewed a separate set of 192 scene images for 3000 ms each and made a two-alternative forced choice judgment about whether the scene was mostly natural or mostly man-made. No changes were presented to subjects for this set of images. This exposure served to familiarize participants with the scenes, but not the changes, that would be used in the stimulus-guided (STIM-guided) condition on Day 2.

Day 2, Test: Twenty-four to forty-eight hours after the training day, participants came in for an fMRI scan session. Trials were presented in blocks of four different conditions: LTM-guided attention (LTM-guided), exogenous stimulus-guided attention (STIM-guided), uncued scenes (No-Cue), and passive scene viewing (Passive). Each block started with a 1 s block cue period and was followed by six 5.9 s trials, for a total block duration of 36.4 s. A total of 12 counterbalanced blocks were presented per run (4 LTM-guided, 4 STIM-guided, 2 No-Cue, 2 Passive). Sets of 4 TRs (10.4 s) of blank screen fixation periods were included at the start, halfway point and end of each run. Each run was 7 min 48 seconds long and eight runs were performed by each participant.

Practice Session: Participants performed practice trials while in the scanner before the scan session began. In these practice trials, participants maintained fixation at the center of the screen. An image for which they had studied a change the day before appeared on the screen for 3000 ms. Simultaneously, a red and white box outline appeared at the location of the studied change for 1500 ms. Participants were instructed to covertly attend to the location of the box/location of studied change. Then the image disappeared for 250 ms and flashed up again for 150 ms before being replaced by a blank screen while responses were collected (2500 ms). Participants were instructed to respond whether or not a change occurred at the cued location (50% of trials). These practice trials served two purposes. First, participants were trained to maintain fixation at the center of the screen and were given verbal feedback if they made

eye movements. Second, participants were reminded of the location of the changes in the 24 images that would be used for the LTM-guided condition. This training also ensured that subjects had three exposures to the location of the changes in the LTM-guided condition (one during the initial encoding and two during this training). Experiment 1B, presented in Chapter 2, suggested that three exposures are sufficient for subjects to learn the location and identity of a single change (Rosen *et al.*, 2014).

Scan session: Participants performed a “single-shot” change detection task under different cueing conditions (Figure 3.1). The initial scene appeared for 3000 ms, followed by a blank gray screen for 250 ms, then either the original or altered scene appeared for 150 ms and finally was replaced by a blank screen for the remainder of each trial (2500 ms) while responses were collected. The single-shot 150 ms probe presentation was chosen to make the attentional selection task difficult, to strongly encourage spatial deployment of attention prior to appearance of the probe, and to prevent subjects from overtly or covertly moving their attentional foci once the probe appeared. The initial image did not provide any information regarding whether a change would occur on that trial. On 50% of the trials, the probe image was different from the initial image (change), and on 50% of trials it was identical to the image presented initially (no-change). Participants made a judgment about whether a change occurred in the probe image compared to the original image. Due to the short duration of the probe stimulus in the change detection task, participants were required to accurately

direct spatial attention in order to detect the image change. In all conditions, participants were instructed to fixate at the center fixation point and direct their attention covertly to the cued location in the scene. In the *long-term memory-guided attention condition (LTM-guided)* (Figure 3.1A), participants viewed one of the 24 images for which they studied changes the prior day. There was no explicit cue on the images. Participants used memory to direct their attention to the spatial location of the studied change. Image changes occurred on 50% of the trials and only occurred at the studied location. In the *stimulus-guided attention condition (STIM-guided)* (Figure 3.1B), participants viewed one of the 192 scenes that they had studied without image changes the prior day with the addition of an explicit cue. The cue was a set of nested red and white square outlines (~1.3 x 1.3 degrees of visual angle) centered on the location of the potential scene change for 1500 ms at the start of the 3000 ms static image phase. Image changes occurred on 50% of the trials, and only occurred at the cued location. In the *no-cue condition (No-Cue)*, participants viewed novel images that had not previously been studied and no cue was provided. Participants were instructed to attend to the entire scene and do their best at detecting changes. The condition was included as a behavioral control in order to demonstrate the impact of LTM-based and stimulus-based cues on behavioral performance. Because this condition had much greater task difficulty, many fewer detected targets, and a greater chance that subjects might incidentally encode the novel scenes and locations of any detected targets, I did not include

it as a baseline fMRI condition or in the imaging data analysis (but it was included as a regressor in the model). In the *passive condition (Passive)*, participants were instructed to fixate as in all other conditions and simply make a random button press whenever the scene appeared for a second time.

Trials were presented in blocks of six, with each block preceded by a cue word on the screen to indicate the block condition: “memory” for LTM-guided, “box” for STIM-guided, “active” for No-Cue, and “passive” for Passive. A total of 408 images were divided into lists of 24 scenes. Scene images used for each condition were counterbalanced across participants such that each list of 24 was presented in each of the four conditions (LTM-guided, STIM-guided, No-Cue and Passive) across the set of participants and each participant viewed all images. The 24 scenes used in the LTM-guided condition for each participant were repeated once per run (eight times total). All other images were only presented once for each participant.

### *3.2.3. MR Data Acquisition*

Functional MRI data were acquired using a 3 Tesla Siemens TIM Trio magnetic resonance (MR) imager located at the Center for Brain Science at Harvard University in Cambridge, Massachusetts. All data were acquired using a 32-channel head coil. Functional scans were acquired using T2\*-weighted, gradient echo, echo-planar images [repetition time (TR) = 2.6 seconds, echo time (TE) = 30 ms; voxel size 3.1 x 3.1 x 3.0 mm] and were collected from 42 slices with no skip, with full brain coverage. Each subject participated in eight functional scans

(each 180 TRs; 7 min 48 sec duration) in one scan session. Functional data were aligned with high-resolution (1.0 x 1.0 x 1.3 mm) T1-weighted images. For 15 participants the high-resolution structural images were acquired at the same facility; for 8 participants they were acquired on an identical scanner and coil at the Martinos Center for Biomedical Imaging at Massachusetts General Hospital in Charlestown, Massachusetts. All high-resolution structural images were used to create a computerized reconstruction of each cerebral cortical hemisphere. Thirteen of the twenty-three participants returned to undergo a resting state scan [TR = 2.6 s, TE = 30 ms; voxel size 3.1 x 3.1 x 3.0 mm, 42 slices, no skip]. During this scan they were instructed to fixate at a center fixation cross and otherwise allow their mind to wander. Participants underwent between six and twelve minutes of resting state scanning.

### *3.2.3. MR Data Analysis:*

For each participant, the cortical surface of each hemisphere was computationally reconstructed from the high-resolution anatomical volume using FreeSurfer software (Dale *et al.*, 1999; Fischl *et al.*, 1999a; Fischl *et al.*, 1999b; Fischl 2012). Both fMRI task data and fMRI resting-state data were analyzed using the FreeSurfer 5.1.0 software package (Charlestown, Massachusetts). For functional data, intensity normalization and motion correction were performed before signal averaging was performed. I analyzed data in two ways: first, using a random-effects model, group average data were projected onto the cortical surface of the FreeSurfer average (fsaverage) brain (Dale *et al.*, 1999); second,

by defining multiple regions of interest (ROIs) for each of three brain networks (CCN, DMN, DAN) in each participant. These regions were taken from a publicly available atlas that was originally defined using cluster-based intrinsic functional connectivity analysis of 1000 brains (Yeo *et al.*, 2011, see below for details). Whole cortex and ROI analyses were performed using a general linear model with regressors that matched the time course of all task conditions (LTM-guided, STIM-guided, No Cue, Passive, Fixation). Resting-state data were analyzed using the cortical ROIs that showed greater activation for LTM-guided attention than STIM-guided attention as seed regions.

Whole-Brain Cortical Surface Analysis: Single participant fMRI data were registered to an average cortical surface space (Freesurfer 'fsaverage' brain) using the boundary of the gray matter and white matter. Analyses were performed separately in each hemisphere on the average cortical surface and data were analyzed for each vertex using a general linear model (GLM) with each condition as a predictor (i.e. one for LTM-guided, STIM-guided, No-Cue, and Passive). Three motion correction regressors were included in the model. The BOLD signal was modeled as a linear, time-invariant system with  $\gamma$  response function assumed for each condition with a delay  $\delta = 2.25$  and a delay time constant  $\tau = 1.25$ . An estimated response was generated by convolving the response function with the block length (i.e. the time in each condition) and minimizing the residual error (FS-FAST, Cortech). Random effects group analyses were performed using surface-based averaging techniques (Fischl *et*

*al.*, 1999b). A *t*-test was performed for each vertex to compare differences in activation between conditions. The significance of these activation differences was projected onto the surface of the Freesurfer 'fsaverage' brain.

To correct for multiple comparisons, I employed FS-FAST to perform Monte-Carlo simulations of a smoothed null hypothesis data set to establish cluster-wise thresholds for the population maps (Forman *et al.*, 1995). The Monte Carlo simulation generated random volumes of normally distributed values that were then smoothed by a 6 mm smoothing kernel. Clusters were defined as areas of contiguous vertices with significance values below a threshold of  $p < 0.01$ . Ten thousand iterations of this simulation established a cluster-size threshold of 140 mm<sup>2</sup> for LTM-guided vs. STIM-guided contrast. Results are presented in Table 3.1.

Region of Interest Analysis within the CCN, DAN and DMN: I examined whether three previously defined cortical networks would be differentially activated in LTM- and STIM-guided attentional conditions: the *dorsal attention network* (DAN) or task-positive network (Corbetta and Shulman, 2002; Raichle *et al.*, 2001), which is involved in top-down endogenous attention, the *default mode network* (DMN) or task-negative network (Raichle *et al.*, 2001; Buckner and Vincent, 2007, Buckner *et al.*, 2008, Vincent *et al.*, 2008), which is recruited in retrieval of long-term memory, and a third network, the *cognitive control network* (CCN, Vincent *et al.*, 2008), some nodes of which lie adjacent to the nodes of the DMN and/or the DAN. I performed both ROI-based analysis and whole-cortex GLM

analysis to contrast the blood oxygen level dependent (BOLD) activation in the LTM-guided and STIM-guided conditions. In the ROI analysis, each condition was contrasted with a passive viewing condition in order to quantify the patterns of activation produced by both forms of attention. The ROI definitions for the CCN, DAN and DMN, were obtained from the Yeo-Krienen-Buckner cortical network atlas, which was constructed from cluster-based analysis of intrinsic functional connectivity of 1000 brains (Yeo *et al.*, 2011). This analysis employed three of the seven Yeo-Krienen-Buckner networks (CCN, DAN, and DMN). Each sub-region of each of these networks was mapped from a pre-defined label on the Freesurfer 'fsaverage' brain onto the appropriate cortical hemisphere of each participant to define each ROI. The *cognitive control network* (CCN) is made up of posterior cortical regions including lateral intraparietal sulcus (latIPS), posterior precuneus (PrC-p), posterior callosal sulcus / mid-cingulate (CaS-p), and posterior lateral temporal cortex (LTC-p), and anterior cortical regions within the prefrontal cortex, including dorsolateral prefrontal cortex (dlPFC), posterior dorsomedial prefrontal cortex (dmPFC-p), and posterior ventrolateral prefrontal cortex (vlPFC-p). I note that the latIPS ROI does not include the fundus of IPS, but rather incorporates the more ventral aspect of the lateral bank of IPS as well as the dorsal most portion of the angular gyrus. The *dorsal attention network* (DAN) includes a region running from intraparietal sulcus/superior parietal lobule through lateral occipito-temporal cortex (IPS/SPL/LOT), as well as superior precentral sulcus (sPCS) and inferior precentral sulcus (iPCS). The *default mode*

*network* (DMN) includes angular gyrus (AnG), posterior cingulate cortex / anterior precuneus (PCC), anterior lateral temporal cortex (LTC-a), anterior dorsal medial prefrontal cortex (dmPFC-a), anterior ventrolateral prefrontal cortex (vlPFC-a), and parahippocampal cortex (PHC). In order to facilitate comparison with earlier work (Summerfield *et al.*, 2006; Stokes *et al.*, 2012), I also included an anatomically defined hippocampal ROI (see below). Percent signal change was extracted for each condition (LTM-guided and STIM-guided) compared to Passive viewing of the stimuli and averaged across blocks and runs to construct time-course data for all vertices/voxels within each of the 17 ROIs (16 cortical ROIs and 1 hippocampal ROI) per hemisphere for each individual subject (see Figures 3.3 and 3.4). A separate 3-way (ROI x Condition x Hemisphere) analysis of variance (ANOVA) was then performed for each network (DAN, CCN, and DMN).

Hippocampal ROI analysis: The hippocampus is known to be involved in long-term memory encoding and retrieval, and the left hippocampus has been shown to be more activated for LTM-guided attention compared to visual stimulus-guided attention when participants search for a target in a visual scene (Summerfield *et al.*, 2006). Therefore, I identified the left and right hippocampi of each individual participant using Freesurfer's automatic parcellation methods (Fischl *et al.*, 2002). The hippocampal ROIs included the entire anterior-posterior extent of the hippocampus. I then performed an ROI analysis in volume space to calculate the percent signal change for each condition (STIM-guided and LTM-

guided) compared to passive viewing. Because of the strong functional and anatomical connections between the hippocampus and the DMN (Vincent *et al.*, 2006; Greicius *et al.*, 2009), the results from the hippocampal ROI analysis are discussed with the DMN results.

ROI analysis using Alternative Network ROIs: On the advice of an anonymous reviewer, I performed *post-hoc* analysis of our results using ROIs derived from two alternative network definitions that also derive from resting-state functional connectivity, the Power *et al.* (2011) study and the Yeo *et al.* (2011) 17-network parcellation. Both analyses identify a network comprised of the mid-cingulate / posterior callosal sulcus and the posterior precuneus / posterior medial parietal cortex. While Yeo and colleagues do not comment on the possible functionality of this network, Power and colleagues performed a meta-analysis of prior work and found evidence that this subnetwork, in conjunction with a small region in lateral parietal cortex, might support some form of memory retrieval processes. The posterior precuneus and posterior callosal sulcus / mid-cingulate coordinates were taken from Power and colleagues (2011), and coordinates for the lateral parietal region (lateral IPS) were taken from a paper cited by Power (posterior IPL in Nelson *et al.*, 2010; Power, personal communication). I performed region of interest analysis on the Montreal Neurological Institute (MNI) coordinates, dilated 8mm, of these three regions. I also performed a subsequent analysis using ROIs from the Yeo *et al.* 17-network parcellation. In the 17-network parcellation, the two medial regions, the posterior precuneus (PrC-p) and the

posterior callosal sulcus / mid-cingulate (CaS-p) break off into a subnetwork (grey-blue network in Yeo *et al.*, 2011). On the lateral surface, the most lateral portion of the IPS (latIPS) forms into a subnetwork including the superior lateral prefrontal cortex and frontal pole (mauve network in Yeo *et al.*, 2011). In order to investigate the more specific parcellation of the posterior nodes of the CCN, I used the 17 network parcellation to define the two medial regions (PrC-p and CaS-p) and the lateral IPS (latIPS), and conduct region of interest analyses.

#### Intrinsic Functional Connectivity Analysis:

Previous work has found that the CCN is positively correlated at rest with the DAN and DMN. Here, I sought to investigate the specific pattern of intrinsic functional connectivity of the three nodes of the CCN that were more strongly recruited during LTM-guided attention than STIM-guided attention. All intrinsic connectivity analyses were performed within hemisphere. Data from resting-state scans were processed in Matlab. Twelve motion regressors (6 motion parameters from Freesurfer and their 6 temporal derivatives) were included in the regression analysis. Nuisance regressors for the white matter, the ventricular cerebrospinal fluid and the global mean waveform were included in the analysis along with the motion regressors (van Dijk *et al.*, 2010). Framewise displacement was calculated by taking the sum of the absolute value of six motion parameters. A threshold of 0.5 mm was set to exclude time points with excessive motion. Runs with more than 10% of time points removed due to excessive motion were removed from further analyses. High motion time points were temporarily

replaced using linear interpolation to avoid artifact spread during band-pass filtering (Power *et al.*, 2012, 2013; Carp *et al.*, 2013). Data were band-pass filtered to extract frequencies between 0.01 Hz and 0.08 Hz and then high motion time points were removed. I defined three seeds (PrC-p, latIPS, and CaS-p) constrained by significant activation ( $p < 0.01$ ) for LTM compared to passive viewing during the task in the group average. A time course was then averaged across vertices for each ROI for each hemisphere. A correlation was then computed between each seed and every vertex in the brain. To correct for multiple comparisons, I again employed FS-FAST to perform Monte-Carlo simulations of a smoothed null hypothesis data set to establish cluster-wise thresholds for the population maps (Forman *et al.*, 1995), as I did for the GLM analysis. The Monte Carlo simulation generated random volumes of normally distributed values that were then smoothed by a 6 mm smoothing kernel. Clusters were defined as areas of contiguous vertices with significance values below a threshold of  $p < 0.00833$  (correction for 6 comparisons) and a significant cluster threshold size of  $164 \text{ mm}^2$  was established.

### **3.3 Results**

#### *3.3.1 Behavioral Results:*

Participants performed well in the challenging one-shot change detection task for the memory-guided attention (LTM-guided) and visual stimulus-guided (STIM-guided) conditions. Behavioral data is reported for 21 of 23 participants; due to technical difficulties behavioral data is not available for two participants. Change

detection performance was not different between the memory-guided (LTM-guided  $d'$ :  $2.64 \pm 0.14$ ) and explicit cue (STIM-guided  $d'$ :  $2.45 \pm 0.09$ ) conditions ( $t(20) = 1.43$   $p = 0.17$ ). Performance in both conditions was significantly greater than in the No-Cue condition ( $d' = 0.94 \pm 0.09$  correct;  $p < 0.0001$ , Holm-Bonferroni corrected). This demonstrates that both forms of cueing have substantial impact on performance and that participants performed at least as well in the LTM-guided condition as in the STIM-guided condition. Because the STIM-guided condition explicitly cued the location of the potential change, these behavioral data also confirm that participants had learned the locations of the changes in the LTM-guided condition images, which did not contain an explicit cue. Additionally, a one factor ANOVA demonstrated that  $d'$  performance did not change over the course of the experiment in the LTM-guided condition ( $F(7,105) = 1.175$ ,  $p = 0.32$ ), suggesting that subjects had fully encoded the locations of the changes in the LTM-guided condition and were not doing any additional learning over the course of the experiment. Furthermore, there was no difference in reaction time between the STIM-guided and LTM-guided conditions (STIM-guided RT:  $1.02 \pm 0.05$  s, LTM-guided  $1.02 \pm 0.05$  s,  $t(20) = 0.1$ ,  $p = 0.92$ ). Note that images and changes were counter-balanced across participants (e.g. one participant's LTM-guided images were another participant's STIM-guided images, No-Cue, or Passive images) and thus performance differences between conditions cannot be attributed to the images or changes themselves.

*Eye movements:* Participants were instructed to maintain central fixation throughout the experiment during fMRI scanning. Eye position was monitored via video camera for all subjects and eye movements in excess of 2 degrees of visual angle were recorded. For three participants (2 male, 1 female), one run was excluded from fMRI analysis due to excessive (> 5% of trials) eye movements during that run. Otherwise participants overall maintained fixation on 99.0% of trials (STIM-guided: 98.3%, LTM-guided: 99.3%; No-Cue =99.1%; Passive = 99.2%).

### 3.3.2. *fMRI Results:*

We performed both whole-cortex surface-based analysis and ROI-based analysis to contrast the BOLD activation in the two behaviorally-matched conditions, LTM-guided and STIM-guided, in order to determine which cortical areas are differentially recruited for memory-guided attention and stimulus-guided attention. The ROI analysis includes both a planned comparison across three cortical networks (cognitive control, dorsal attention and default mode) and a post-hoc analysis of subnetworks suggested during the review process. The non-task 'Passive' condition, which includes stimulus presentation and a button press, served as the baseline condition.

Whole-Cortex Surface-Based Analyses: As an initial step, I performed whole-cortex GLM analysis (see Figure 3.2). This analysis (LTM-guided > STIM-guided) demonstrated that memory-guided attention differentially activated bilateral regions in posterior precuneus (PrC-p), posterior callosal sulcus / mid-cingulate

(CaS-p), anterior dorsolateral prefrontal cortex (dlPFC-a), lateral intraparietal sulcus / angular gyrus (latIPS/AnG), right anterior cingulate (ACC) and right cuneus (See Table 3.1). However, three areas identified in this contrast (LTM-guided > STIM-guided), bilateral dlPFC-a, right ACC and right cuneus, actually reflect strong deactivation in those vertices in the STIM-guided condition, while no activation is apparent in those vertices for the LTM-guided condition. Therefore, three key bilateral regions demonstrated activation for the LTM-guided spatial attention condition: PrC-p, CaS-p / mid-cingulate, and latIPS/AnG.

The reverse contrast (STIM-guided > LTM-guided) revealed greater bilateral activation in several nodes of the *dorsal attention network*: superior precentral sulcus (sPCS), inferior precentral sulcus (iPCS), intraparietal sulcus / lateral superior parietal lobule / lateral occipital complex (IPS/SPL/LOC) (see Table 3.1). Bilateral activation was also observed in the mid insula and anterior inferior frontal sulcus / gyrus (IFS-a), and anterior superior temporal sulcus (STS-a). Unilateral activation was observed in right lateral orbitofrontal cortex (OFC), and left posterior cingulate cortex / anterior precuneus (PrC-a) (see Table 3.1).

#### Network ROI Analysis I – Yeo 7-Network Parcellation:

In order to quantify the patterns of activation produced by both forms of attention, I contrasted the LTM-guided and STIM-guided conditions with a passive viewing non-task condition and performed ROI-based analysis. My primary interests were in the *cognitive control*, *dorsal attention*, and *default mode networks* (CCN, DAN and DMN, respectively). To identify ROIs, I employed an atlas constructed from

cluster-based analysis of intrinsic functional connectivity of 1000 brains (Yeo *et al.*, 2011, 7 network parcellation). This atlas contains several subregions within each of the three networks (CCN, DAN and DMN). I mapped these ROIs onto the brains of each subject and extracted percent signal change for each region.

Cognitive Control Network: Nodes of the CCN were activated by both the STIM-guided and LTM-guided conditions relative to passive viewing (Fig 3A; Table 3.2). A repeated measures Hemisphere x ROI x Condition ANOVA was performed and all statistics are lower-bound corrected (Mauchly's test for sphericity was not met for any of the main effects or interactions;  $p < 0.001$ ). This ANOVA revealed a main effect of Condition such that there was significantly greater activation in the CCN in the LTM-guided condition compared to the STIM-guided condition ( $F(1,22) = 5.29$ ,  $p = 0.031$ ). The ANOVA also revealed a significant main effect of ROI ( $F(1,22) = 14.05$ ,  $p = 0.001$ ). There was no main effect of Hemisphere, no interaction for Hemisphere x Condition or Hemisphere x ROI, and no three-way Hemisphere x ROI x Condition interaction ( $F(1,22) = 3.90$ ,  $p = 0.06$ ;  $F(1,22) = 2.01$ ,  $p = 0.170$ ;  $F(1,22) = 0.229$ ,  $p = 0.637$ ;  $F(1,22) = 1.726$ ,  $p = 0.202$  respectively), therefore I combined data across hemispheres in subsequent analyses.

There was also a significant ROI x Condition interaction ( $F(1,22) = 21.00$ ,  $p < 0.001$ ). A more in-depth look revealed that this interaction was driven specifically by two posterior medial ROIs within the CCN, posterior precuneus (PrC-p) and posterior callosal sulcus / mid-cingulate (CaS-p). These regions

were also found to be significantly more activated in the LTM-guided condition compared to the STIM-guided condition in the whole cortex analysis (see above). Percent signal change is presented in Table 3.2 for all regions of interest. Post-hoc paired t-tests (Holm-Bonferroni corrected for 34 total ROIs) revealed significantly greater activation for LTM-guided vs. STIM-guided in the PrC-p and CaS-p (both  $p < 0.001$ ). Lateral IPS (latIPS) exhibited a similar but weaker activation pattern that did not survive statistical correction for the multiple ROIs; no other CCN areas exhibited significant activation differences between LTM-guided and STIM-guided conditions (see Table 3.2). These findings, taken together with the whole-cortex analysis, demonstrate that the two medial posterior nodes of the *cognitive control network*, PrC-p and CaS-p, make significant contributions to long-term memory-guided attention.

The maps of the group-level averages for both LTM-guided and STIM-guided compared to passive viewing (see Figure 3.3) reveal that the activation differences within PrC-p and CaS-p are precisely captured within the ROIs defined by the Yeo-Krienen-Buckner atlas. Although regions abutting the PrC-p are activated in the STIM-guided condition, PrC-p is essentially devoid of significantly activated vertices in the STIM-guided condition. In contrast, nearly all of PrC-p is significantly activated in the LTM-guided condition. CaS-p is activated (relative to passive viewing) in both the STIM-guided and LTM-guided conditions, but the relative increase in activation for the LTM-guided condition (vs. STIM-guided) can be seen to be restricted to the boundaries of the ROI (Figure 3.3C,

D). These results also help to functionally validate these CCN ROI definitions of the Yeo-Krienen-Buckner atlas.

The results for latIPS in the ROI analysis are more ambiguous than in the whole-cortex analysis (Figure 3.2). LTM-guided attention appears to drive posterior portions of the bilateral latIPS ROIs, while the STIM-guided condition fails to drive any portion of the ROIs (Figure 3.3 E, F); however the anterior portion of the latIPS ROI is not activated in either condition. A closer analysis reveals a shift in the location of the latIPS peak between the LTM-guided vs. STIM-guided contrast (Table 3.2, shown on the whole-cortex; Figure 3.2) and the LTM-guided vs. baseline contrast (shown on the ROIs; Figure 3.3 E,F) of 16.7mm and 11.6mm ventrolaterally, in the left and right hemispheres, respectively. The peak shift reflects the fact that a deactivated DMN region, angular gyrus, lies adjacent to the activated latIPS region and that the DMN border region is more deactivated during the STIM-guided condition (see Discussion).

Dorsal Attention Network: As expected, the DAN was activated by both the STIM-guided and LTM-guided conditions compared to passive viewing (see Figure 3.4A-C, Figure 3.5). A repeated measures Hemisphere x ROI x Condition ANOVA was performed and all statistics are lower-bound corrected (Mauchly's test for sphericity was not met for any of the main effects or interactions;  $p < 0.001$ ). In contrast to the CCN, the DAN showed significantly greater activation in the STIM-guided condition compared to the LTM-guided condition, revealed by a

main effect of Condition ( $F(1,22) = 35.93, p < 0.001$ ). There was also a main effect of ROI but no main effect of Hemisphere ( $F(1,22) = 6.51, p = 0.018$  and  $F(1,22) = 3.11, p = 0.09$ , respectively). All three two-way interactions emerged as significant (ROI x Condition:  $F(1,22) = 11.54, p = 0.003$ ; ROI x Hemisphere:  $F(1,22) = 14.47, p = 0.001$ ; and Hemisphere x Condition:  $F(1,22) = 10.62, p = 0.004$ ). The three-way interaction was also significant ( $F(1,22) = 4.65, p = 0.042$ ). Therefore, all post-hoc *t*-tests were performed separately for each hemisphere ROI and Holm-Bonferroni corrected for 34 ROIs. All subdivisions of the DAN were significantly more activated by the STIM-guided than by the LTM-guided attention conditions (all  $p < 0.02$  corrected, post-hoc paired *t*-tests; see Table 3.2). The Hemisphere x Condition interaction reflected a stronger difference between STIM-guided and LTM-guided activation in the right hemisphere compared to the left. The ROI x Hemisphere interaction was driven by significantly greater activation of the iPCS in the right hemisphere (RH) compared to the left hemisphere (LH) (iPCS:  $t(22) = 3.77, p = 0.001$ ; IPS/SPL/LOC:  $p = 0.11$ ; sPCS:  $p = 0.42$ ). Thus, the STIM-guided attention condition more strongly taxed the dorsal attention network than did the LTM-guided attention condition, even though no significant behavioral differences were observed.

Default Mode Network and Hippocampus: In contrast to the DAN and CCN, there was no main effect of Condition in the DMN ( $F(1,22) = 3.34, p = 0.081$ ). Also, many nodes of the DMN were deactivated compared to passive viewing (see

Figure 3.4E,F). The results within this network are more complex and heterogeneous than in the other two networks. The repeated measures ANOVA revealed a main effect of ROI ( $F(1,22) = 13.60, p = 0.001$ ) and no main effect of Hemisphere in the DMN ( $F(1,22) = 3.50, p = 0.075$ ). Neither of the two-way interactions involving Hemisphere were significant (ROI x Hemisphere:  $F(1,22) = 1.24, p = 0.278$ ; Hemisphere x Condition interaction  $F(1,22) = 3.85, p = 0.063$ ). However, there was a significant three-way interaction (Hemisphere x ROI x Condition,  $F(1,22) = 5.20, p = 0.033$ ). Therefore, post-hoc *t*-tests were performed separately for each hemisphere for each ROI and Holm-Bonferroni corrected for 34 total ROIs. The heterogeneity of results is indicated by the significant ROI x Condition interaction ( $F(1,22) = 18.79, p < 0.001$ ). The two medial temporal lobe structures, parahippocampal cortex (PHC) and hippocampus (HC), showed greater activation in the STIM-guided condition compared to the LTM-guided condition (all  $p < 0.001$ , corrected; see 3.2). The medial temporal lobe activation in the STIM-guided condition may reflect encoding processes; in each STIM-guided trial the location of a potential change in an image is shown for the first time and it is likely that participants are encoding this information, while participants have already learned the change locations for LTM-guided trial images.

Bilateral posterior cingulate cortex (PCC) showed greater activation in the LTM-guided than STIM-guided condition (both  $p < 0.01$ , corrected; see Table 3.2). However, LTM-guided attention did not drive significant positive activation

relative to baseline in any of these ROIs, suggesting that the difference in the LTM-guided vs. STIM-guided contrast results from deactivation during the STIM-guided condition. A possible explanation is that suppressive influences from the DAN, which is more activated in the STIM-guided condition than the LTM-guided condition, may differentially suppress these medial nodes of the DMN during the STIM-guided condition. No other regions within the DMN showed significant activation differences between the LTM-guided and STIM-guided conditions.

#### Network ROI Analysis II – Alternative Network Definitions:

The ROI analysis above employed a network parcellation based on intrinsic functional connectivity analysis. The 3 subnetworks of the Yeo *et al.* 7-Network parcellation were an *a priori* choice for ROI analysis. However, two other prominent cortical network parcellations have been reported that are also derived from intrinsic functional connectivity analysis: the Power parcellation (Power *et al.*, 2011) and the Yeo 17-Network parcellation (Yeo *et al.*, 2011). At the suggestion of an anonymous reviewer, I performed a post-hoc analysis of these results using ROIs from the Power and Yeo 17 parcellation, in order to better isolate the pattern of activation seen in the contrast of LTM-guided attention vs. STIM-guided attention. Both resting-state parcellations reveal a subnetwork on the medial surface that appears remarkably similar to the CaS-p and PrC-p ROIs activated in the LTM-guided attention task (Figure 3.5). In order to attempt to identify a possible function for this previously undescribed network, Power *et al.* performed a meta-analysis of task data that suggested that this subnetwork

might perform memory retrieval functions (Power *et al.*, 2011). Notably, this analysis also suggested that a small ROI in the lateral IPS, previously identified in Nelson *et al.*, 2010 was also part of this network and I included this region in the *post-hoc* analysis. From Yeo and colleagues, I used sub regions reported in the 17-network parcellation that correspond to this network in the latIPS, PrC-p, and CaS-p (see Methods). All three of the regions, latIPS, PrC-p and CaS-p, showed significantly greater activation during the LTM-guided condition compared to the STIM-guided condition (all  $p < 0.001$  Holm-Bonferroni corrected, Table 3.3, Figure 3.5). This was true for both the Yeo 17-network and Power/Nelson parcellations (Yeo *et al.*, 2011; Power *et al.*, 2011; Nelson *et al.*, 2010). Thus, the Yeo 17-network and the Power/Nelson parcellations more precisely captured the pattern of activation that I observed in the memory-guided attention task than did the Yeo 7-network parcellation. Although *post-hoc* analyses, these ROIs capture the observed pattern of activation remarkably well (Figure 3.6).

#### Intrinsic Connectivity Analysis:

We examined the intrinsic connectivity within the CCN, focusing on the three posterior nodes of the CCN recruited for LTM-guided attention. During rest, PrC-p is strongly correlated within each hemisphere with the other two regions recruited in LTM-guided attention, the latIPS and CaS-p (Figure 3.5, Table 3.4), with less extensive connectivity to the other nodes of the CCN. CaS-p is the strongly correlated with PrC-p and moderately correlated with latIPS, but largely

uncorrelated with the rest of the CCN (Figure 3.7, Table 3.4). LatIPS shows strong connectivity with almost the entire CCN at rest, aside from moderate connectivity with the CaS-p (Figure 3.7, Table 3.4). Taken together, these findings suggest that these three regions may form a subnetwork at rest in which PrC-p serves as a local hub and latIPS connects this subnetwork to the rest of the CCN.

### **3.4 Discussion**

Memory-guided attention is key to our high level of visual performance in familiar environments, serving to efficiently direct our limited attentional resources. The present fMRI experiments investigated cortical networks serving memory-guided attention (Hutchinson and Turk-Browne, 2012), contrasting long-term memory-guided attention with stimulus-guided attention and a baseline condition, using a change detection paradigm. I hypothesized that the Cognitive Control Network (CCN) would be differentially recruited for LTM-guided attention and the results support this hypothesis. Closer investigation demonstrates that within the broader CCN, a posterior subnetwork exists and it is preferentially recruited for LTM-guided attention. This subnetwork consists of a region of lateral intraparietal sulcus (latIPS), and two medial structures, posterior precuneus (PrC-p) and posterior callosal sulcus / mid-cingulate (CaS-p). Lateral parietal structures, especially on the left hemisphere, have been strongly suggested in prior studies to play an important memory retrieval role (e.g., Wagner *et al.*, 2005; Vilberg and Rugg, 2008; Ciaramelli *et al.*, 2008; Hutchinson *et al.*, 2009,

2014; Sestieri *et al.*, 2010). In contrast, the two medial structures have received limited attention in the literature (Power *et al.*, 2011, 2014; Nelson *et al.*, 2013). My definition of the CCN derives from analysis of a 1000-brain database (Yeo *et al.*, 2011) and is similar to prior functional connectivity reports (Dosenbach *et al.*, 2007; Vincent *et al.*, 2008); however, note that some task-based definitions of the cognitive control network differ by including much of the dorsal attention network and exclude posterior regions, which are the focus of these results (e.g., Cole and Schneider, 2007; Braver, 2012).

We also examined two other networks, the Dorsal Attention Network (DAN) and the Default Mode Network (DMN). While the DAN was significantly activated in both LTM-guided and STIM-guided conditions, it was more strongly activated for the STIM-guided condition. Since there were no behavioral differences, this activation cannot be attributed to task difficulty, *per se*; however, the BOLD activation difference suggests that LTM-guided attention was less taxing on the DAN than was STIM-guided attention. Although it is not inconceivable that the greater DAN activation could result from the presence of the explicit spatial cue in the STIM-guided condition, this explanation seems unlikely given that early visual cortex does not exhibit corresponding robust increases in activation for the STIM-guided condition. Thus, the suggestion that LTM-guided attention reduces demands on the DAN deserves further investigation.

We did not observe a main effect for the Default Mode Network and no coherent pattern emerges across the ROIs of the DMN. One notable prior study (Summerfield et al., 2006) observed greater LTM-guided attention activation than stimulus-guided attention activation within left hippocampus, while here the hippocampus was significantly more activated by the STIM-guided condition. Recent work also demonstrated hippocampal activation during the cueing phase of LTM-guided attention (Stokes *et al.*, 2012). In this change-detection paradigm, the STIM-guided trials likely activated memory *encoding* mechanisms; any time a change occurred in a STIM-guided trial, it was the first time participants saw a change in that image and it is likely that participants encoded this location into long-term memory. Previous research has demonstrated that memory encoding robustly activates the hippocampus (e.g., Stern *et al.*, 1996; Wagner *et al.*, 1998). I do not take the present results to contradict the hippocampal involvement in LTM-guided attention in previous studies. I note that in the present study, stimuli and stimuli changes in the LTM-guided condition were well-learned (see Behavioral results) while in learning may have still been occurring over the course of scanning in Summerfield et al (2006). This activation in the hippocampus in previous studies may reflect the critical role that the hippocampus plays in binding of relational information (Ryan et al., 2000; Yee et al., 2014). I believe that in the current study, the LTM-guided condition does not rely on the hippocampus because the stimuli and changes were well-learned. In contrast, the additional encoding of the changes in the STIM-guided scenes

resulted in overall more activation in the hippocampus for the STIM-guided scenes than the LTM-guided scenes.

Previous work has shown that the activity within the CCN is positively correlated with both the DMN and DAN at rest (Spreng *et al.*, 2013) suggesting these regions may be well positioned to act as an intermediary between regions of the DMN and DAN. Here, I sought to characterize the specific intrinsic connectivity profile of each of the regions within the CCN recruited for LTM-guided attention. No prior studies have described the connectivity patterns between all three of these nodes. When the PrC-p was used as a seed for resting-state functional connectivity I found strong positive correlations with CaS-p and latIPS, but less extensive connectivity with the other nodes of the CCN (Figure 3.5, Table 3.4). CaS-p exhibited strong resting-state functional connectivity only with PrC-p and itself (Figure 3.6A, Table 3.4); this observation is consistent with prior reports that CaS-p and PrC-p form a distinct two-node resting-state network (Power *et al.*, 2011, 2014; Yeo *et al.*, 2011). In contrast, latIPS exhibits strong resting-state functional connectivity throughout the broader CCN (Figure 3.6B). Therefore, I suggest that PrC-p serves as a local hub in this three-node memory-guided attention network and that latIPS serves as hub to the broader CCN. Thus, this analysis illuminates a subnetwork of the CCN and its potential role in memory-guided attention. A recent fMRI study (Nelson *et al.*, 2013) noted that these three regions may contribute in a broader range of

memory-retrieval operations. The full functional range of this network deserves further investigation.

Involvement of CaS-p, PrC-p and latIPS was not reported in the two prior studies employed fMRI to investigate memory-guided attention (e.g. Summerfield *et al.*, 2006; Stokes *et al.*, 2012). The present study likely benefitted from the use of pre-defined cortical surface ROIs, as some CCN regions lie between DMN and DAN regions and could be obscured by volume-based group-averaging methods. Of these prior studies only one study directly contrasted memory-guided attention with exogenous stimulus-guided attention (Summerfield *et al.*, 2006); the present findings differ significantly, but there are some important similarities. Summerfield *et al.* (2006) observed that both memory-guided attention and exogenous stimulus-guided attention drove a common network of brain regions including the mid-cingulate as well as multiple regions of the fronto-parietal DAN. Here, I confirm that the mid-cingulate and the DAN were activated in both conditions, but I also observed significant activation differences between conditions. The mid-cingulate cortex exhibited greater activation for LTM-guided attention, while the DAN exhibited greater activation for STIM-guided attention.

This study provides the first evidence that three regions within the broader CCN are preferentially recruited for memory-guided attention and the first to explicitly investigate the connectivity profiles of each of these nodes. While one recent study (Nelson *et al.*, 2013) has identified these three regions in a memory retrieval experiment, this work makes a novel and substantial contribution to

understanding these regions as a subnetwork and their function in supporting memory-guided attention.

The posterior precuneus (PrC-p) ROI within the CCN is thin and crescent shaped and thus could be easily obscured in volume-based group-averaging techniques. Despite this unusual shape, memory-guided attention activation falls neatly within the boundaries of this ROI (Figure 3.3D). A similarly located region, referred to as the medial superior parietal lobule, has been implicated in an array of task-switching paradigms (Chiu and Yantis, 2009; Esterman *et al.*, 2009). In the current task, participants switch attention between their internal representation of the scene change and the external scene. Here, the PrC-p could be participating in this switching between internally directed to externally directed attention. Retrieval of episodic memories also produces activation in this vicinity (Sestieri *et al.*, 2010). Together the data suggest this region is well positioned to aid in the cooperation of LTM and attention systems.

The posterior callosal sulcus (CaS-p) within the CCN is a long, thin region that may also be described as the rostro-ventral portion of posterior cingulate cortex (Brodmann area 23) or simply as mid-cingulate cortex. Anatomical studies in monkeys and connectivity studies in humans reveal that both the hippocampus and posterior parietal cortex make substantial connections with the mid-cingulate cortex (Beckmann *et al.*, 2009; Vogt *et al.*, 2006; Baleyrier and Mauguier, 1987). The anatomy suggests that this region is well positioned to support the interaction between memory retrieval and attention. Prior functional connectivity

and task activation studies suggest that posterior cingulate cortex consists of several functionally distinct subregions (Beckmann *et al.*, 2009; Leech *et al.*, 2011; Vogt, *et al.*, 2006). Prior task-based fMRI studies have reported CaS-p/mid-cingulate activation during retrieval of visual LTM (Huijbers *et al.*, 2011) and retrieval of visual working memory (Schon *et al.*, 2009). Reduced CaS-p/mid-cingulate activation has been observed in clinical populations during cognitive control tasks such as task-switching and N-back working memory tasks (Gundersen *et al.*, 2008; Tamm *et al.*, 2004). Generally, CaS-p/mid-cingulate has been understudied and underemphasized; future studies would be required to more fully explore the functional roles of CaS-p. These task-based findings demonstrate a strong role for this region in long-term memory guidance of attention.

A bilateral region in lateral IPS / AnG was significant in the whole-cortex cluster analysis, did not emerge as significant in the planned Yeo 7-Network ROI analysis, and was highly significant in the *post hoc* analysis suggested by a reviewer. I interpret these results to indicate that there is a region of lateral IPS contributes to LTM-guided visual attention, but that this region was not well captured by the Yeo 7-Network parcellation. Here, the latIPS/AnG activation peak is located near regions previously identified in neuroimaging studies examining the role of parietal cortex in episodic memory retrieval (Wagner *et al.*, 2005; Vilberg and Rugg, 2008; Ciaramelli *et al.*, 2008; Hutchinson *et al.*, 2009, 2014; Sestieri *et al.*, 2010). The MNI coordinates for the left latIPS/AnG in the

LTM-guided > STIM-guided contrast (-48.6, -58.9, 38.2) lies within 3.5 mm of the average of the locations identified in two meta-analyses of left parietal lobe involvement in episodic memory retrieval for recollection (Vilberg and Rugg, 2008: -43, -66, 38) and bottom-up attentional capture by retrieved memory contents (Ciaramelli *et al.*, 2008: -50, -57, 38). A peak shift effect (between LTM-guided vs. STIM-guided and LTM-guided vs. passive) that I observed here may help to explain anatomical variability in the location of episodic memory retrieval-based activation in lateral parietal cortex reported across prior studies (see also Hutchinson *et al.*, 2014); the degree of DMN deactivation in the control condition determines the size of the shift. The latIPS region appears to roughly correspond to a lateral IPS region sensitive to source memory that may act as a mnemonic accumulator and in the service of memory-guided action selection (Hutchinson *et al.*, 2014). Other studies have also suggested that a region in this vicinity may act in post retrieval processes (Sestieri *et al.*, 2011; Nelson *et al.*, 2010). In the present study, the latIPS may be holding spatial information that has already been retrieved and/or accumulating information about whether a stimulus matches what is stored in memory at that location and thus be acting as a memory-guided action selector. Another recent study has implicated this region in violations of an expected memory response (i.e. unexpected familiarity or unexpected novelty), suggesting this region may reflect general orienting mechanisms during memory retrieval (Jaeger *et al.*, 2013).

Memory consists of multiple systems, and it follows that memory-guided attention is likely not a single entity (see also Jiang *et al.*, 2013). Here, I have focused on the mechanisms by which explicit memory guides visuospatial attention. Retrieval of explicit memories to guide attention may be critical to CCN recruitment, and CCN recruitment may not occur in implicit memory-guided attention paradigms such as contextual cueing (Chun and Jiang, 1998; Chun, 2000). The spatial nature of the attentional task may have biased CCN activation toward the posterior nodes, as spatial processing is often associated with posterior cortex (e.g. Posner *et al.*, 1984; Postle *et al.*, 2000); alternately, this may reflect episodic memory influences on reactive cognitive control mechanisms (Braver, 2012). In the present study, functional connectivity results and task activations demonstrate functional heterogeneity within the CCN (see also Cole and Schneider, 2007), and point to memory-guided attention as one key function of some CCN nodes.

Traditionally, attention and long-term memory have been distinct fields of study, examined by different sets of researchers focused on different brain structures. Recent work examining the role of parietal cortex in episodic memory retrieval (Vilberg and Rugg, 2008; Ciaramelli *et al.*, 2008, 2010; Wagner *et al.*, 2005; Nelson *et al.*, 2010; Hutchinson *et al.*, 2009, 2014; Sestieri *et al.*, 2010, 2011) and work investigating long-term memory influences on attention (Chun and Jiang, 1998, 2003; Henderson and Hollingworth, 1999; Moores, *et al.*, 2003; Hollingworth, 2004, 2005; Summerfield *et al.*, 2006, 2011; Chun and Turk-

Browne, 2007; Olivers, 2011; Stokes *et al.*, 2012) have started to break through this divide. The present study makes a significant contribution to the field by highlighting the role that this posterior subnetwork within the greater Cognitive Control Network plays in aiding cooperative interactions between memory and attention.

## 3.5 Chapter 3 Figures

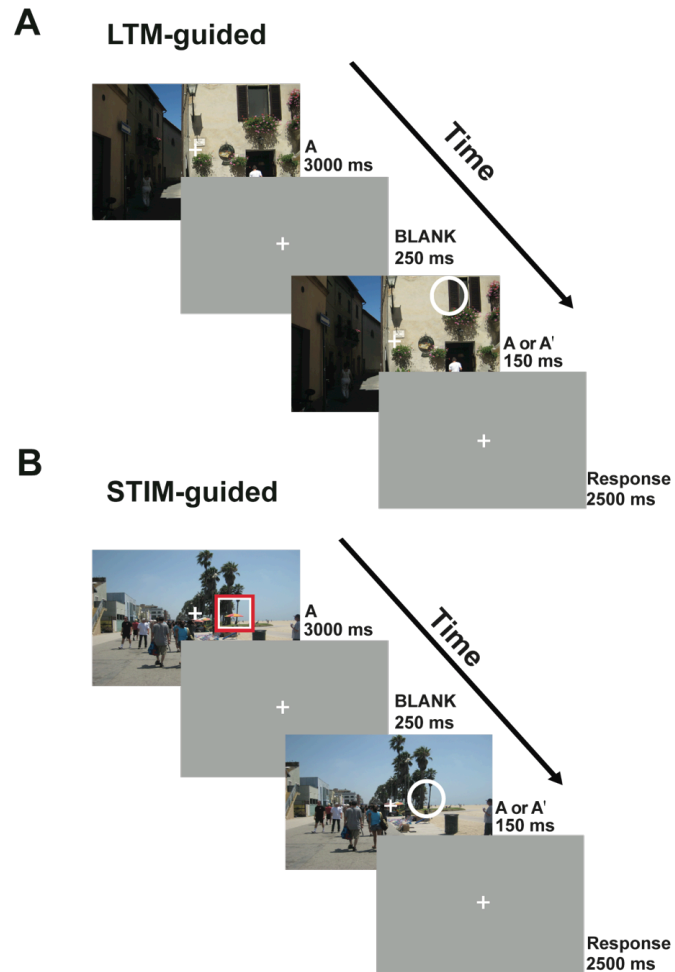


**Figure 3.1.** One-shot Change Detection Paradigms. A scene (S) was presented for 3000 ms, followed by a blank screen (250 ms), a very brief presentation (150 ms) of either an identical or altered image (S or S'), and another blank screen (2500 ms). Participants held central fixation while trying to detect whether or not a single change occurred in the scene. A) LTM-guided condition: Participants viewed scenes for which they had previously learned the location of changes.

Participants were instructed to covertly direct attention to the remembered location of the potential change; no explicit spatial cue was provided. B) STIM-guided condition: Participants viewed scenes that they had previously studied without exposure to scene changes. A red and white square explicitly cued the location of the potential scene change, and then disappeared prior to the image change. Note that the white circle was used in this figure for illustration purposes to highlight the scene change, but no such stimulus appeared on the images.

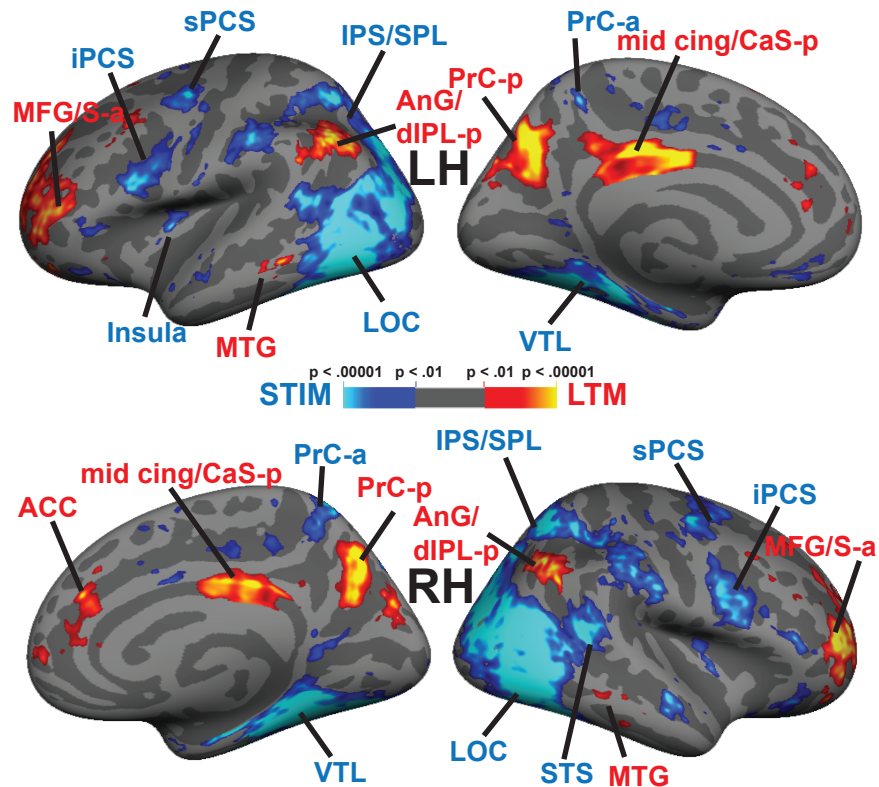


**Figure 3.2** Long-Term Memory-Guided Attention vs. Stimulus-Guided Attention:

A whole-cortex surface-based GLM analysis averaged over all participants (n=23) shows areas that respond differentially to LTM-guided vs. stimulus-guided attention. Hot colors represent LTM-guided > STIM-guided and cool colors represent STIM-guided > LTM-guided. See Table 3.1 for details.

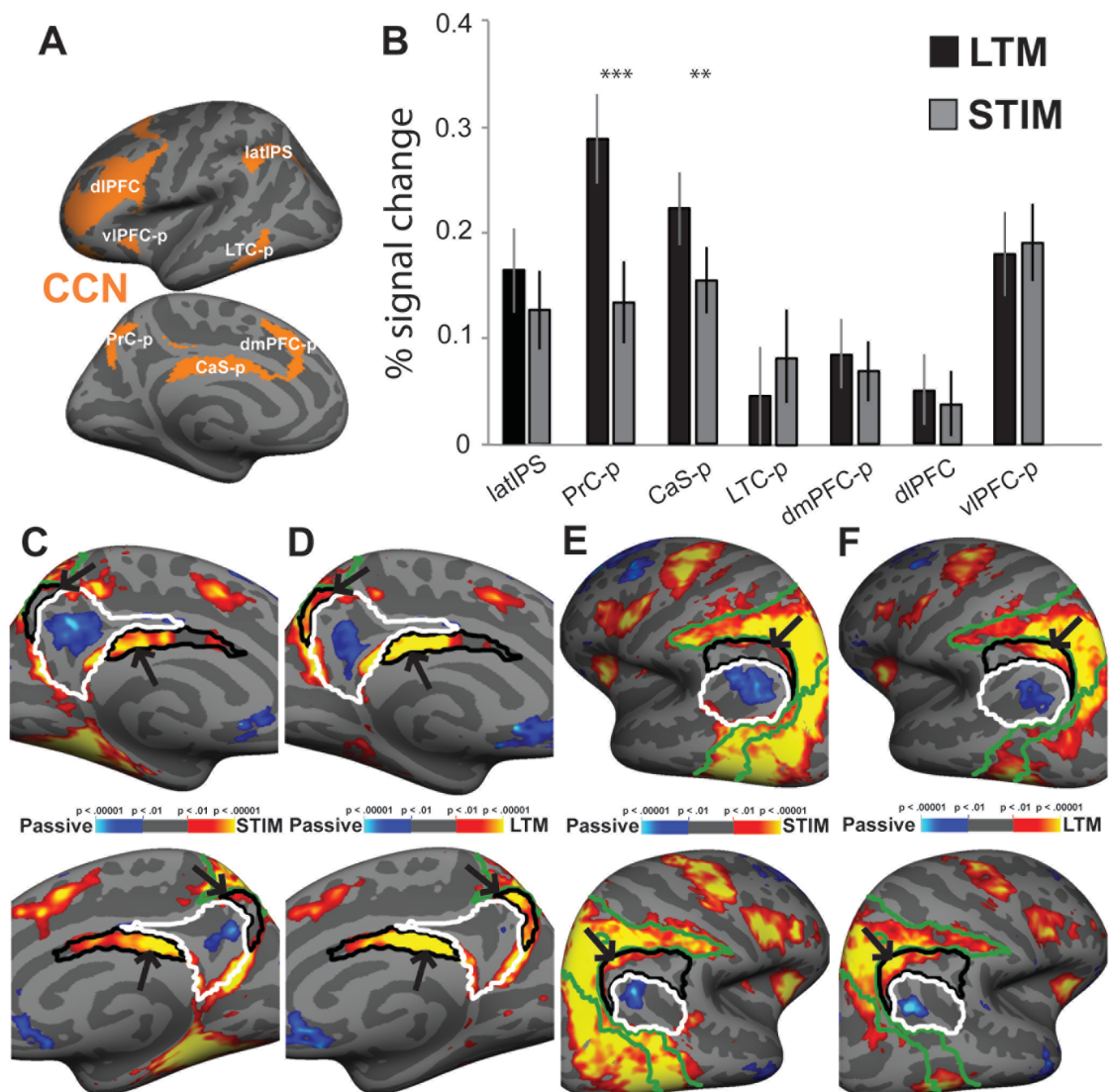


**Figure 3.3** ROI analysis for the *cognitive control network*: A) ROIs were obtained from an intrinsic functional connectivity analysis of 1000 brains (Yeo, Krienen *et al.*, 2011) and were projected onto the cortical surface of each individual participant. B) A region of interest (ROI) analysis was performed on each ROI within the CCN for LTM-guided and STIM-guided conditions. The bar graph presents percent signal change between each condition compared to passive viewing. Error bars reflect SEM. C and E show zoomed in images of the medial

and lateral left (top) and right (bottom) cortical surfaces during the STIM-guided condition (vs. passive viewing). D and F show the same views for the LTM-guided (vs. passive viewing). CCN ROIs are outlined in black, DMN ROIs are outlined in white and DAN ROIs are outlined in green. Black arrows indicate differences between the STIM-guided condition activation and the LTM-guided condition activation. \* indicates  $p < 0.05$ , \*\* indicates  $p < 0.01$ , and \*\*\* indicates  $p < 0.0001$ , Holm-Bonferroni corrected.

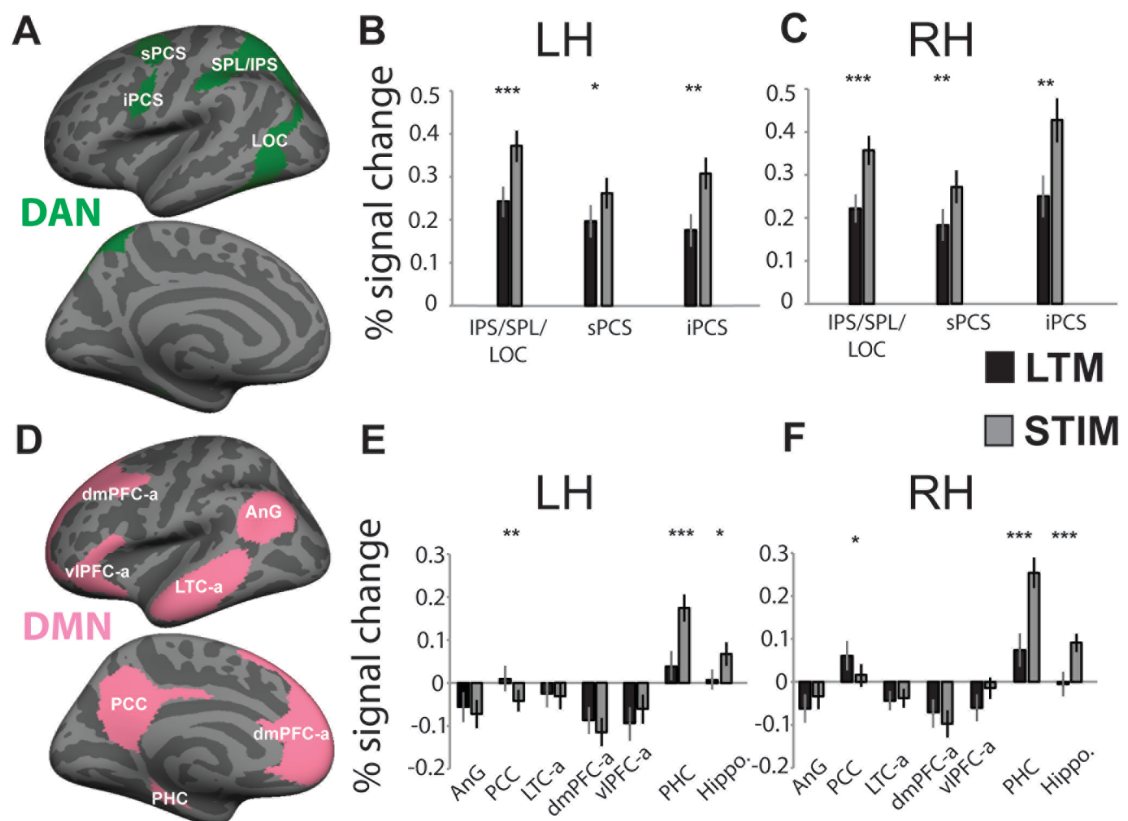


**Figure 3.4:** ROI analyses for the *dorsal attention* and *default mode networks* (DAN and DMN): A and B) ROIs were obtained from an intrinsic functional connectivity analysis of 1000 brains (Yeo, Krienen *et al.*, 2011) and were projected onto the cortical surface of each individual participant. ROIs from the DAN and DMN are presented. C, D, E, F) Bar graphs illustrate percent signal change in the LTM-guided and STIM-guided conditions compared to passive viewing for each ROI within the DAN and DMN. \* Indicates  $p < 0.05$ , \*\* indicates

$p < 0.01$ , and \*\*\* indicates  $p < 0.0001$ , Holm-Bonferroni corrected. Error bars reflect SEM.

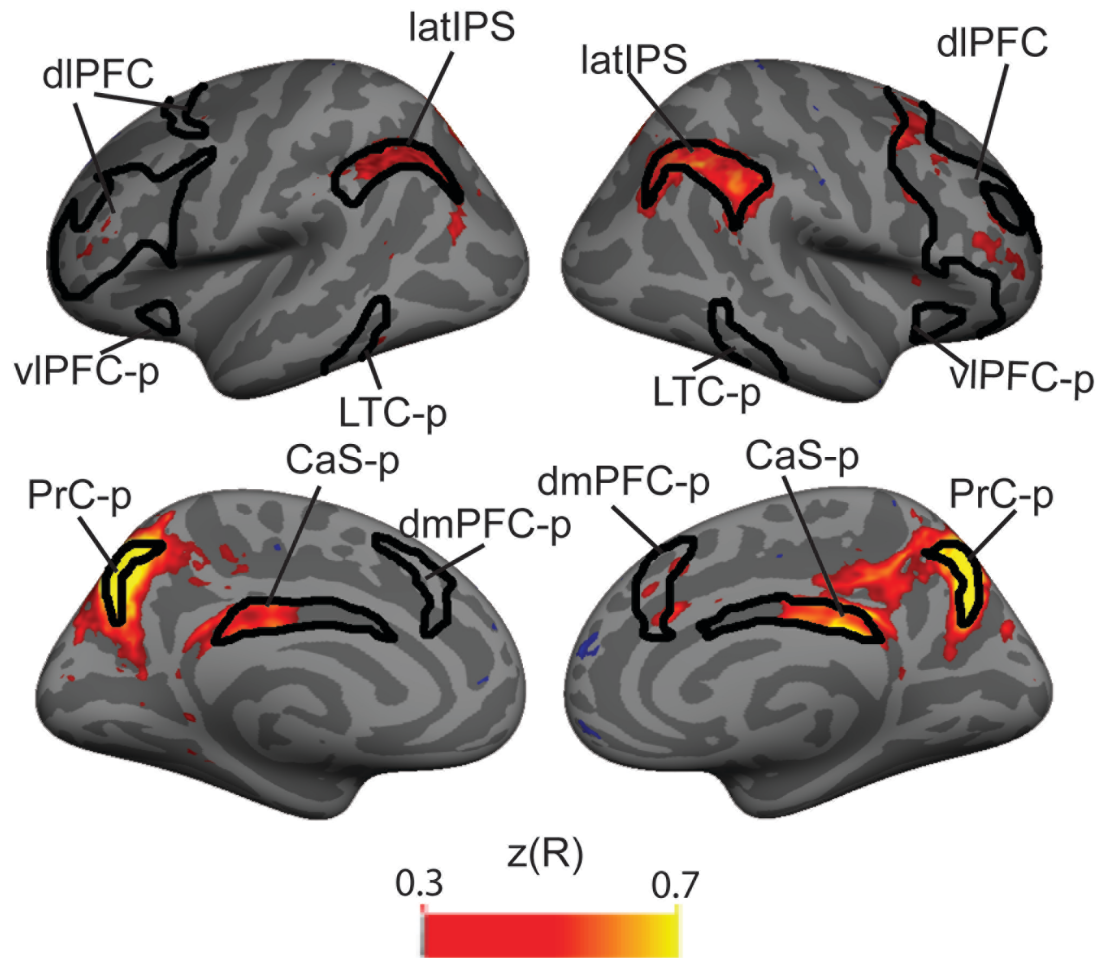


**Figure 3.5:** Posterior Precuneus Seed-Based Intrinsic Connectivity Analysis: Black lines outline the Cognitive Control Network. Time courses from each vertex in the brain were correlated with the time course of the PrC-p. Hot colored regions reflect vertices whose timecourses were positively correlated with the PrC-p (Fisher's z transformed R value).

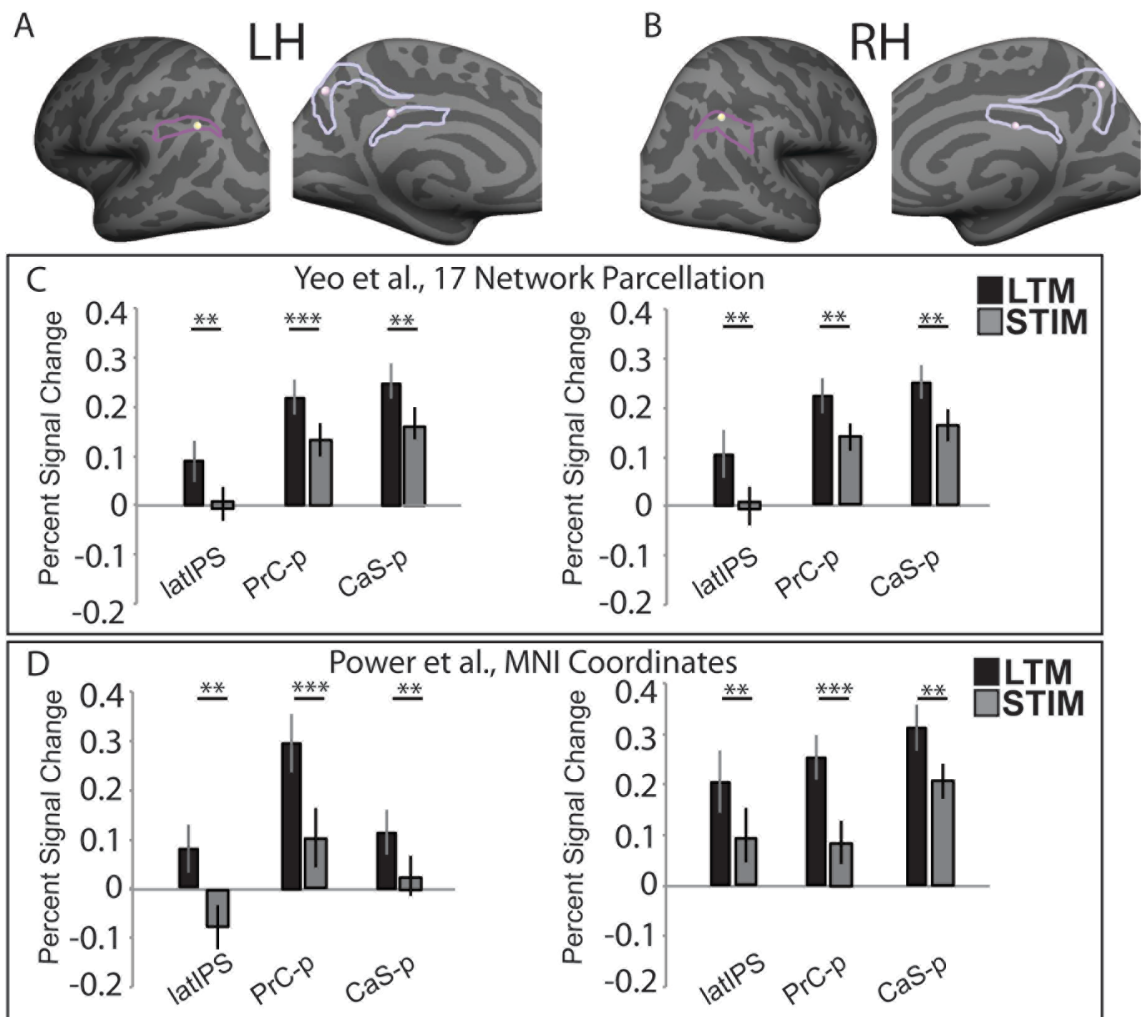


**Figure 3.6:** Post-hoc analysis using alternative ROI definitions. A and B show left and right hemispheres with ROI definitions. Outlines are from Yeo et al., 2011 17 network parcellation, spheres are MNI coordinates diluted 8mm from Power et al., (2011). C and D show percent signal change for LTM-guided and STIM-guided compared to passive viewing for each from Yeo et al and Power et al., definitions, respectively. \*\* indicates  $p < 0.01$ , and \*\*\* indicates  $p < 0.0001$ , Holm-Bonferroni corrected. Error bars reflect SEM.

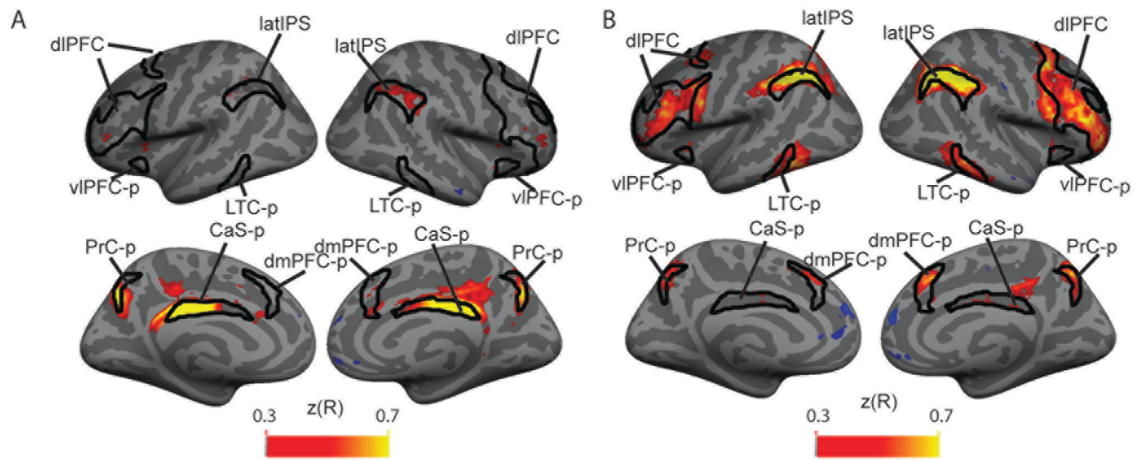


**Figure 3.7:** Posterior Callosal Sulcus and Lateral Intraparietal Sulcus Seed-Based Connectivity Analysis. Black lines outline the Cognitive Control Network. Time courses from each vertex in the brain were correlated with the time course of the PrC-p. Hot colored regions reflect vertices whose time courses were positively correlated with CaS-p in A and latIPS in B. (Fishers z-transformed R values).

### 3.6 Chapter 3 Tables

**Table 3.1:** Significant areas of activation in the contrast of LTM-Guided vs STIM-Guided conditions

#### LTM-Guided > STIM-Guided Attention

| <u>Anatomical Region</u>     | <u>Hemisphere</u> | <u>x</u> | <u>y</u> | <u>z</u> | <u>Size(mm<sup>2</sup>)</u> | <u>t-value</u> |
|------------------------------|-------------------|----------|----------|----------|-----------------------------|----------------|
| Posterior                    | L                 | -5.8     | -64.5    | 30.7     | 1107.61                     | 7.755          |
| Precuneus                    | R                 | 12.7     | -64.2    | 38.6     | 774.24                      | 7.15           |
| Mid Cingulate/               | L                 | -4       | -22.3    | 31       | 794.16                      | 7.518          |
| Callosal Sulcus              | R                 | 5.3      | -25.7    | 29.5     | 481.18                      | 6.939          |
| Anterior Dorsal Lateral      | L                 | -22.3    | 43.9     | 27.7     | 2060.02                     | 5.975          |
| Prefrontal Cortex            | L                 | -39.7    | 19.8     | 39.7     | 173.09                      | 3.829          |
|                              | R                 | 33.7     | 48.1     | 5        | 1490.59                     | 6.688          |
| Angular Gyrus/               | L                 | -48.6    | -58.9    | 38.2     | 1195.22                     | 5.751          |
| Lateral Intraparietal Sulcus | R                 | 45.5     | -56.9    | 43.2     | 751.61                      | 5.757          |
| Anterior Cingulate Cortex    | R                 | 12.7     | 36.4     | 21.8     | 253.91                      | 5.114          |
| Cuneus                       | R                 | 7.2      | -74.8    | 30       | 330.09                      | 4.807          |

#### STIM-Guided > LTM-Guided Attention

| <u>Anatomical Region</u> | <u>Hemisphere</u> | <u>x</u> | <u>y</u> | <u>z</u> | <u>Size(mm<sup>2</sup>)</u> | <u>t-value</u> |
|--------------------------|-------------------|----------|----------|----------|-----------------------------|----------------|
| Ventral Temporal         | L                 | -46.2    | -60.8    | -2       | 10937.29                    | 8.905          |
| Cortex/Lateral           | L                 | -22.6    | -15.3    | -22.4    | 142.09                      | 4.999          |

|   |   |       |       |       |          |        |
|---|---|-------|-------|-------|----------|--------|
| Occipital Complex/                                | L | -52.7 | -27.2 | 32.7  | 634.03   | 5.23   |
| Intraparietal Sulcus/<br>Supramarginal Gyrus      | R | 28.9  | -67.8 | -5.6  | 14690.27 | 11.246 |
| Superior Precentral<br>Sulcus                     | L | -35.8 | -5.8  | 43.3  | 525.42   | 7.007  |
|   | R | 31.6  | -7.5  | 46.2  | 916.79   | 5.989  |
| Inferior Precentral<br>Sulcus                     | L | -39.9 | 11.7  | 20.3  | 737.76   | 5.371  |
|   | R | 45    | 5.2   | 26.3  | 1035.83  | 5.326  |
| Anterior Superior Temporal<br>Sulcus              | R | 48    | -13.6 | -10.6 | 249.47   | 5.18   |
| Insula  | L | 36.5  | -4.2  | 7.3   | 140.28   | 5.149  |
|   | R | 37.8  | -1.6  | 1.5   | 152.49   | 4.283  |
| Anterior Inferior Frontal<br>Sulcus/ Gyrus        | L | -40.9 | 27.6  | 2     | 153.97   | 3.425  |
|   | R | 45.6  | 31.2  | 5.7   | 164.18   | 4.661  |
| Lateral Orbitofrontal<br>Cortex                   | R | 33.3  | 30.5  | -10.8 | 311.81   | 4.589  |
| Anterior Precuneus/<br>Posterior Cingulate Sulcus | L | -15.3 | -15.8 | 38.3  | 153.55   | 3.702  |
| Parietal Occipital Sulcus/<br>Calcarine Sulcus    | R | 21.8  | -50.6 | 7.8   | 175.41   | 3.599  |

**Table 3.2:** Percent signal change in Regions of Interest of the Cognitive Control, Dorsal Attention and Default Mode Networks, defined from the Yeo 7-Network Parcellation

**Cognitive Control Network**

| <u>Region of interest</u> | <u>Hemisphere</u> | <u>LTM-guided</u> | <u>STIM-guided</u> | <u>t-value</u> | <u>p-value</u> |
|---------------------------|-------------------|-------------------|--------------------|----------------|----------------|
| PrC-p                     | L                 | 0.28±0.05         | 0.13±0.05          | 5.04           | 0.0012         |
| PrC-p                     | R                 | 0.30±0.04         | 0.13±0.04          | 6.84           | <0.0001        |
| CaS-p                     | L                 | 0.20±0.04         | 0.14±0.03          | 5.98           | 0.0001         |
| CaS-p                     | R                 | 0.24±0.03         | 0.17±0.03          | 4.46           | 0.0043         |
| latIPS                    | L                 | 0.16±0.04         | 0.12±0.04          | 1.62           | 1.00           |
| latIPS                    | R                 | 0.17±0.05         | 0.13±0.04          | 1.79           | 1.00           |
| LTC-p                     | L                 | 0.02±0.06         | 0.08±0.06          | 2.06           | 0.725          |
| LTC-p                     | R                 | 0.08±0.04         | 0.09±0.04          | 0.55           | 1.00           |
| dmPFC-p                   | L                 | 0.06±0.03         | 0.05±0.03          | 0.57           | 1.00           |
| dmPFC-p                   | R                 | 0.11±0.03         | 0.08±0.03          | 1.39           | 1.00           |
| dIPFC                     | L                 | 0.04±0.03         | 0.02±0.03          | 0.838          | 1.00           |
| dIPFC                     | R                 | 0.07±0.03         | 0.05±0.03          | 0.814          | 1.00           |
| viPFC-p                   | L                 | 0.17±0.04         | 0.18±0.04          | 0.218          | 1.00           |
| viPFC-p                   | R                 | 0.19±0.05         | 0.20±0.04          | 0.777          | 1.00           |

**Dorsal Attention Network**

| <u>Region of interest</u> | <u>Hemisphere</u> | <u>LTM-guided</u> | <u>STIM-guided</u> | <u>t-value</u> | <u>p-value</u> |
|---------------------------|-------------------|-------------------|--------------------|----------------|----------------|
| IPS/SPL                   | L                 | 0.24±0.04         | 0.37±0.04          | 6.54           | <0.0001        |

|         |   |           |           |      |         |
|---------|---|-----------|-----------|------|---------|
| IPS/SPL | R | 0.22±0.04 | 0.36±0.04 | 6.81 | <0.0001 |
| iPCS    | L | 0.18±0.04 | 0.31±0.04 | 4.51 | 0.0029  |
| iPCS    | R | 0.25±0.05 | 0.43±0.05 | 6.12 | <0.0001 |
| sPCS    | L | 0.20±0.04 | 0.26±0.04 | 3.83 | 0.0144  |
| sPCS    | R | 0.18±0.04 | 0.27±0.04 | 4.77 | 0.0016  |

### Default Mode Network

| <u>Region of interest</u> | <u>Hemisphere</u> | <u>LTM-guided</u> | <u>STIM-guided</u> | <u>t-value</u> | <u>p-value</u> |
|---------------------------|-------------------|-------------------|--------------------|----------------|----------------|
| PHC                       | L                 | 0.04±0.03         | 0.17±0.04          | 6.92           | <0.0001        |
| PHC                       | R                 | 0.07±0.04         | 0.25±0.04          | 7.34           | <0.0001        |
| Hippo.                    | L                 | 0.007±0.02        | 0.067±0.03         | 3.53           | 0.0265         |
| Hippo.                    | R                 | -0.004±0.03       | 0.091±0.02         | 6.35           | <0.0001        |
| PCC                       | L                 | 0.01±0.03         | -0.04±0.03         | 4.80           | 0.0021         |
| PCC                       | R                 | 0.06±0.03         | 0.02±0.03          | 3.61           | 0.0308         |
| dmPFC-a                   | L                 | -0.09±0.03        | -0.11±0.03         | 2.41           | 0.2729         |
| dmPFC-a                   | R                 | -0.07±0.03        | -0.09±0.03         | 2.11           | 0.4647         |
| vlPFC-a                   | L                 | -0.10±0.04        | -0.06±0.03         | 2.62           | 0.1863         |
| vlPFC-a                   | R                 | -0.06±0.03        | -0.01±0.03         | 2.81           | 0.1329         |
| AnG                       | L                 | -0.06±0.04        | -0.07±0.04         | 1.06           | 0.6712         |
| AnG                       | R                 | -0.06±0.03        | -0.03±0.03         | 1.92           | 0.6096         |
| LTC-a                     | L                 | -0.02±0.03        | -0.02±0.03         | 0.68           | 1.0            |
| LTC-a                     | R                 | -0.04±0.02        | -0.03±0.03         | 0.58           | 1.0            |

**Table 3.3: Post-hoc Alternative Network ROI Analysis**

Percent signal change in Regions of Interest of the defined by Yeo et al., 17

Network Parcellation and Power et al., 2011 MNI coordinates

| ROI                                   | x, y, z     | Hemisphere | LTM-Guided | STIM-Guided | <i>t-value</i> | <i>p-value</i> |
|---------------------------------------|-------------|------------|------------|-------------|----------------|----------------|
| <b>Yeo et al., (2011, 17 network)</b> |             |            |            |             |                |                |
| PrC-p                                 |             | L          | 0.22±0.04  | 0.13±0.03   | 4.21           | 0.001          |
| PrC-p                                 |             | R          | 0.23±0.04  | 0.14±0.03   | 4.48           | 0.0009         |
| CaS-p                                 |             | L          | 0.25±0.04  | 0.17±0.03   | 6.04           | <0.0001        |
| CaS-p                                 |             | R          | 0.25±0.02  | 0.17±0.03   | 5.49           | 0.0001         |
| latIPS                                |             | L          | 0.09±0.04  | -0.003±0.04 | 4.16           | 0.0014         |
| latIPS                                |             | R          | 0.11±0.05  | 0.005±0.04  | 4.80           | 0.0005         |
| <b>Power et al., (2011)</b>           |             |            |            |             |                |                |
| PrC-p                                 | -7, -71, 42 | L          | 0.30±0.06  | 0.10±0.06   | 5.86           | <0.0001        |
| PrC-p                                 | 11, -66, 42 | R          | 0.25±0.04  | 0.08±0.04   | 6.45           | <0.0001        |
| CaS-p                                 | -2, -35, 31 | L          | 0.11±0.05  | 0.02±0.03   | 5.28           | 0.0002         |
| CaS-p                                 | 2, -24, 30  | R          | 0.10±0.02  | 0.07±0.01   | 4.19           | 0.0014         |
| <b>Nelson et al., (2010)</b>          |             |            |            |             |                |                |
| latIPS                                | 40, -62, 8  | L          | 0.07±0.05  | -0.07±0.05  | 4.78           | 0.0005         |
| latIPS                                | 44, -56, 41 | R          | 0.20±0.06  | 0.10±0.05   | 3.11           | 0.0051         |

**Table 3.4:** Within Hemisphere Intrinsic Connectivity

Intrinsic connectivity using PrC-p (left: -9.5 -67.3, 42.8; right: 10.1, -65.9, 41.2), CaS-p (left: -6.0, -23.1, 29.3; right: 6.6, -17.9, 29.8), and latIPS (left: -36.5, -56.2, 38.2; right: 37.5, -57.3, 40.5) as seed regions within the hemisphere

**Left PrC-p Seed**

| <u>Anatomical Region</u> | <u>x</u> | <u>y</u> | <u>z</u> | <u>Size(mm<sup>2</sup>)</u> | <u>t-value</u> |
|--------------------------|----------|----------|----------|-----------------------------|----------------|
| PrC-p (CCN)              | -9.0     | -69.8    | 46.3     | 4326.51                     | 8.630          |
| CaS-p (CCN)              | -8.4     | -36.8    | 25.3     | 645.53                      | 5.285          |
| dIPFC (CCN)              | -40.8    | 28.5     | 21.9     | 879.40                      | 4.490          |
| latIPS (CCN)             | -39.9    | -60.1    | 41.7     | 1956.53                     | 4.485          |
| LTC-p (CCN)              | -53.6    | -55.0    | -16.9    | 196.23                      | 4.121          |
| Occipital Pole (Visual)  | -11.4    | -96.6    | -10.8    | 433.47                      | 3.436          |
| IPS (DAN)                | -41.6    | -76.8    | 15.6     | 286.14                      | 3.324          |

**Right PrC-p Seed**

| <u>Anatomical Region</u> | <u>x</u> | <u>y</u> | <u>z</u> | <u>Size(mm<sup>2</sup>)</u> | <u>t-value</u> |
|--------------------------|----------|----------|----------|-----------------------------|----------------|
| PrC-p(CCN)               | 8.7      | -67.3    | 40.5     | 3522.27                     | 8.830          |
| CaS-p(CCN)               | 6.5      | -30.6    | 29.0     | 781.59                      | 6.690          |
| latIPS (CCN)             | 42.1     | -70.2    | 35.4     | 3655.26                     | 5.445          |
| dmPFC-p (CCN)            | 13.6     | 23.9     | 28.5     | 204.94                      | 4.712          |
| dIPFC (CCN)              | 45.7     | 29.8     | 22.9     | 1724.41                     | 4.680          |
|                          | 39.3     | 51.3     | 8.0      | 264.14                      | 3.229          |
| dmPFC-p (CCN)            | 7.6      | 19.3     | 46.8     | 204.72                      | 3.878          |
| insula (VAN)             | 30.5     | 19.4     | 9.0      | 201.66                      | 3.430          |

**Left CaS-p Seed**

| <u>Anatomical Region</u> | <u>x</u> | <u>y</u> | <u>z</u> | <u>Size(mm<sup>2</sup>)</u> | <u>t-value</u> |
|--------------------------|----------|----------|----------|-----------------------------|----------------|
| CaS-p (CCN/DMN)          | -5.2     | -34.7    | 29.1     | 1421.10                     | 11.708         |
|                          | -8.3     | 22.8     | 27.1     | 515.48                      | 4.786          |
| PrC-p (CCN)              | -15.3    | -70.8    | 36.4     | 1184.83                     | 6.660          |
| latIPS/TPJ (DAN/VAN)     | -53.8    | -42.6    | 45.5     | 242.23                      | 4.934          |
| insula (VAN)             | -34.6    | 14.5     | -3.5     | 469.08                      | 5.292          |
|                          | -35.8    | 39.4     | 10.5     | 164.47                      | 2.653          |

### Right CaS-p Seed

| <u>Anatomical Region</u> | <u>x</u> | <u>y</u> | <u>z</u> | <u>Size(mm<sup>2</sup>)</u> | <u>t-value</u> |
|--------------------------|----------|----------|----------|-----------------------------|----------------|
| CaS-p (CCN)              | 5.8      | -28.7    | 30.5     | 2217.54                     | 10.446         |
| PrC-p (CCN)              | 14.2     | -69.1    | 38.9     | 955.38                      | 5.631          |
| latIPS (CCN)             | 52.6     | -45.3    | 37.8     | 1123.63                     | 5.051          |
|                          | 35.5     | -69.7    | 42.7     | 211.65                      | 4.152          |
| vIPFC-p (CCN/VAN)        | 31.6     | 15.0     | -8.3     | 511.28                      | 3.129          |

### Left latIPS Seed

| <u>Anatomical Region</u> | <u>x</u> | <u>y</u> | <u>z</u> | <u>Size(mm<sup>2</sup>)</u> | <u>t-value</u> |
|--------------------------|----------|----------|----------|-----------------------------|----------------|
| latIPS(CCN/DAN)          | -40.7    | -45.9    | 36.6     | 3582.97                     | 9.621          |
| PrC-p (CCN)              | -5.9     | -65.2    | 43.5     | 831.41                      | 4.550          |
| dIPFC/iPCS (CCN/DAN)     | -42.9    | 1.8      | 24.9     | 4672.24                     | 7.305          |
| LTC-p/LOC (CCN/DAN)      | -47.6    | -56.9    | -8.7     | 1790.88                     | 5.019          |
| dmPFC-p (CCN)            | -6.7     | 26.3     | 41.4     | 351.82                      | 5.008          |
| Occipital pole (Visual)  | -19.3    | -100.9   | -4.7     | 226.64                      | 3.134          |
| LOC (Visual)             | -36.2    | -88.0    | -11.1    | 318.03                      | 2.619          |

**Right latIPS Seed**

| <u>Anatomical Region</u> | <u>x</u> | <u>y</u> | <u>z</u> | <u>Size(mm<sup>2</sup>)</u> | <u>t-value</u> |
|--------------------------|----------|----------|----------|-----------------------------|----------------|
| latIPS (CCN)             | 34.4     | -58.1    | 44.2     | 3446.39                     | 9.659          |
| PrC-p (CCN)              | 6.6      | -61.5    | 41.1     | 1099.37                     | 5.533          |
| dIPFC(CCN)               | 28.3     | 6.8      | 48.6     | 6695.62                     | 7.054          |
| dmPFC-p (CCN)            | 8.5      | 29.4     | 40.9     | 395.19                      | 6.707          |
| CaS-P (CCN)              | 5.8      | -38.9    | 24.0     | 1002.28                     | 5.708          |
| insula (VAN)             | 32.7     | 18.9     | 2.1      | 205.87                      | 5.263          |
| LTC-p (CCN)              | 62.4     | -38.5    | -13.5    | 1471.81                     | 5.093          |

**CHAPTER 4: Posterior Parietal Network is Recruited Specifically for  
Long-Term Memory-Guided Attention**

## 4.1 Introduction

Human attentional and short-term memory capacity is extremely limited while real-world human visual performance is remarkably excellent, especially in familiar environments. This apparent discrepancy between superior visual performance and limited attentional capacity can be reconciled by taking into account the role of long-term memory, which can guide attention to the most relevant information in an environment (Chun, 2000; Summerfield *et al.*, 2006; Hutchinson and Turk-Browne, 2012; Rosen *et al.*, 2015). A rich literature has highlighted the behavioral advantage of memory in guiding attention (Chun and Jiang, 1998; Jiang and Chun, 2003; Henderson and Hollingworth, 1999; Moores, *et al.*, 2003; Hollingworth, 2004, 2005; Olivers, 2011), however the neural mechanisms underlying this cooperation are understudied (Hutchinson and Turk-Browne, 2012).

Visual spatial attention engages the dorsal attention network (Corbetta and Shulman, 2002) while memory retrieval engages the default mode network (Buckner *et al.*, 2008). The question of how memory and attention cooperate is complicated by the fact that these networks have strongly competitive interactions (e.g., Sestieri *et al.*, 2010; Spreng *et al.*, 2012). One previous study from Summerfield and colleagues (2006) directly contrasted memory-guided and stimulus guided attention and found that the left hippocampus is recruited for memory-guided attention. Critically, this study found largely overlapping cortical regions engaged for both long-term memory-guided and stimulus-guided

attention. However, it is possible that volume-based group averaging techniques obscured cortical differences in these two attentional states.

In the experiment presented in Chapter 3, I used a change detection paradigm with natural scenes in which subjects learned the location of changes in the scene images and later used this memory to guide their attention. I compared subjects' ability to detect scene changes using LTM to guide visuospatial attention to their ability to detect changes when an explicit visuospatial cue guided their attention (Rosen et al., 2015). In that study, I hypothesized that a third network, the cognitive control network (CCN), would be recruited when long-term memory guides attention. I directly contrasted long-term memory-guided attention with visual stimulus-guided attention (Rosen *et al.*, 2015) and analyzed the cortical data using regions of interest defined on individual subjects. I found that three posterior nodes of the cognitive control network were more strongly recruited for long-term memory-guided attention than stimulus guided attention, including the posterior precuneus (PrC-p), the posterior callosal sulcus (CaS-p), and the lateral intraparietal sulcus (latIPS). This was the first study to show distinct recruitment of cortical regions within the cognitive control network for long-term memory guided spatial attention. I suggested that posterior CCN nodes support processing that integrate memory- and stimulus-based representations and that a memory retrieval sub-network exists that is preferentially recruited for long-term memory-guided attention (Rosen et al., 2015). However, in the previous study, long-term memory retrieval

and long-term memory-guided attention were not distinguished from one another. Therefore, the open question remains whether the posterior cognitive control network is recruited for long-term memory retrieval in general or long-term memory-guided attention specifically. The present study was designed to directly test this question.

One of the three regions that I identified in the study presented in Chapter 3, the latIPS, lies in the vicinity of previously reported activation in several fMRI studies of long-term memory retrieval (Kahn et al., 2004; Wagner et al., 2005; Cabeza et al., 2008; Vilberg and Rugg 2007, 2008, 2009; Nelson et al., 2010; Hutchinson et al., 2009; 2014; Sestieri et al., 2010, 2011). The precise role of the parietal cortex in memory retrieval is hotly debated. A dissociation exists such that dorsal parietal cortex is recruited more for familiarity type judgments while ventral parietal cortex is recruited for recollection type judgments (Cabeza et al., 2008; Vilberg and Rugg, 2008; Hutchinson et al., 2009). Some hypotheses argue that this activity indicates a true episodic contribution of the parietal lobe to long-term memory retrieval. One hypothesis suggests that inferior parietal cortex is a site of Baddeley's proposed episodic buffer, such that it holds retrieved information in working memory until a decision can be made about that information (Vilberg and Rugg, 2007, 2008, 2009). Conversely, other hypotheses rely on known functional roles of the parietal lobes, such as attentional processes. The dual attention to memory hypothesis posits that the dissociation between retrieval of vivid and weak memories in the parietal cortex reflects an

established dissociation between bottom-up and top-down attention respectively (Cabeza *et al.*, 2008; Cabeza, 2008; Ciaramelli *et al.*, 2010). The latIPS region seen recruited in the previous study, lies in the vicinity of a region recruited during memory retrieval but thought to act as a mnemonic accumulator (Hutchinson *et al.*, 2014) or in post-retrieval action selection (Sestieri *et al.*, 2010; Nelson *et al.*, 2010).

However, the recruitment of the PrC-p and CaS-p has been less widely investigated. A recent study using resting state methods to parcellate the human cortex into networks noted that these three regions often cluster together (Power *et al.*, 2011), however, only the two medial areas, PrC-p and CaS-p, met their criteria for a network; similarly, Yeo *et al.* (2011), in a 17-network parcellation of cortex, reported a two node network consisting of regions that closely match PrC-p and CaS-p. Power and colleagues (2011) conducted a meta-analysis investigating all three regions and found that these regions are most often reported in memory-retrieval studies. Furthermore, a recent study from Nelson and colleagues (2013) found recruitment of these three regions when subjects restudied words compared to their original study. Collectively, these data are consistent with the notion that the latIPS, CaS-p and PrC-p form a subnetwork and this network is recruited for LTM-guided attention; however, important questions remain. A key question is whether activation in these regions reflects a generalized response to memory retrieval or whether activation exhibits specificity for LTM-guided attention.

In the current study, I designed a novel target detection task with a *long-term memory-guided attention condition*, along with two control conditions: an *attention control (stimulus-guided attention)* in which the visuospatial attentional demands were matched and a *memory control (LTM retrieval)* in which the memory retrieval demands were matched. The first goal of the current study was to replicate the findings presented in Chapter 3 that three regions of the posterior cognitive control network are recruited more strongly for LTM-guided attention than stimulus-guided attention by comparing LTM-guided attention to stimulus-guided attention. My second goal was to determine whether activation of the posterior cognitive control network is specific to LTM-guided attention or whether it is more general to memory retrieval by comparing the pattern of activation during the LTM retrieval condition to that of the LTM-guided attention condition. If these areas serve a general memory retrieval function, I would expect to see greater recruitment during memory retrieval compared to stimulus-guided attention condition. If however, these regions are specific to LTM-guided attention, I should not see stronger recruitment of these regions during the LTM retrieval compared to the stimulus-guided attention. I quantified these differences using a region of interest analyses in each of the three regions recruited for LTM-guided attention in Chapter 3 (PrC-p, CaS-p, and latIPS) and directly contrasted LTM-guided attention with the stimulus-guided attention and the LTM retrieval in order to further demonstrate that activation within these regions is strongest for LTM-guided attention.

## **4.2 Methods**

### *4.2.1 Participants:*

Twenty-five healthy human participants (13 male, 12 female) with normal or corrected-to-normal vision were recruited from Boston University and the greater Boston community. All participants were compensated and gave written informed consent to participate in the study, which was approved by the Institutional Review Board of Boston University. All participants were right handed, between the ages of 22 and 34, and participated in two sessions (training and test) across two days. One female participant was excluded from all analyses due to persistent sleepiness during the scan session and below chance performance, leaving twenty-four subjects included in the analyses.

### *4.2.2. Visual Stimuli and Experimental Paradigm:*

Experiments were conducted over two sessions on separate days, with the training session on Day 1 and the fMRI scanning session on Day 2. The main condition of interest was the LTM-guided attention condition. I designed two control conditions to determine brain activation that is unique to the cooperation between LTM-guided attention: a stimulus-guided attention and an LTM retrieval. The stimulus-guided attention was designed to be well matched with the LTM-guided attention condition in its attentional demands, but vary in its memory demands, while the LTM retrieval was designed to be well matched with the LTM-guided attention condition in its memorial demands but vary in its

visuospatial attention demands. A visual-motor control was also included as a baseline for the region of interest analyses.

Day 1: Three separate training paradigms were conducted for each subject for stimuli that were used in the three different experimental conditions, an LTM-guided spatial attention condition, an LTM retrieval, and a stimulus-guided attention. For each subject, eight groups of object categories were used for each experimental condition. Each group of categories contained four exemplars. Training was conducted separately for each condition and the order of study was counterbalanced across subjects. Within each condition, subjects studied all four exemplars of each of the eight stimuli categories in a random order. Each exemplar was studied four times.

LTM-guided attention training: Subjects were presented with Word A presented above and below fixation and with a red arrow pointing to one of eight peripheral locations and a picture of Object A at the cued location (e.g. the word “lamp” appeared with picture of a lamp). Then subjects were presented with only Word A followed by a blank screen and instructed to anticipate the expected location of the object before it appeared. Subjects studied 8 word-location pairings.

LTM retrieval training: Subjects studied a series of Word B - Object C pairings. Subjects viewed Word B above and below fixation (e.g. “hourglass”) with Object C presented (e.g. picture of a telephone) at fixation. This pairing was repeated four times with each of the four exemplars. Then subjects were presented with

only Word B followed by a blank screen and were instructed to anticipate the object before it appeared. Subjects studied 8 word-object pairings.

Stimulus-guided attention, visual-motor control and distractor images training:

Subjects studied each additional stimulus that would be presented during scanning in order to equate familiarity with the object stimuli across all conditions and reduce encoding of the stimuli during scanning. They studied images that would be used in the visuospatial attention condition (8 objects with 4 exemplars each, for a total of 32 objects), in the visual-motor control condition (9 additional exemplars taken from the distractor categories) and as distractors (24 objects with 4 exemplars each for a total of 96 objects). Each stimulus appeared on screen for 1 second (same duration as the LTM-guided attention and LTM retrieval training) and were asked to make a judgment about each object (e.g., “Will it fit in a shoebox?”) They saw each stimulus exemplar four times. This was done to ensure that subjects saw each stimulus across all conditions an equal number of times during the study phase.

Explicit Memory Test: At the end of Day 1, I tested that subjects had encoded all word-location and word-object pairings. Subjects were asked to perform an explicit memory test in which they used a mouse cursor to drag object images onto their associated location (LTM-guided attention) or word (LTM retrieval).

Day 2:

While undergoing fMRI scanning, subjects performed a task with four conditions with the same basic structure. In all conditions, a word was presented on the

screen for 1.85 seconds above and below a fixation cross. An arrow cue was located at the center of the screen. In three conditions, this arrow was uninformative and irrelevant (a double headed horizontal arrow), while in one condition (visual stimulus guided attention) the arrow pointed to the location to which subjects should attend (Figure 4.1). The word and arrow cues disappeared for 1 second. Then, nine objects (8 equally spaced in the periphery and 1 at fixation) flashed up on the screen for 150 ms, followed by a 2 second response window. In the stimulus-guided attention condition (Figure 4.1A), the cue word was not a word for which subjects studied an associated object or location. However subjects were presented with a red arrow at the center of the screen that pointed to one of the eight peripheral locations. They were instructed to use that cue to deploy their attention to that location. They were asked if the object that appears at that location was a match or a non-match to the word (i.e. if the word “telephone” appeared, subjects should try to detect a picture of a telephone at the cued location). In the LTM retrieval condition (Figure 4.1B), the word cue was a word studied with an associated object. Subjects were asked to retrieve the object associated with the word and then respond whether the object that appeared at the center of the screen was a match (50% of trials) or a non-match. In the LTM-guided attention condition (Figure 4.1C), the cue word was a word that was studied with an associated location. Subjects were instructed to retrieve the associated location and deploy their attention covertly to that location. They then responded whether the object that appeared at that location was a match or

a non-match to the word. On non-match trials, the target appeared at one of the other seven peripheral locations to ensure that subjects were not diffusely attending to the entire periphery, but rather were attending to only one location. In the visual-motor control or baseline condition, subjects saw the word “passive” above and below fixation. After a blank, nine objects appeared and subjects made a random button press. The same nine objects (taken from the distractor categories) appeared in different configurations for every visual-motor control trial.

#### *4.2.2. MR Data Acquisition:*

Functional scans were acquired using simultaneous multi slice EPI (3 slices at a time) [repetition time (TR) = 2.0 seconds, echo time (TE) = 30 ms; voxel size 2.0 mm isotropic] and were collected from 69 slices with no skip, with full brain coverage. Each participant participated in nine to twelve functional scans (each 191 TRs; 6 min 22 sec duration) in one scan session. Functional data were aligned with high-res T1-weighted images.

#### *4.2.4. MR Data Analysis:*

Functional data were aligned with high-resolution (1.0 x 1.0 x 1.3 mm) T1-weighted images. For 17 participants the high-resolution structural images were acquired at the same facility; for 7 participants they were acquired on an identical scanner and coil at the Martinos Center for Biomedical Imaging at Massachusetts General Hospital in Charlestown, Massachusetts. These high-resolution

structural images were used to create a computerized reconstruction of each cerebral cortical hemisphere.

Functional MRI data were preprocessed using FreeSurfer 5.3.0 (Charlestown, MA). First, slice time correction to account for the multi slice acquisition. Whole cortex and ROI analyses were performed using a general linear model (GLM) with regressors that match the time course of task conditions.

Single participant fMRI data were registered to an average cortical surface space (Freesurfer 'fsaverage' brain) using the boundary of the gray matter and white matter. Analyses were performed separately in each hemisphere on the average cortical surface and data were analyzed for each vertex using a general linear model (GLM) with each condition as a predictor (i.e. one for LTM-guided, stimulus-guided attention, LTM retrieval, visual-motor control). Three motion correction regressors were included in the model. The BOLD signal was modeled as a linear, time-invariant system with  $\gamma$  response function assumed for each condition with a delay  $\delta = 2.25$  and a delay time constant  $\tau = 1.25$ . An estimated response was generated by convolving the response function with the block length (i.e. the time in each condition) and minimizing the residual error (FS-FAST, Cortech). Random effects group analyses were performed using surface-based averaging techniques (Fischl *et al.*, 1999b). A *t*-test was performed for each vertex to compare differences in activation between conditions. The significance of these activation differences was projected onto the surface of the Freesurfer 'fsaverage' brain (Figure 4.2A and 4.2B).

To correct for multiple comparisons, I employed FS-FAST to perform Monte-Carlo simulations of a smoothed null hypothesis data set to establish cluster-wise thresholds for the population maps (Forman *et al.*, 1995). The Monte Carlo simulation generated random volumes of normally distributed values that were then smoothed by a 6 mm smoothing kernel. Clusters were defined as areas of contiguous vertices with significance values below a threshold of  $p < 0.01$ . Ten thousand iterations of this simulation established a cluster-size threshold of  $130 \text{ mm}^2$  for LTM-guided vs. stimulus-guided attention contrast. Results are presented in Table 4.1.

Regions of interest were defined from Yeo *et al.*, 2011 7 network parcellation definition of the cognitive control network (CCN). The study presented in Chapter 3 of this dissertation showed that three regions within the CCN, including lateral intraparietal sulcus (latIPS), posterior callosal sulcus (CaS-p) and posterior precuneus (PrC-p) were more strongly activated during LTM-guided attention than stimulus-guided attention (Rosen *et al.*, 2015). The present study was designed test the hypothesis that these three regions form a subnetwork that is specifically recruited for LTM-guided attention and do not serve a more general long-term memory retrieval function. Each region was mapped from a pre-defined label on the Freesurfer 'fsaverage' brain onto the appropriate cortical hemisphere of each participant to define each ROI. Percent signal change was extracted for each condition (LTM-Guided visuospatial attention, LTM retrieval, and stimulus-guided attention) compared to visual-motor

control and averaged across blocks and runs to construct time-course data for all vertices/voxels within each of the 6 ROIs (3 cortical ROIs) per hemisphere for each individual subject (Figure 4.2C). A separate 2-way (Condition x Hemisphere) analysis of variance (ANOVA) was then performed for each ROI (Table 4.2).

### 4.3 Results

Performance in all three task conditions was strong. An ANOVA revealed a main effect of Condition  $F(2,46) = 7.462$ ,  $p = 0.007$ ). Post-hoc t-tests revealed that there was no significant difference in performance between the LTM-guided attention (Mean =  $94.0\% \pm 0.01$ ) and stimulus-guided attention conditions (Mean =  $95.0 \pm 0.01$ ;  $t(23) = 1.02$ ,  $p = 0.32$ ). As expected, performance in the LTM retrieval was excellent (Mean =  $97.19\% \pm 0.005$ ) and superior to that of the attentional conditions (both  $p < 0.01$ ).

Three whole cortex analyses (Table 4.1) were conducted. First I sought to replicate the results presented in Chapter 3 that LTM-guided attention activates the posterior cognitive control network more strongly than stimulus-guided attention (Figure 4.2A). The next goal was to determine whether memory retrieval in general also activates these regions more strongly than stimulus-guided attention. This would allow me to determine whether activation in these regions serves a general memory retrieval function or is specific for LTM-guided attention (Figure 4.2B). The contrast between LTM-guided and stimulus-guided attention revealed results consistent with the results presented in Chapter 3 of

this dissertation including the posterior precuneus (PrC-p), posterior callosal sulcus (CaS-p) and lateral intraparietal sulcus (latIPS) (Table 4.1). This result provides a replication of the novel result that LTM-guided attention recruits the posterior nodes of the cognitive control network in an independent dataset with a different task (Figure 4.2B). There was also additional recruitment of the dorsolateral prefrontal cortex, perhaps reflecting the working memory demands of LTM-guided attention, and of the dorsal anterior cingulate cortex (see Table 4.1). Also consistent with the study presented in Chapter 3, there was significantly stronger recruitment of the lateral occipital complex in stimulus-guided attention compared to LTM-guided attention, likely reflecting the additional processing of object stimuli in that condition. In contrast to the previous study, results from this study did not point to stronger recruitment of the dorsal attention network for stimulus-guided attention compared to LTM-guided attention.

The contrast of the LTM retrieval condition compared to stimulus-guided attention condition did not show significant recruitment of the three regions of the posterior cognitive control network (Figure 4.2B). Activation in the LTM retrieval condition was largely left lateralized, consistent with previous accounts (Wagner et al., 2005; Hutchinson et al., 2014). There was significant recruitment of the left angular gyrus, which has been implicated consistently in long-term memory retrieval (Wagner et al., 2005; Berryhill et al., 2007; Vilberg and Rugg, 2007). Results also revealed significant recruitment of the insula, which has been shown

to be important for declarative memory (Chen et al., 2009). Taken together with the above results, this suggests that the three regions of the CCN, CaS-p, latIPS, and PrC-p, do not serve a general memory retrieval function. Finally, bilateral recruitment of the occipital pole likely reflects the fact that participants were processing stimuli presented foveally in the LTM retrieval condition compared to peripherally in the stimulus-guided attention condition (Table 4.1). The contrast between stimulus-guided attention and LTM retrieval revealed significantly stronger recruitment of the dorsal attention network (IPS, sPCS and iPCS), retrosplenial cortex, lateral occipital complex, and parahippocampal cortex, which likely reflect the increased attentional demands of this task and the increased processing of the object stimuli.

Finally, the contrast between LTM-guided attention and the LTM retrieval showed significant recruitment of the dorsal attention network as well as the three regions of the posterior cognitive control network previously shown to be recruited for LTM-guided attention in Chapter 3. This finding provides additional evidence that the posterior cognitive control network is uniquely recruited to support long-term memory-guided attention and not simply attention or memory functioning in isolation. The contrast of LTM retrieval compared to LTM-guided attention also found significant recruitment of the posterior insula, superior temporal sulcus, dorsal medial prefrontal cortex, and occipital pole (Table 4.1).

Based on the findings of my prior fMRI study, presented in Chapter 3, of LTM-guided attention using a change-detection paradigm with real world scenes,

I approached this study with three *a priori* selected regions of interest per hemisphere: *posterior precuneus (PrC-p)*, lateral IPS (*LatIPS*), and *posterior callosal sulcus / mid-cingulate (CaS-p)*. The results confirmed my hypothesis that each of these three posterior cognitive control network regions would be more significantly activated in the LTM-guided attention condition than in either the stimulus-guided attention condition or the LTM retrieval condition ( $p < 0.05$  for all comparisons in each ROI in each hemisphere). Three two-way (Hemisphere x Condition) ANOVAs were performed for each of the three regions of interest.

*PrC-p*: There was a significant main effect of Condition in PrC-p ( $F(2,46) = 33.578$ ,  $p < 0.001$ ) and no main effect of Hemisphere ( $F(1,23) = 0.143$ ,  $p = 0.709$ ), but a significant Hemisphere x Condition interaction ( $F(2,46) = 4.950$ ,  $p = 0.011$ ). Post-hoc t-tests reveal that activation was highest in the PrC-p during LTM-guided attention compared to both stimulus-guided attention and LTM retrieval in both the left and right hemispheres (all  $p < 0.05$ , corrected. See Table 4.2).

*LatIPS*: There was a significant main effect of Condition in PrC-p ( $F(2,46) = 20.516$ ,  $p < 0.001$ ) a main effect of Hemisphere ( $F(1,23) = 19.071$ ,  $p < 0.001$ ), and a significant Hemisphere x Condition interaction ( $F(2,46) = 13.4218$ ,  $p < 0.001$ ). Overall, activation was strongest in the left hemisphere, and this effect was driven by greater activation in the left hemisphere in both the LTM-guided condition and LTM retrieval condition (Figure 4.2). This finding is consistent with the literature reporting left lateral posterior parietal cortex activation for long-term

memory retrieval (e.g. Wagner et al., 2005; Nelson et al., 2010; Hutchinson et al., 2009, 2014). Post-hoc t-tests reveal that activation was highest in the latIPS during LTM-guided attention compared to both stimulus-guided attention and LTM retrieval in both the left and right hemispheres (all  $p < 0.05$ , corrected. See Table 4.2), but that the effect was strongest in the right hemisphere. This was due to the fact that activation in this region was significant in the LTM retrieval condition compared to the visual-motor control condition in the left hemisphere but not the right.

*CaS-p*: There was a significant main effect of Condition in PrC-p ( $F(2,46) = 11.197$ ,  $p < 0.001$ ) and no main effect of Hemisphere ( $F(1,23) = 0.105$ ,  $p = 0.749$ ), but a significant Hemisphere x Condition interaction ( $F(2,46) = 3.917$ ,  $p = 0.027$ ). Post-hoc t-tests reveal that activation was highest in the CaS-p during LTM-guided attention compared to both stimulus-guided attention and LTM retrieval in both the left and right hemispheres (all  $p < 0.05$ , corrected. See Table 4.2).

#### **4.4. Discussion**

In the present study, I investigated the neural mechanism underlying the cooperation of long-term memory and attention. The lateral intraparietal sulcus (latIPS), posterior precuneus (PrC-p), and posterior callosal sulcus (CaS-p) were found to be most strongly recruited for long-term memory-guided attention compared to both a LTM retrieval condition, matched on memory retrieval demands, and a stimulus-guided attention condition, matched on visuospatial

attention demands. The work presented in Chapter 3 identified these three regions for memory-guided attention in a change detection task using real-world scenes (Rosen et al., 2015). The present study replicated these findings in a novel target detection task (Figure 4.2A) and further expanded on these findings by including a memory retrieval condition.

The inclusion of this memory retrieval condition allowed me to test the hypothesis that these three regions are specifically coming online when memory is cooperating with attention during LTM-guided attention and that they are not serving a general memory retrieval function (Figure 4.2B). Indeed, the results show that these three regions are more strongly recruited for memory-guided attention than for stimulus-guided attention or memory retrieval alone. A recent study from Power and colleagues (2011) used graph theoretic analysis to attempt to functionally parcellate the human cortex. This study identified three subgraphs without previously known functions. Power and colleagues performed a meta-analysis of memory retrieval studies and found colocalization between an unidentified subgraph including regions in the vicinity of the lateral IPS, posterior callosal sulcus and posterior precuneus. In Chapter 3, I showed that the regions identified by Power et al (2011) directly overlap with the regions recruited more strongly for LTM-guided attention than stimulus-guided attention. In Chapter 3, I suggest that within the broader cognitive control network exists a memory retrieval subnetwork that is specifically recruited for LTM-guided attention. However, the results presented by Power and colleagues were arrived to via

reverse inference. In the present study, I directly tested the hypothesis that these regions are recruited for long-term memory-guided attention specifically and that they do not serve a general memory retrieval function. Bilateral CaS-p, left latIPS, and left PrC-p were all significantly recruited for LTM retrieval compared with visual-motor control. These results are consistent with the well-documented left lateralized long-term memory retrieval effects (Wagner et al., 2005; Hutchinson et al., 2009; 2014) and consistent with the findings of Power and colleagues' meta-analysis. However, these regions were also significantly recruited for stimulus-guided attention and critically, all three of these regions were bilaterally most strongly recruited for LTM-guided attention. The results of the present study suggest do not confirm the idea presented in Chapter 3 that these three regions of the posterior cognitive control network form a memory retrieval subnetwork that is preferentially recruited for LTM-guided attention. Rather, these results indicate that these three regions are preferentially recruited when long-term memory and attention cooperate to a greater extent than when memory or attention is acting alone. This finding suggests that rather these regions are specifically recruited to support processing that integrates memory- and stimulus-based representations rather than memory retrieval alone.

One potential confound of this study is that performance was higher for the LTM retrieval condition than the LTM-guided attention and stimulus-guided attention conditions. This is likely due to the fact that participants were attending foveally in the LTM retrieval condition and peripherally in the other two conditions

and visual acuity declines the farther a stimulus is from the center of gaze. The greater activation in early visual cortex seen for LTM retrieval compared to the other conditions is likely due to the direction of attention to the fovea as well. However, I cannot fully rule out the possibility the lack of recruitment of the posterior precuneus, posterior callosal sulcus and lateral IPS in the LTM retrieval condition is attributed to the difference in task difficulty. One would expect that if these regions were simply sensitive to task difficulty no differences would be seen between the LTM-guided and stimulus-guided attention conditions in which performance was equated. Therefore, it is unlikely that the lack of recruitment in these regions in the LTM retrieval condition is simply due to task difficulty alone. I argue instead that these regions are recruited specifically to support LTM-guided attention.

Activation in the lateral posterior parietal cortex especially in the left hemisphere has been repeatedly found in fMRI studies of long-term recognition or episodic memory retrieval (reviewed in Hutchinson et al., 2009; School *et al.*, 2011). Results from a recent study have indicated that the activation seen in lateral parietal cortex in memory retrieval does not reflect a unitary function, but rather that there are at least four distinct regions within lateral parietal cortex supporting different aspects of long-term memory retrieval (Hutchinson et al., 2014). The region of latIPS, recruited here for LTM-guided attention, has been suggested to act as a mnemonic accumulator, increasing activation with additional information regarding the nature of a memory before making a

decision (Hutchinson et al., 2014). In the present study, recruitment of the left latIPS for the LTM retrieval task was significant (Figure 4.2B), consistent with previous literature reporting left lateral parietal recruitment for memory retrieval (e.g. Wagner et al., 2005; Nelson et al., 2010; Hutchinson et al., 2014). This was the only region that showed this laterality effect. The latIPS may be holding spatial information that has already been retrieved and/or accumulating information about whether the stimulus presented in the remembered location matches the item stored in memory and thus be acting as a memory-guided action selector.

The posterior precuneus has been attributed to attentional switching (Shomstein and Yantis, 2004, 2006; Chiu and Yantis, 2009), as well as in memory of previously viewed items compared to novel items (Wagner et al., 2005; Sestieri et al., 2010). These findings together suggest that this region is well positioned to switch attention between internal memory representation and external stimuli, as is necessary for LTM-guided attention. Furthermore, results from Chapter 3 (Rosen et al., 2015), using intrinsic connectivity suggested that this region acts as a local hub within the subnetwork recruited for LTM-guided attention, showing the greatest specificity for connectivity with both the CaS-p and latIPS.

The CaS-p has generally been underemphasized in many studies. Importantly, this region has been shown to be recruited for both retrieval of working memory and long-term memory (Schon et al., 2009; Huijbers et al.,

2011). It has been suggested that working memory, the ability to hold information in mind and manipulate it in some way, is an emergent property of interactions between attention and long-term memory (Oberauer, 2002; Postle, 2006, see also Courtney, 2004). Furthermore, working memory has been broken down into two parts, information that is in the focus of attention which has a limited capacity, and information that is outside the focus of attention, but in an active state of long-term memory and thus more easily accessible (Cowan, 1988; Lewis Peacock and Postle, 2008). It is possible that the regions that show greater activity during LTM-guided attention compared to stimulus-guided attention and LTM retrieval reflect this bringing of information into the activated portion of long-term memory in order for it to be accessible for attentional purposes.

In addition the regions within the posterior cognitive control network identified a priori for region of interest analysis, a whole brain exploratory analysis revealed several significantly activated clusters in the LTM-Guided attention condition overlapping with other regions of the cognitive control network (Table 4.1). These included the dorsal anterior cingulate (dACC), the dorsolateral prefrontal cortex, the anterior insula, and the middle temporal sulcus. Activation in the majority of these regions reflected a change in deactivation, such that they were less deactivated in the LTM-guided attention condition compared to the stimulus-guided attention and LTM retrieval conditions. However, two regions, the right dACC and bilateral anterior insula were significantly recruited for LTM-guided attention compared to both stimulus-guided attention and LTM retrieval.

The recruitment of these additional regions may reflect additional statistical power in the present study compared to the experiment presented in Chapter 3 or perhaps task difficulty differences. Further investigation will be required to determine the precise role of the dACC and anterior insula in LTM-guided attention.

Long-term memory and attention have historically been studied by distinct groups of scientists. Furthermore, the advent of neuroimaging has highlighted that the dorsal attention network, which supports top-down goal directed attention, and the default mode network, which supports memory retrieval and other internal cognitive processes, competitively interact with one another (Fox et al., 2005; Todd et al., 2005; Sestieri et al., 2010). However, previous experience with a stimulus or environment often provides a behavioral advantage in both processing speed and accuracy (Summerfield et al., 2006; Chun and Jiang, 1998). The present study was designed to investigate the interaction between long-term memory and visuospatial attention. Results indicated that three regions within the posterior cognitive control network (latIPS, PrC-p and CaS-p) are recruited for LTM-guided attention compared to stimulus-guided attention. This finding provides an important replication of the results presented in Chapter 3 with a novel task and different stimuli. Furthermore, the present study extends these findings by showing that these regions are not recruited for LTM retrieval in general, but rather specifically recruited most strongly for LTM-guided attention. Taken together, these findings provide evidence that the cooperation between

long-term memory and attention is supported by distinct brain regions located within the posterior cognitive control network. Future studies should use an event-related task design in order to further illuminate at what point in the LTM-guided attention process these regions are recruited as well as what happens when one's mnemonic expectations are violated.

## 4.5 Chapter 4 Figures

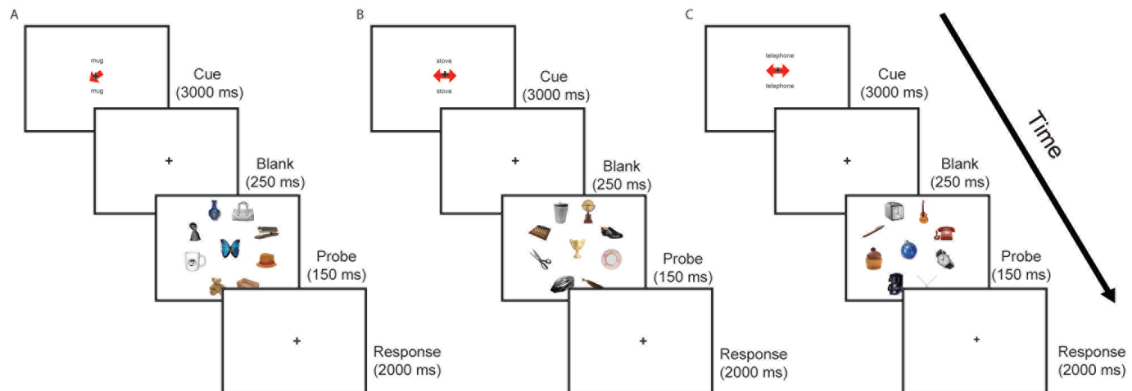


**Figure 4.1.** Behavioral paradigms and trial timing. A) Stimulus-guided attention. Subjects used a word (e.g. ‘mug’) and an arrow cue to guide their attention covertly to one of eight peripheral locations. After a delay, an array of objects appeared. On 50% of trials, the target appeared at the correct location, and on 50% it appeared at another location. B) LTM retrieval. On Day 1, subjects studied word-object associations (e.g. ‘stove’ with a picture of a trophy). On Day 2 in the scanner, subjects were presented with the word and were instructed to retrieve the object associated with the word. On 50% of trials, the object that appeared centrally was the paired associate and on 50% of trials it was not. C) LTM-Guided Attention. On Day 1, subjects studied a word-location association (e.g. ‘telephone’ paired with a picture of a telephone at a peripheral location). On Day 2 in the scanner, subjects were presented with a word and instructed to retrieve the location associated with that word and covertly attend to that location. On 50% of trials the target appeared at the correct location and on 50% it appeared at a different location.

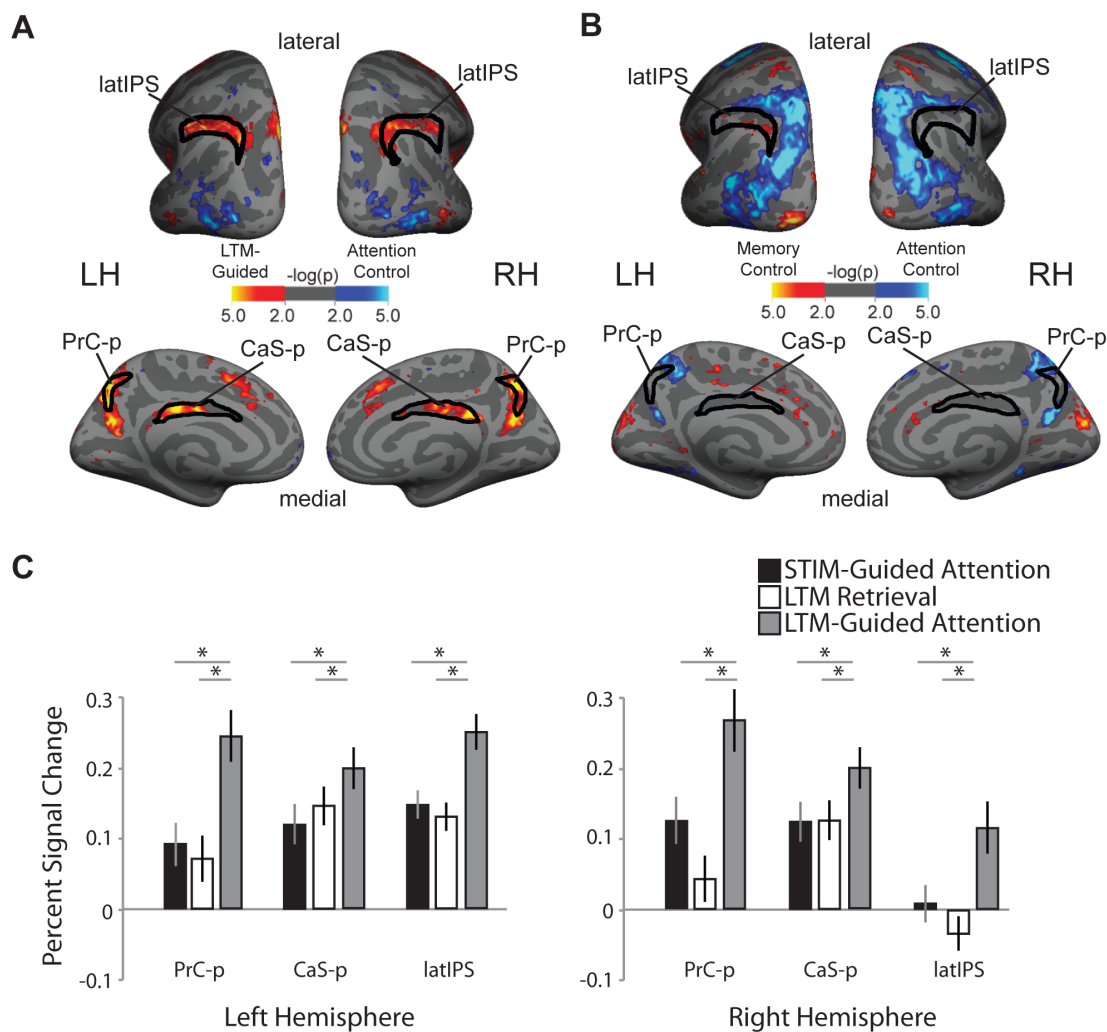


Figure 4.2. A) Whole brain analysis displaying the contrast of LTM-Guided attention vs. stimulus-guided attention and B) LTM retrieval vs stimulus-guided attention. Black outlines are regions of interest from the cognitive control network (Yeo et al., 2011) that were found to be more strongly recruited for LTM-guided attention compared to Stimulus-guided attention in Chapter 3 of this thesis (Rosen et al., 2014). C) Region of Interest Analysis. Percent signal change was

extracted for each condition compared to a visual-motor control condition. A Hemisphere x Condition ANOVA was performed for each ROI. There was a significant main effect of Condition in both the PrC-p and CaS-p. Post-hoc paired t-tests revealed significantly greater activation in these regions for the LTM-Guided Attention condition compared to both the stimulus-guided attention and the LTM retrieval conditions. There was a significant Hemisphere x Condition interaction in the latIPS. Post hoc t-tests revealed significantly greater activation in the LTM-Guided condition than stimulus-guided attention and LTM retrieval condition with the right hemisphere showing greater specificity.

## 4.6 Chapter 4 Tables

**Table 4.1: Cluster-size corrected analysis:** Significant areas of activation in the contrast of LTM-Guided vs. Stimulus-guided, LTM Retrieval vs. Stimulus-guided and LTM-Guided vs LTM Retrieval conditions

### LTM-Guided > Stimulus-guided attention

| <i>Anatomical Region</i>  | <i>Hemisphere</i> | <i>x</i> | <i>y</i> | <i>z</i> | <i>Size(mm<sup>2</sup>)</i> | <i>t-value</i> |
|---------------------------|-------------------|----------|----------|----------|-----------------------------|----------------|
| Posterior Precuneus       | L                 | -13.7    | -71.5    | 39.3     | 1773.89                     | 8.013          |
|                           | R                 | 7        | -69.2    | -40.8    | 1498                        | 7.74           |
| Posterior Callosal Sulcus | L                 | -8       | -24.2    | 30.6     | 436.03                      | 6.656          |
|                           | R                 | 8.5      | -38.6    | 28.3     | 427.27                      | 6.77           |
| DLPFC/Anterior MFG        | L                 | -38.9    | 45.8     | 3.9      | 1758.53                     | 5.918          |
|                           | R                 | 39.2     | 48.7     | 9.6      | 2559.21                     | 6.332          |
| Lateral IPS/SMG           | L                 | -54.2    | -44      | 44.4     | 2084.71                     | 5.359          |
|                           | R                 | 36       | -72.7    | 42.2     | 1935.29                     | 5.165          |
| Anterior Insula           | L                 | -26.5    | 24.3     | -7.1     | 553.76                      | 5.602          |
|                           | R                 | 33       | 17.4     | 2.1      | 420.77                      | 4.598          |
| Dorsal ACC                | L                 | -9       | 9.9      | 47.1     | 499.89                      | 4.22           |
|                           | R                 | 7.8      | 22.2     | 43.9     | 547.13                      | 4.413          |
| Middle Temporal Gyrus     | L                 | -55.7    | -43.5    | -14.3    | 326.96                      | 3.913          |
|                           | R                 | 55.2     | -47.8    | -6.8     | 336.92                      | 4.182          |
| Superior DLFPC            | L                 | -30.6    | 8.9      | 54.1     | 827.78                      | 4.466          |
|                           | R                 | 22.9     | 11.8     | 46.2     | 936.08                      | 3.856          |
|                           | R                 | 19.5     | 17.9     | 57.5     | 134.66                      | 3.32           |

**Stimulus-guided attention > LTM-Guided Attention**

| <u>Anatomical Region</u>     | <u>Hemisphere</u> | <u>x</u> | <u>y</u> | <u>z</u> | <u>Size(mm<sup>2</sup>)</u> | <u>t-value</u> |
|------------------------------|-------------------|----------|----------|----------|-----------------------------|----------------|
| Lateral Occipital Cortex     | L                 | -44.5    | -72.3    | -5.9     | 1514.14                     | 6.744          |
|                              | R                 | 41.5     | -69.1    | -4.5     | 1547.59                     | 6.11           |
| Superior and Transverse OccR |                   | 24.8     | -78.3    | 26.6     | 152.1                       | 3.282          |

**LTM retrieval > Stimulus-guided attention**

| <u>Anatomical Region</u> | <u>Hemisphere</u> | <u>x</u> | <u>y</u> | <u>z</u> | <u>Size(mm<sup>2</sup>)</u> | <u>t-value</u> |
|--------------------------|-------------------|----------|----------|----------|-----------------------------|----------------|
| Anterior Insula          | L                 | -39.2    | 26       | 6.7      | 1167.42                     | 6.788          |
| Posterior Insula         | L                 | -39.8    | -24.6    | 21.1     | 431.86                      | 4.318          |
| Angular Gyrus            | L                 | -45      | -59.1    | 40.8     | 374.03                      | 4.702          |
| Mid insula               | L                 | -54.5    | 3.5      | 3        | 189.07                      | 4.803          |
| Mid Insula               | L                 | -36.4    | -15.1    | 3.9      | 208.2                       | 4.293          |
| Superior Occipital Gyrus | L                 | -7.9     | -90.9    | 27       | 620.91                      | 4.018          |
| OFC                      | L                 | -30.2    | 37.5     | -7.5     | 237.62                      | 3.589          |
| Cuneus                   | R                 | 7        | -82.2    | 17.5     | 725.78                      | 5.065          |
| Occipital Pole           | L                 | -22.2    | -98.9    | -4.6     | 742.5                       | 6.419          |
|                          | R                 | 23.3     | -98.6    | -1       | 223.82                      | 4.328          |
| Postcentral Sulcus       | L                 | -21.9    | -38.2    | 57.8     | 252.29                      | 3.426          |
|                          | R                 | 22.2     | -43.2    | 58.8     | 183.96                      | 3.792          |
| Postcentral Gyrus        | L                 | -33.6    | -30.6    | 63.3     | 214.16                      | 3.2            |
| Central Sulcus           | R                 | 15.8     | -33      | 65.1     | 270.84                      | 3.461          |

**Stimulus-guided attention > LTM retrieval**

| <u>Anatomical Region</u>   | <u>Hemisphere</u> | <u>x</u> | <u>y</u> | <u>z</u> | <u>Size(mm<sup>2</sup>)</u> | <u>t-value</u> |
|----------------------------|-------------------|----------|----------|----------|-----------------------------|----------------|
| Superior Precentral Sulcus | L                 | -20.9    | -4.3     | 48.7     | 956.65                      | 8.558          |
|                            | R                 | 32.8     | -7.6     | 46.7     | 2232.97                     | 6.252          |
| SPL/IPS/LOC                | L                 | -29.1    | -74.3    | 16.6     | 7595.04                     | 8.02           |
|                            | R                 | 16.1     | -63      | 59.1     | 8171.96                     | 7.994          |
| Retrosplenial Cortex       | L                 | -16.8    | -60.8    | 22.8     | 208.65                      | 5.532          |
|                            | R                 | 20.9     | -57.5    | 21.9     | 420.81                      | 7.275          |
| Parahippocampal            | R                 | 34.1     | -41      | -9.2     | 155.67                      | 4.726          |

**LTM-Guided Attention > LTM retrieval**

| <u>Anatomical Region</u>   | <u>Hemisphere</u> | <u>x</u> | <u>y</u> | <u>z</u> | <u>Size(mm<sup>2</sup>)</u> | <u>t-value</u> |
|----------------------------|-------------------|----------|----------|----------|-----------------------------|----------------|
| Superior Parietal/IPS      | L                 | -10.9    | -72.3    | 49.4     | 6234.84                     | 8.518          |
| Retrosplenial Cortex       | L                 | -16.2    | -61.1    | 24.1     | 535.67                      | 7.004          |
|                            | R                 | 17.6     | -60.2    | 26.4     | 9082.59                     | 9.669          |
| Posterior Callosal Sulcus  | L                 | -7.7     | -46.6    | 17.4     | 261.91                      | 4.36           |
| Anterior Insula            | L                 | -29.8    | 20       | -4.2     | 323.09                      | 6.222          |
| sPCS/DLPFC                 | R                 | 33.7     | 6.7      | 55.7     | 5823.88                     | 7.216          |
| Inferior Precentral Sulcus | L                 | -49.2    | 2.8      | 28.6     | 377.72                      | 4.926          |
| Anterior Insula            | R                 | 30.3     | 22.5     | 0.3      | 492.05                      | 7.177          |
| Middle Temporal            | R                 | 52.4     | -53.8    | -4.6     | 967.39                      | 6.269          |
| Superior Precentral Sulcus | L                 | -20.7    | -3       | 49.1     | 1401.26                     | 7.662          |
| Dorsal Anterior Cingulate  | R                 | 8.5      | 28.9     | 46.8     | 850.01                      | 5.925          |
| Lateral OFC                | R                 | 21.6     | 42.5     | -11.7    | 150.06                      | 4.867          |

|          |   |       |       |       |        |       |
|----------|---|-------|-------|-------|--------|-------|
| Fusiform | L | -29   | -57.2 | -13.5 | 791.96 | 3.981 |
|          | L | -40.4 | -56.8 | -9.2  | 413.28 | 3.633 |

### LTM retrieval > LTM-Guided Attention

| <u>Anatomical Region</u>       | <u>Hemisphere</u> | <u>x</u> | <u>y</u> | <u>z</u> | <u>Size(mm<sup>2</sup>)</u> | <u>t-value</u> |
|--------------------------------|-------------------|----------|----------|----------|-----------------------------|----------------|
| Posterior Insula               | L                 | -38.6    | -24.5    | 20.8     | 587.58                      | 6.806          |
|                                | L                 | -34.4    | -15      | -3       | 262.46                      | 4.034          |
|                                | L                 | -56.2    | -3.7     | 8.4      | 150.58                      | 3.952          |
| Postcentral Sulcus             | L                 | -26      | -46.1    | 58.7     | 259.43                      | 4.286          |
|                                | R                 | 20.6     | -41.9    | 58.7     | 231.79                      | 6.208          |
| Central Sulcus                 | L                 | -21.3    | -31.6    | 68.2     | 442.15                      | 3.39           |
|                                | R                 | 21.1     | -32      | 59.9     | 500.04                      | 5.089          |
| Occipital Pole                 | L                 | -24.4    | -96.7    | 0.3      | 365.68                      | 4.109          |
|                                | R                 | 25.7     | -97.9    | -2       | 337.23                      | 4.787          |
| Sup Occipital Gyrus            | L                 | -7.4     | -88.6    | 30.4     | 512.98                      | 5.391          |
|                                | R                 | 6.4      | -85.2    | 29.3     | 627.98                      | 4.499          |
| Circular Insula(very anterior) | L                 | -37.8    | 28.7     | 4.2      | 375.73                      | 5.183          |
| Dorsal Medial PFC              | L                 | -8       | 56.5     | -8.9     | 385.91                      | 4.782          |
| Orbitofrontal Cortex           | L                 | -30.2    | 37.5     | -7.5     | 154.85                      | 4.117          |
| Superior Temporal Sulcus       | L                 | -52.3    | -40.1    | 5        | 270.7                       | 3.721          |
|                                | L                 | -65.2    | -34.5    | 8.1      | 263.16                      | 3.681          |

**Table 4.2 ROI Analysis**

Percent signal change in Regions of Interest of the three posterior nodes of the cognitive control network from Yeo and colleagues (2011). Activation during the LTM-guided condition was compared to activation in the stimulus-guided attention condition and compared to the LTM retrieval condition. All values reflect percent signal change relative to the visual-motor control condition (\*\*\*) =  $p < .001$ ; \*\* =  $p < .01$ ; \* =  $p < .05$ )

| ROI    | Hemi | LTM-Guided Attention | Stimulus-Guided Attention | t-value | Sig. | LTM Retrieval | t-value | Sig. |
|--------|------|----------------------|---------------------------|---------|------|---------------|---------|------|
| PrC-p  | L    | 0.24±0.04            | 0.09±0.03                 | 10.75   | ***  | 0.07±0.03     | 5.29    | ***  |
| PrC-p  | R    | 0.27±0.04            | 0.13±0.03                 | 6.83    | ***  | 0.04±0.03     | 7.49    | ***  |
| CaSp   | L    | 0.20±0.03            | 0.12±0.03                 | 5.59    | ***  | 0.15±0.03     | 2.68    | *    |
| CaSp   | R    | 0.20±0.03            | 0.12±0.03                 | 5.29    | ***  | 0.13±0.03     | 4.33    | ***  |
| latIPS | L    | 0.17±0.04            | 0.05±0.02                 | 5.64    | ***  | 0.08±0.03     | 3.86    | **   |
| latIPS | R    | 0.12±0.04            | 0.01±0.03                 | 4.59    | ***  | -0.03±0.02    | 6.65    | ***  |

**CHAPTER 5: Influences of Long-Term Memory-Guided Attention and  
Stimulus-Guided Attention on Visuospatial Representations  
Within Human Intraparietal Sulcus**

## 5.1 Introduction

Damage to the right parietal cortices can result in inattention to the contralesional hemifield, a neurological syndrome known as left hemispatial neglect (Corbetta *et al.*, 2011), but damage to the homologous regions in the left hemisphere very rarely results in right neglect. Early models of hemispatial neglect suggested that the right hemisphere may contain representational maps of the visual world that encompass both the left and right hemifields whereas the left hemisphere only contains a map of the right visual field (Heilman and Van Den Abell, 1980). This idea stands in direct contrast to the frequently replicated observation that under purely visual drive, the visuotopically mapped regions within the parietal cortex contain maps of the visual field that have a strong symmetric contralateral bias (Serenio *et al.*, 2001; Swisher *et al.*, 2007; Wandell, *et al.*, 2007; Silver and Kastner, 2009).

The human parietal lobe plays a central role in coding visuospatial information and multiple regions in the vicinity of the intraparietal sulcus are known to contain maps of the contralateral visual field (e.g., Swisher *et al.*, 2007; Silver and Kastner, 2009). These visuotopic maps exhibit a high degree of hemispheric symmetry when examined with standard fMRI retinotopic mapping analysis. In contrast to this symmetry, two forms of parietal lobe hemispheric asymmetry have been well documented. A right hemisphere bias occurs for spatial attention and prior studies identify the right temporo-parietal junction, a region that lies far lateral to IPS, as the key structure in this attentional

hemispheric bias (e.g., Mesulam, 1981; Gitelman et al., 1999; Corbetta & Shulman, 2011). A left hemisphere bias occurs during successful retrieval of long-term memories (e.g. Wagner et al., 2005; Vilberg and Rugg, 2007); although the role of this region in LTM retrieval is still under investigation, the region has been clearly localized to lie lateral to visuotopic IPS (Hutchinson et al., 2014; Rosen et al., 2015). Thus, lateral portions of parietal lobe appear to exhibit hemispheric asymmetries, while the visuotopic maps along the medial bank of IPS appear symmetric. However, recent fMRI studies (Szczepanski *et al.*, 2010; Sheremata *et al.*, 2010; Sheremata and Silver, 2015) employing demanding attention or short-term memory tasks have found visuotopically mapped regions IPS0, IPS1 and IPS2 in right, but not left hemisphere dynamically change their spatial representations to code targets across the full visual field; the resulting hemispheric asymmetry in IPS spatial representations is consistent with key predictions of representational models of neglect (Heilman and Van Den Abell, 1980; Mesulam, 1981). These findings leave unanswered the question of what other cognitive factors might shape spatial representations in the IPS.

We adapted a change-detection paradigm (Rensink *et al.*, 1997; Rosen *et al.*, 2015) such that subjects had only one shot to determine whether a change occurred between the target and probe image. Subjects use either long-term memory (LTM-guided) or a visual stimulus (STIM-guided) to guide their attention to the location of the potential change. Critically, here I can assess when subjects are attending to the left or right visual field in either the LTM-guided or STIM-

guided condition. Including the STIM-guided condition allowed me to replicate the previous finding that during an attentionally demanding task, the left hemisphere continues to code for the contralateral visual field, whereas the right hemisphere codes for targets in both the contralateral and ipsilateral fields, using complex visual scenes. Furthermore, I tested two alternative hypotheses to address how visuotopically mapped IPS regions may be flexibly recruited during long-term memory-guided attention. One possibility is that the left IPS will have a full field representation while the right will have a strong contralateral bias (Asymmetry: LH Full Field). Alternatively both the left and right IPS could code for the full field (Symmetrically Full Field) due to the presence of both high attention and memory demands of the task.

## **5.2 Materials and Methods**

### *5.2.1 Participants:*

Twenty-two healthy human participants (13 male) between 22 and 33 years of age, with normal or corrected-to-normal vision participated in all experiments; however two subjects were dropped from analysis due to weak retinotopic maps within intraparietal sulcus (see below). All participants were compensated and gave written informed consent to participate in the study, which was approved by the Institutional Review Board of Boston University.

### *5.2.2 Visual Stimuli and Experimental Paradigms:*

Day 1, Training: Participants performed two behavioral tasks on Day 1 intended to give them experience with the specific images to be used in the scanner on

Day 2. The location of scene changes were trained in the first experiment, but no changes were presented in the second experiment. On Day 2, stimuli from the first experiment were used in the LTM-guided attention scans and stimuli from the second experiment were used in the stimulus-guided attention scans. Each participant viewed all images and scene images used for each condition were counterbalanced between conditions across the participant pool.

Change-detection Encoding Task: Participants were shown 24 scene images in a change-detection flicker paradigm (Rensink *et al.*, 1997; Rosen *et al.*, 2014). Each scene was an outdoor scene obtained from Google Images that was altered using Adobe Photoshop (*e.g.*, removed tree, added window, changed color of car, etc.), thus creating two versions of each scene (original, altered). On a given trial, a scene appeared on the screen for 1000 ms, followed by a blank screen for 250 ms, and the same scene, containing one change, for another 1000 ms flickering on and off for 15 s. Participants were instructed to visually search for the change and to click on the scene change when they detected the change. Following the flicker period was a “reveal period” in which the original and the altered scene alternated without a blank screen for 10 s. The reveal period ensured that all participants saw all changes and reinforced the location and identity of the change.

Man-made/Natural Judgment Encoding Task: Participants viewed 192 scene images for 3000 ms each and made a two-alternative forced choice judgment about whether the scene was mostly natural or mostly man-made with no image

changes presented. This exposure served to familiarize participants with the scenes, but not the changes, that would be used in the stimulus-guided (STIM-guided) cueing condition on Day 2.

Day 2, Test: Twenty-four to forty-eight hours after the training day, participants came in for an fMRI scan session. Conditions contrasted LTM-guided attention and stimulus-guided attention in left and right visual hemifields, along with control conditions. Trials were presented in twelve counterbalanced blocks per run (2 LTM-guided: Left, 2 LTM-guided: Right, 2 STIM-guided: Left, 2 STIM-guided: Right, 1 No-Cue: Left, 1 No-Cue: Right, 2 Passive). Each block started with a 1 s block cue period and was followed by six 5.9 s trials, for total block duration of 36.4 s. Sets of 4 TRs (10.4 s) of blank screen fixation periods were included at the start, halfway point and end of each run. Each run was 7 min 48 seconds long and eight runs were performed by each participant.

Participants performed a “single-shot” change detection task under different cueing conditions (Figure 5.1). The initial scene appeared for 3000 ms, followed by a blank gray screen for 250 ms, then either the original or altered scene appeared for 150 ms and finally was replaced by a blank screen for the remainder of each trial (2500 ms) while responses were collected. The 150 ms probe presentation was chosen to make the attentional selection task difficult, to strongly encourage spatial deployment of attention prior to appearance of the probe, and to prevent subjects from overtly or covertly moving their attentional foci once the probe appeared. Image changes occurred on 50% of the trials.

Participants reported whether or not a change occurred in the probe image compared to the original image.

In all conditions, participants were instructed to fixate at the center and direct their attention covertly to the cued location in the scene. In the *long-term memory-guided attention condition (LTM-guided)* participants directed attention based on learned spatial location; that is, LTM was the only source of cueing information. In the *stimulus-guided attention condition (STIM-guided)*, participants directed attention to an exogenously cued (set of nested red and white square outlines subtending  $\sim 1.3 \times 1.3$  degrees of visual angle) spatial location in previously viewed scenes. In the *no cue* condition, participants were not provided with any cue but instructed to actively attend to the whole novel scene, and in the *passive condition*, participants simply made a button press to novel scenes presented in the same manner as all other conditions (Figure 5.1). The twenty-four scenes used in the LTM-guided condition for each participant were repeated once per run (eight times total). All other images were only presented once for each participant.

### 5.2.3 MR Data Acquisition:

Functional MRI data were acquired using a 3 Tesla Siemens TIM Trio magnetic resonance (MR) imager located at the Center for Brain Science at Harvard University in Cambridge, Massachusetts. All data were acquired using a 32-channel head coil. Functional scans were acquired using T2\*-weighted, gradient echo, echo-planar images [repetition time (TR) = 2.6 seconds, echo time (TE) =

30 ms; voxel size 3.1 x 3.1 x 3.0 mm] and were collected from 42 slices with no skip, with full brain coverage. Each participant participated in eight functional scans (each 180 TRs; 7 min 48 sec duration) in one scan session. Functional data were aligned with high-resolution (1.0 x 1.0 x 1.3 mm) T1-weighted images. For 14 participants the high-resolution structural images were acquired at the same facility; for 8 participants they were acquired on an identically equipped scanner and coil at the Martinos Center for Biomedical Imaging at Massachusetts General Hospital in Charlestown, Massachusetts.

*MR Data Analysis:* For each participant, the cortical surface of each hemisphere was computationally reconstructed from the high-resolution anatomical volume using FreeSurfer software (Fischl *et al.*, 2012). fMRI task data were analyzed using the FreeSurfer 5.1.0 software package (Charlestown, Massachusetts). Intensity normalization and motion correction were performed before signal averaging was performed. Whole cortex and ROI analyses were performed using a general linear model with regressors that matched the time course of all task conditions.

Whole-Brain Cortical Surface Analysis: Single participant fMRI data were registered to an average cortical surface space (FreeSurfer 'fsaverage' brain) using the boundary of the gray matter and white matter. Analyses were performed separately in each hemisphere on the average cortical surface and data were analyzed for each vertex using a GLM with each condition as a predictor. Three motion correction regressors were included in the model. The

BOLD signal was modeled as a linear, time-invariant system with  $\gamma$  response function assumed for each condition with a delay  $\delta = 2.25$  and a delay time constant  $\tau = 1.25$ . An estimated response was generated by convolving the response function with the block length (i.e. the time in each condition) and minimizing the residual error (FS-FAST, Cortech). Random effects group analyses were performed using surface-based averaging techniques (Fischl *et al.*, 1999). A *t*-test was performed for each vertex to compare differences in activation between conditions. The significance of these activation differences were then projected onto the cortical surface of an individual subject for the purposes of comparing activation maps to visuotopic maps.

Retinotopic Mapping and Region of Interest Definition: To map the visual field representations within intraparietal sulcus, I employed the phase-encoded protocol described in Swisher *et al.*, 2007. Briefly, a flickering chromatic radial wedge checkerboard swept around a fixation point at the center of the screen at a periodicity of 55.46 s (12 cycles per 665.6 second run). I performed alternating runs of clockwise and counterclockwise rotation. Subjects fixated at a center fixation point and made a button press when the fixation point dimmed at random throughout the run. The phase of responses was used to determine the polar angle receptive field of each vertex. These data were then visualized on the cortical surface. ROIs for areas IPS0, IPS1, IPS2, IPS3 and IPS4 were drawn based on reversals in the polar angle phases (e.g. Wandell *et al.*, 2007; Swisher 2007, Figure 5.2A). Regions of interest were then further restricted to those

vertices which were significantly activated ( $p < 0.05$  uncorrected) by the retinotopic mapping analysis. For two subjects, all five IPS regions could not be drawn using this statistical threshold and therefore these subjects were dropped from all analyses.

Percent signal change was extracted for each region of interest for each contrast compared to passive viewing (e.g. LTM-guided: Left vs. Passive). The results will be discussed according to cue-type and visual field in the results (e.g. left hemisphere LTM-guided: Contra refers to the right visual field whereas left hemisphere LTM-guided: Ipsi refers to the left visual field). In order to quantify the contralateral bias in each IPS region for each condition (LTM-guided and STIM-guided), I computed a Contralateral Index (CI) using the following equation:

$$CI = \frac{(Contra - Ipsi)}{\sqrt{\sigma_{Contra} + \sigma_{Ipsi}}}$$

Where Contra and Ipsi refer to the percent signal change for targets in the contralateral and ipsilateral visual fields, respectively, for a hemisphere ROI. Where Contra and Ipsi refer to the percent signal change for ta

### **5.3 Results**

#### *5.3.1 Behavioral Performance:*

Subjects performed well both in LTM-guided attention and stimulus-guided attention conditions and in both visual hemifields. A Condition x Visual Field ANOVA revealed no significant main effect of condition, visual field, or interaction

(all  $p > 0.1$ ; STIM-guided LVF  $d' = 2.52 \pm 0.34$ , STIM-guided RVF  $d' = 2.37 \pm 0.58$ , LTM-guided LVF =  $2.72 \pm 0.81$ , LTM-guided RVF =  $2.56 \pm 0.69$ ).

### 5.3.2 fMRI Analysis:

Standard retinotopic mapping was performed in each subject and, as expected, revealed multiple maps of the contralateral visual field within the intraparietal sulcus (IPS) of each hemisphere. Although both right and left IPS exhibited a strong bias for stimuli in the contralateral visual field, these patterns appeared highly symmetric between the two hemispheres (e.g., Figure 5.2A).

In the attention task scans, fMRI activation in each hemisphere was contrasted between contralateral and ipsilateral visual field target stimuli. A strong hemispheric asymmetry was observed within IPS for the STIM-guided attention condition (see Figure 5.2B). In the left hemisphere, a strong contralateral bias is present in IPS for STIM-guided attention exhibited by the greater activation for targets in the contralateral visual field (right) than in the ipsilateral visual field (left). Right IPS showed comparatively diminished contralateral bias, exhibited by the reduced difference between targets in the contralateral visual field (left) compared to the ipsilateral visual field (right).

In contrast to the STIM-guided attention condition, no such hemispheric asymmetry was observed in IPS during the LTM-guided attention condition. Both left and right IPS exhibited only weak contralateral biases (see Figure 5.2C). These observations suggest that both attentional conditions affect the visual field

selectivity within IPS from their standard strong contralateral bias and that the two forms of attention produce different changes in IPS spatial responsivity.

In order to quantify these attention-driven dynamic changes in the visual field representations within IPS a region of interest analysis was performed for retinotopically mapped IPS0, IPS1, IPS2, IPS3, and IPS4 in each hemisphere of each subject. This analysis was restricted to only those voxels that exhibited significant contralateral bias during retinotopic mapping and task activation in each condition was contrasted with passive viewing (see Materials and Methods). I performed three-factor (Hemisphere x Condition x Visual Field) ANOVAs for each IPS region. The critical test for differences in hemispheric asymmetry between the LTM-guided attention and stimulus-guided attention conditions is a three-way interaction between hemisphere, attentional condition, and visual hemifield. IPS0, IPS1 and IPS2 all revealed this significant interaction (see Table 5.1, all  $p < 0.05$ ), while IPS3 and IPS4 did not. Post-hoc t-tests revealed with that within IPS0, IPS1 and IPS2, activation in response to contralateral targets was stronger than ipsilateral targets in both LTM-guided and STIM-guided conditions in both the left and right hemisphere. However, that these differences appeared to be greatest in the left hemisphere during STIM-guided attention, indicating a stronger contralateral bias under these conditions. All IPS regions (IPS0-4) revealed a significant main effect of Condition, such that activation was greater in the STIM-guided condition than the LTM-guided

condition (all  $p < 0.0001$ ) and none of the regions showed a main effect of Hemisphere (all  $p > 0.05$ ).

The attentionally-driven dynamic changes in visual field coding within IPS0, IPS1 and IPS2 are summarized in Figure 5.3. The distribution of preferred visual field polar angles reveal a very robust bias for stimuli presented in the contralateral visual field under the minimal attention conditions of retinotopic mapping and this bias is highly symmetric between hemispheres (see Figure 5.3A). To quantify contralateral biases in LTM-guided and STIM-guided attention, I computed a contralateral index (CI) for IPS0, IPS1, and IPS2 in each hemisphere (see Methods). All three regions showed a significantly stronger CI in STIM-guided attention in the left hemisphere compared to the right hemisphere (all  $p < 0.01$ , see Figure 5.3B), and none of the regions showed a significant difference in CI between hemispheres in the LTM-guided attention condition (all  $p > 0.5$ ; see Figure 5.3C). Furthermore, in each region the CI was significantly stronger in the left hemisphere for STIM-guided attention than for LTM-guided attention (IPS0: STIM-guided =  $0.37 \pm 0.03$ , LTM-guided =  $0.14 \pm 0.03$ ,  $p < 0.0001$ , IPS1: STIM-guided =  $0.25 \pm 0.03$ , LTM-guided =  $0.11 \pm 0.03$ ,  $p = 0.0028$ , IPS2: STIM-guided =  $0.26 \pm 0.04$ , LTM-guided =  $0.10 \pm 0.03$ ,  $p = 0.0023$ ). In contrast, there was no difference in the CI in the right hemisphere across condition (IPS0: STIM-guided =  $0.20 \pm 0.03$ , LTM-guided =  $0.14 \pm 0.03$ ,  $p = 0.16$ , IPS1: STIM-guided =  $0.09 \pm 0.03$ , LTM-guided =  $0.15 \pm 0.03$ ,  $p = 0.06$ , IPS2: STIM-guided =  $0.07 \pm 0.03$ , LTM-guided =  $0.12 \pm 0.03$ ,  $p = 0.08$ ).

## 5.4 Discussion

These results demonstrate two forms of attentionally-driven changes in the spatial selectivity within human intraparietal sulcus. Under simple stimulus conditions, spatial coding is strongly biased to the contralateral field and highly symmetric between the hemispheres. Under stimulus-guided attention conditions, a hemispheric asymmetry emerges as the right hemisphere IPS0-2 strongly respond strongly to stimuli in both visual hemifields but the left hemisphere IPS0-2 maintains a strong contralateral bias. In contrast, during LTM-guided attention, this hemispheric asymmetry vanishes as IPS0-2 in both left and right hemispheres respond robustly to targets in both visual hemifields. The dynamic changes under stimulus-guided attention that I observe replicate prior findings by our lab and others (Szczepanski *et al.*, 2010; Sheremata *et al.*, 2010). The dynamic changes under LTM-guided attention are novel and unexpected.

The finding that during STIM-guided attention the right IPS has a reduced contralateral bias whereas the left hemi IPS has a strong contralateral bias is consistent with early models of lateralization of visual attention in the human brain and previous studies of attention and VSTM (Heilman and Van Den Abell, 1980; Mesulam, 1981; Szczepanski *et al.*, 2010; Sheremata *et al.*, 2010). Sheremata and colleagues found that the left hemisphere showed increased activation in IPS0-2 with high visual short term memory load in the contralateral visual field compared to the ipsilateral visual field. The activation of IPS

increased according to the number of items successfully remembered. In contrast, right IPS did not exhibit this contralateral bias, showing increased activation as a function of the number of items successfully remembered regardless of location in the visual field. This hemispheric asymmetry only becomes apparent at high VSTM loads. Taken together, these studies provide support for the models of neglect that argue that the right dorsal parietal cortex contains maps of both the contralateral and ipsilateral visual field while the left dorsal parietal cortex only contains a map of the contralateral visual field (Heilman and Van Den Abell, 1980; Mesulam, 1981). However, it is uncommon that damage to the dorsal parietal cortex causes hemispatial neglect. Instead, lesions causing hemispatial neglect tend to be to the nodes in the right ventral attention network, including the temporoparietal junction and inferior frontal gyrus (Corbetta *et al.*, 2011), which are important for bottom-up attentional capture and reorienting. It is therefore likely, that the visual field dependent deficits seen in hemispatial neglect are a result of the acute decrease in activity in the right dorsal parietal cortex following right ventral attention network damage. Neglect of the left half of space following right hemisphere stroke may then be the result of an indirect effect of the damage to the ventral attention network such that the dorsal network no longer receives reorienting information and therefore has reduced activity (Sheremata *et al.*, 2010; Ptak and Schneider, 2010).

In recent years, numerous fMRI studies have reported activation within the left parietal cortex for long-term memory retrieval (e.g. Wagner *et al.*, 2005;

Vilberg and Rugg, 2008; Ciaramelli *et al.*, 2010; Hutchinson *et al.*, 2014). The precise contributions of the parietal cortex to long-term memory retrieval is hotly debated and several studies have suggested that at least some of the parietal activation is due to attentional contributions to long-term memory retrieval (Cabeza *et al.*, 2008; Ciaramelli *et al.*, 2010; Hutchinson *et al.*, 2014). The attention to memory hypothesis (Cabeza *et al.*, 2008; Ciaramelli *et al.*, 2010), posits that retrieval of a weak memory requires top-down attention in order to retrieve and thus results in activation of the dorsal parietal cortex, including the IPS and superior parietal lobule. In support of this claim, patients with dorsal parietal cortex damage do not exhibit improved recognition accuracy for validly cued old words and thus could not use memory cues to direct attention to the correct memory representation (Ciaramelli *et al.*, 2010). Furthermore, a recent study found that visuotopically mapped IPS regions tracked reaction time of retrieval responses suggesting that when a memory is more difficult to retrieve and therefore takes more time to make a response, these regions are recruited (Hutchinson *et al.*, 2014).

Activation in the ventral parietal cortex, including the angular gyrus, has been reported widely for strong episodic memory retrieval (Vilberg and Rugg, 2008; Wagner *et al.*, 2005; Hutchinson *et al.*, 2014). It has been debated whether this activation is due to bottom up attentional capture and activation of the homologue to the right temporoparietal junction (Cabeza *et al.*, 2008; Ciaramelli *et al.*, 2010), or whether it is a location of Baddeley's episodic buffer, a temporary

multimodal memory store that allows for interaction between episodic memory retrieval and working memory (Vilberg and Rugg, 2008; Hutchinson et al., 2014). Regardless of the precise contributions of this region to memory retrieval, it is possible that this non-spatiotopic mnemonic activation in the angular gyrus influences activation within spatiotopically mapped IPS in the left hemisphere, just as non-spatiotopic attentional mechanisms influence activation in the right IPS during STIM-guided attention and other attentionally demanding tasks (Sheremata *et al.*, 2010; Szczepanski *et al.*, 2010).

It should be noted that during LTM-guided attention, both the right and left IPS regions showed a reduced contralateral bias (Symmetrically Full Field). I believe this response to the full field in the left hemisphere is due to the high mnemonic demands of this task and the full field response in the right hemisphere is due to the high attentional demands still present in the LTM-guided attention condition. It is possible that in a task with lower attentional demands that an asymmetry would emerge such that the left IPS had a full field representation while the right IPS had a strong contralateral bias.

In a classic study, Bisiach and Luzzatti (1978) asked two patients with hemispatial neglect to recall the details of the Piazza del Duomo in Milan. First, they asked the patients to imagine standing on the steps of the cathedral and describe what they saw. Both patients described the right side of the piazza in great detail while neglecting much of the left side of the piazza. Then, they asked them to imagine standing on the opposite side of the square, facing the

cathedral, and describe what they saw. Again, they described the right side of space, which had previously been the left, neglected, side of space when standing at the opposite end of the piazza. This study provided strong evidence that hemispatial neglect persists when subjects are recreating a mental image using long-term memory, a phenomenon known as representational neglect.

If as the present study suggest, long-term memory-guided attention results in the left IPS regions coding for the full visual field, this could contradict what was found in by Bisiach and Luzzatti. One would expect that if the left hemisphere switches to a full field representation during long-term memory-guided attention, that these patients would not demonstrate neglect of the left visual field during recall of the piazza, because the intact left hemisphere could code for the ipsilateral side of space. Importantly, however, these patients were not engaging in long-term memory guided attention, but rather in mental imagery. A recent study (Moreh *et al.*, 2014), presented neglect patients with stimuli on the left and right side of the screen. They were asked to immediately recall the items presented and after a delay were given a long-term recognition test. The patients exhibited a similar effect as in Bisiach and Luzzatti during the long-term recognition test, such that items originally presented in the left were often categorized as new in the patients. Critically, items that the patients had initially recalled in the immediate recall test did not exhibit the same spatial bias. Items that were immediately recalled were just as likely to be recognized during the long-term memory test if they were presented in the left or right visual field.

Moreh and colleagues suggest that because these items are originally given a verbal tag during the initial encoding task, they do not fall subject to the representational neglect. Furthermore, subjects were able to recall the spatial location in which these items were initially presented, suggesting that these items not only retain a semantic tag, but also a spatial tag. Thus, the present findings can be reconciled with those of Bisiach and Luzzatti by considering the fact that subjects likely had a verbal and spatial tag for each image (i.e. tree in upper left corner), and that subjects had explicit immediate memory for the changes.

The present study provides novel evidence on the influence of memory retrieval on attention. I found that the same vertices within the intraparietal sulcus dynamically change their representations depending on the task demands. During visual drive alone, maps in the left and right IPS have a symmetric contralateral bias. When attentional demands are high, the right IPS switches to respond to both contralateral and ipsilateral targets, while the left IPS continues to have a contralateral bias. Finally, when memory is used to guide spatial attention both the left and right IPS respond to targets in the contralateral and ipsilateral visual fields resulting in diminished contralateral biases in both hemispheres.

## 5.5 Chapter 5 Figures

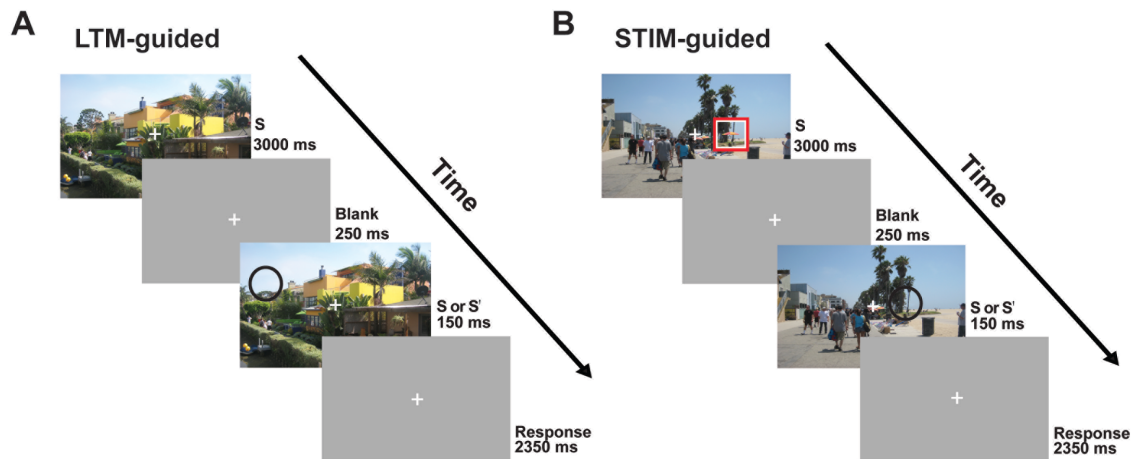


**Figure 5.1** One-shot Change Detection Paradigms. A scene (S) was presented for 3000 ms, followed by a blank screen (250 ms), a very brief presentation (150 ms) of either an identical or altered image (S or S'), and another blank screen (2500 ms). Participants held central fixation while trying to detect whether or not a single change occurred in the scene. A) LTM-guided condition: Participants were instructed to covertly direct attention to the remembered location of the potential change; no explicit spatial cue was provided. B) STIM-guided condition: Participants viewed scenes that they had previously studied without exposure to scene changes. A red and white square explicitly cued the location of the potential scene change, and then disappeared prior to the image change. Trials were blocked such that subjects were attending to either the right or left visual field.

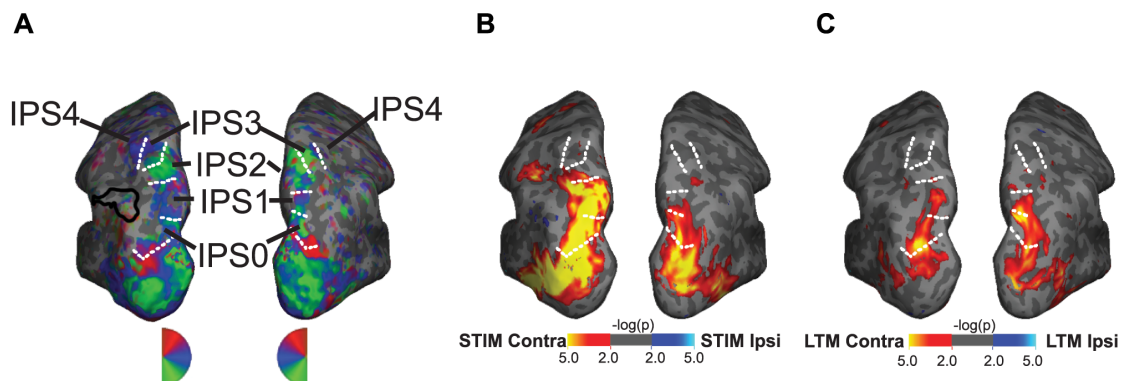


**Figure 5.2** Activation maps for visuoaptic mapping, STIM-guided and LTM-guided Attention. A) IPS0 – IPS4 from a representative subject. B and C) Group average of activation in response to Contralateral vs. Ipsilateral targets in STIM-guided and LTM-guided attention, respectively. Data are mapped onto the brain of the same representative subject as A and white dotted lines represent boundaries between that subject's IPS0-4.

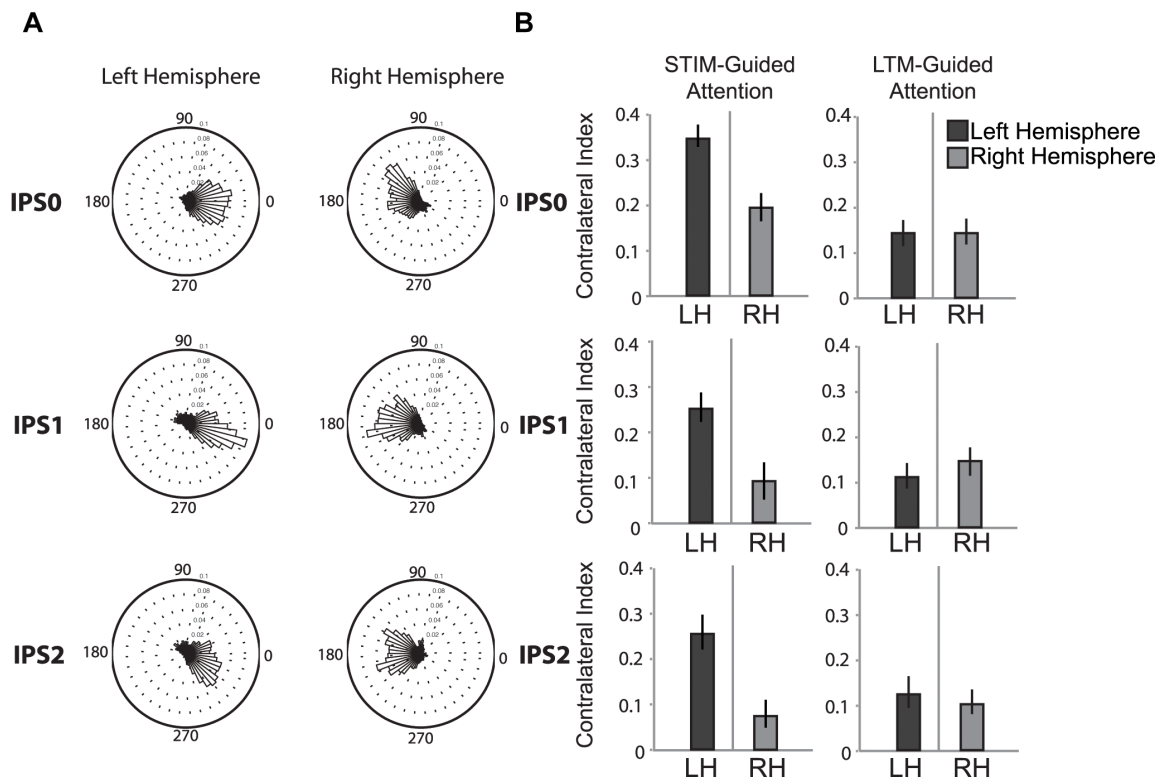


**Figure 5.3** Comparison of contralateral bias during visuotopic mapping, STIM-guided and LTM-guided attention. A) Preferred visual angle for vertices activated during mapping in left and right IPS0 to IPS2. B) Contralateral bias for each IPS region (0-2) for STIM and LTM-guided attention in left and right hemispheres.

## 5.6 Chapter 5 Tables

| Region | Left Hemisphere |           |             |           | Right Hemisphere |           |             |           |       |     |
|--------|-----------------|-----------|-------------|-----------|------------------|-----------|-------------|-----------|-------|-----|
|        | LTM-Guided      |           | STIM-Guided |           | LTM-Guided       |           | STIM-Guided |           | F     | sig |
|        | Contra          | Ipsi      | Contra      | Ipsi      | Contra           | Ipsi      | Contra      | Ipsi      |       |     |
| IPS0   | 0.23±0.04       | 0.13±0.04 | 0.47±0.05   | 0.24±0.05 | 0.17±0.04        | 0.07±0.05 | 0.38±0.05   | 0.25±0.05 | 5.08  | *** |
| IPS1   | 0.32±0.05       | 0.23±0.06 | 0.49±0.05   | 0.30±0.05 | 0.31±0.05        | 0.20±0.04 | 0.48±0.06   | 0.42±0.04 | 11.40 | *** |
| IPS2   | 0.41±0.05       | 0.34±0.05 | 0.58±0.06   | 0.40±0.04 | 0.43±0.05        | 0.34±0.05 | 0.56±0.05   | 0.50±0.05 | 14.05 | *** |
| IPS3   | 0.36±0.07       | 0.32±0.06 | 0.48±0.05   | 0.38±0.05 | 0.31±0.06        | 0.26±0.06 | 0.46±0.07   | 0.42±0.07 | 1.13  | .   |
| IPS4   | 0.29±0.06       | 0.24±0.05 | 0.43±0.07   | 0.33±0.05 | 0.32±0.06        | 0.26±0.05 | 0.47±0.07   | 0.44±0.06 | 1.41  | .   |

**Table 5.1** Percent signal change within left and right retinotopically mapped IPS0-4 during LTM-guided and STIM-guided attention to the contralateral and ipsilateral visual field. Activation is compared to passive viewing. F statistics and p-values refer to the significance of the three-way (Hemisphere x Condition x Visual Field) interaction ( \*\*\* reflects  $p < 0.0001$ , . reflects  $p > 0.05$ )

**Chapter 6: Summary and Discussion**

## **6.1 Summary of Results**

### *6.1.1 Restatement of Original Goals*

The experiments presented here were conducted to elucidate the mechanisms of long-term memory-guided attention. Here, I presented four experiments with the following goals: A) to test the hypothesis that humans can use long-term memory to guide attention to multiple discrete locations simultaneously [Chapter 2], B) use fMRI to determine whether the cognitive control network supports long-term memory-guided attention in a change detection task [Chapter 3], C) show that recruitment of the cognitive control network during long-term memory-guided attention does not reflect general memory retrieval, but is specific to the cooperation between attention and long-term memory [Chapter 4], and finally D) to differentiate how LTM-guided and stimulus-guided attention differentially affect the spatial responsivity of maps within the intraparietal sulcus.

### *6.1.2 Summary of Results from Experiment 1*

Experiments 1A and 1B were behavioral experiments designed to determine whether humans can use long-term memory to guide attention to multiple spatial locations in a change detection task. Experiment 1A used a change detection task in which participants learned 0, 1, 2, or 3 changes in scene photographs. At test, they were presented with a target image and instructed to covertly attend to all possible change locations. After a brief blank

screen, a probe image was presented and participants responded whether or not a change occurred between the target and probe. Results indicated that prior exposure to scene changes in the 1, 2, or 3 change condition significantly improved performance compared to the 0-studied change condition. Moreover, capacity was significantly higher in the 2- and 3-studied change condition than the 1-studied change condition indicating that participants were able to attend to more information in these conditions. However, capacity did not increase above 1, making claims that participants were able to divide attention difficult.

In Experiment 1A, participants were only exposed to each image and each change once. I hypothesized that participants did not have enough exposure to have robust memory for each of the changes in each scene. Therefore, in Experiment 1A, I exposed participants to fewer scenes, each with three changes, for a total of four exposures. I also measured the reaction time to find each change at each exposure. Reaction time to find the changes decreased with each exposure. Furthermore, reaction times were used to estimate how many changes participants had encoded after each exposure and found that after the third exposure, participants had encoded all changes. At test, subjects performed the same one-shot change detection task. However, in Experiment 1B, the probe duration varied. Results indicated that capacity for the three change images was significantly higher than 1, and that performance did not change across different probe durations, suggesting that participants were not using extra time to move their attentional spotlight from one location to another. These results suggest that

participants are able to divide their attention to more than one discrete location using a long-term memory cue simultaneously. Furthermore, the experiments designed in Experiment 1A and 1B were adapted for use in the second and fourth functional MRI presented in Chapters 3 and 5, respectively.

### *6.1.3 Summary of Results from Experiment 2*

The second experiment, presented in Chapter 3, was designed to determine the neural networks underlying long-term memory-guided attention in a functional MRI study. The goals were to determine 1) whether long-term memory-guided attention recruits distinct cortical regions from stimulus-guided attention 2) whether these regions are located within the cognitive control network and 3) whether these regions are functionally connected to one another at rest, forming a subnetwork. Using a modified version of the task developed in Experiment 1, I directly contrasted long-term memory-guided attention with stimulus-guided attention in the same participants. I independently defined regions of interest based on a publically available functional parcellation of the cortex. Results indicated that three posterior nodes of the cognitive control network (posterior precuneus, posterior callosal sulcus, and lateral intraparietal sulcus), were more strongly recruited for long-term memory-guided attention than stimulus-guided attention. Moreover, at rest these three regions form a subnetwork. This is the first experiment to show distinct cortical regions recruited for memory-guided attention compared to stimulus-guided attention and the first to explicitly map out the connectivity between these regions. I conclude that

within the broader cognitive control network, a subnetwork exists that is recruited for memory-guided attention.

#### *6.1.4 Summary of Results from Experiment 3*

The third experiment, presented in Chapter 4, was designed to 1) replicate the findings of Experiment 2 in a different paradigm 2) determine whether the regions found to be more strongly recruited for memory-guided attention compared to stimulus-guided attention were specific to long-term memory-guided attention or are recruited for a more general memory retrieval function. Results showed that in a target detection task using objects, I also saw recruitment of the posterior precuneus, posterior callosal sulcus, and lateral intraparietal sulcus for long-term memory-guided attention compared to stimulus-guided attention. Furthermore, I found no differences in activation within these regions between the long-term memory retrieval task and the stimulus-guided attention task. Taken together, these findings indicate that these three regions are preferentially recruited when long-term memory is used to guide spatial attention and not when memory or attention is functioning alone.

#### *6.1.5 Summary of Results from Experiment 4*

Finally, the fourth experiment, presented in Chapter 5, investigated how visual and memory cues affect the spatial responsivity of maps within the parietal cortex. I performed visuotopic mapping on each participant to define IPS0-IPS4. Results showed that over 85% of the vertices in both the left and right IPS regions responded preferentially to a visual stimulus in the contralateral visual

field, indicating a strong contralateral bias under visual stimulation alone. Under purely visual drive, the spatial responsivity of the maps in left and right parietal cortex are symmetrically contralateral. Using the same change-detection data from Experiment 2, I was able to directly compare when participants are attending to the left or right visual field using a memory or visual cue. During the visual stimulus-guided attention condition, the visuotopically mapped IPS in the left hemisphere continued to have a strong contralateral bias, while right visuotopically mapped IPS responded strongly to targets in both the contralateral and ipsilateral visual fields, and thus showed a reduced contralateral bias. This finding indicates that during an attentionally demanding task, an asymmetry emerges such that the spatial responsivity of the right IPS switches to the full visual field, whereas the responsivity of the left IPS remains strongly contralateral. When participants used long-term memory to guide attention, both left and right visuotopically mapped IPS responded strongly to targets in both the left and right visual fields, indicating a reduced contralateral bias in both hemispheres, illustrating that the spatial responsivity of both the left and right IPS switches to be symmetrically bilateral under LTM-guided attention conditions. The results from the stimulus-guided attention condition replicated previous results from our laboratory and other groups that at high attentional load, the right hemisphere IPS maps respond to the full visual field while the left IPS continues to code strongly for the contralateral visual field. These results suggest that the right hemisphere may contain non-spatiotopic attentional mechanisms that

change the response pattern of spatiotopically mapped IPS. The results from the memory-guided attention condition further suggest that the maps within the left IPS can also change their spatial responsivity if memory is used to guide spatial attention, suggesting that the left hemisphere contains non-spatiotopic mnemonic mechanisms that can influence the spatial responsivity of visuotopically mapped IPS. It is likely that the right IPS also showed a reduced contralateral bias in the long-term memory-guided condition due to the high attentional demands of the task.

## **6.2 Discussion**

In our everyday lives, we are bombarded with far more visual information than our attentional capacities are equipped to process. Yet, human visual performance in complex visual environments is superb. One important factor that helps enhance visual performance is long-term memory, which can help guide attention to the most relevant information. Historically, attention and memory have been studied by distinct groups of scientists and competition between attention and memory in the brain has been the focus of much of the neural literature (e.g. Fox et al., 2005; Sestieri et al, 2010). However, recent research has highlighted that cooperation between these systems may underlie an important aspect of our ability to process complex visual environments (Chun and Jiang, 1998, Summerfield et al., 2006, 2011; Stokes et al., 2012; Hutchinson and Turk-Browne, 2012). The experiments discussed in this dissertation examined the mechanisms by which long-term memory guides spatial attention.

### *6.2.1 Long-Term Memory Guided Divided Attention*

The visual world contains more information than our attentional capacities can process at a given moment; dividing the attentional spotlight into multiple spotlights can aid efficient processing (Shaw and Shaw, 1977; Awh and Pashler, 2000; McMains and Somers, 2004; 2005). While much debate has surrounded whether humans can divide attention and process stimuli in parallel or whether this phenomenon reflects rapid switching of attention (Tsal et al., 1983; Jans et al., 2010), the behavioral advantage of selecting multiple objects to attend to is clear. Previous studies of attention to multiple spatial locations have all used exogenous or endogenous cues. The experiments presented in the Chapter 2 of this dissertation expand on this literature by exploring whether long-term memory can be used as a cue to guide attention to multiple discrete locations. Results from these experiments suggest that once stimuli are well learned, humans can indeed attend to more than one spatial location. Furthermore, these experiments found no behavioral benefit when participants were given additional time to process the probe image, suggesting that they were not moving their attentional spotlight rapidly, but rather dividing the spotlight to discrete locations simultaneously. Finally, the use of naturalistic scenes and long-term memory cues may provide a more ecologically relevant example of how humans attend to complex visual environments in the real world.

### *6.2.2 Cortical Mechanisms Supporting Long-Term Memory-Guided Attention*

The results of this dissertation elucidate the contributions of a subnetwork within the cognitive control network, including the posterior precuneus, the posterior callosal sulcus and lateral intraparietal sulcus, to long-term memory-guided attention. These experiments are the first to find cortical regions are recruited more strongly for long-term memory-guided attention than stimulus-guided attention and make important contributions to understanding the mechanisms by which previous experience can guide attention.

The dorsal attention network is recruited for top-down, goal directed attentional tasks (Corbetta et al., 2002). In contrast, long-term memory retrieval is supported by the default mode network and medial temporal lobe structures (Buckner et al., 2008). These cortical networks have strongly competitive interactions such that when one is activated, the other is deactivated (Raichle et al., 2001; Fox et al., 2005; Todd et al., 2005; Sestieri et al., 2010; 2011; Spreng et al., 2012). In fact, the default mode network was first defined as the “task-negative network” because researchers continually reported a network of brain regions that were deactivated during an attentionally demanding task (Raichle et al., 2001). Despite this neural competition, a rich behavioral literature in the last twenty years has highlighted the behavioral advantage that long-term memory can provide in guiding attention (Chun and Jiang, 1998; Chun, 2000; Werner and Thies, 2000, Summerfield et al., 2006; Olivers, 2011). Previous work has highlighted largely overlapping cortical regions of the dorsal attention network that support long-term memory-guided attention and stimulus-guided attention

with the only unique region recruited for long-term memory-guided attention being the hippocampus (Summerfield et al., 2006). However, the use of volume-based group averaging techniques may have made it difficult to identify the unique cortical contributions to long-term memory-guided attention. Other studies have not directly contrasted long-term memory-guided and stimulus-guided attention and therefore have been unable to report regions that uniquely support cooperation between long-term memory and attention (Stokes et al., 2012).

Experiments in this dissertation extend the prior literature by directly contrasting long-term memory-guided and stimulus-guided attention and using pre-defined surfaced based regions of interest. Here, I showed that three regions of the cognitive control network, latIPS, CaS-p and PrC-p are all recruited more strongly during long-term memory guided attention compared to stimulus-guided attention.

Furthermore, these regions have been shown to have reduced cortical thickness in children with ADHD (Nars et al., 2009; Shaw et al., 2006; McLaughlin et al., 2014). It is possible that if these regions are not functioning properly in patients with ADHD that the symptoms of this disorder are partially impacted by a deficit in the ability to interface between attention and memory. The results from this dissertation provide an important contribution to the growing literature on memory-guided attention (Hutchinson and Turk-Browne, 2012).

*6.2.3 The long-term memory-guided attention subnetwork is specifically recruited for LTM-guided attention and not memory retrieval*

The results presented in Chapter 3 made an important discovery that regions within the cognitive control network are specifically recruited for long-term memory-guided attention compared to stimulus-guided attention. However, recent work has suggested that these three regions, the posterior precuneus, posterior callosal sulcus, and lateral intraparietal sulcus, are recruited for long-term memory retrieval (Power et al., 2011, 2014; Nelson et al., 2013). In the experiment presented in Chapter 3 of this dissertation, long-term memory-guided attention and long-term memory retrieval are confounded. Therefore, the experiment presented in Chapter 4 of this dissertation was designed to contrast long-term memory guided attention with an LTM retrieval condition and a stimulus-guided attention condition in the same participants and scan session. Results from this experiment found that these regions are uniquely recruited for long-term memory-guided attention and likely not serving a general memory retrieval function. Taken together, the results from this dissertation indicate that regions of the cognitive control network are recruited specifically when long-term memory is used to guide spatial attention compared to when attention or long-term memory are acting alone.

#### *6.2.4 Visuotopic maps in parietal cortex change their spatial specificity depending on attentional cue type*

Results from this dissertation indicate that visuotopically mapped regions of the IPS can change their spatial responsivity depending on the task demands. Under purely visual drive, these maps have a symmetrically contralateral bias.

During an attentionally demanding task, such as the stimulus-guided attention condition, presented here, a hemispheric asymmetry emerges such that the right hemisphere responds to targets in the full visual field while the left continues to have a strong contralateral bias. Finally, during LTM-guided attention, the symmetry between the hemispheres is restored, but both the left and right IPS have a reduced contralateral bias and respond to targets in the full visual field.

Hemispatial neglect is a common neurological disorder that results from damage to the right parietal or frontal cortex (Buxbaum et al., 2004; Corbetta et al., 2005; Corbetta and Shulman, 2011). Unilateral neglect is common for the left visual field, but very rare for the right visual field (Stone et al., 1993). Early models of neglect suggested that the right hemisphere contains representational maps of the visual world that encompass both the left and right hemifields whereas the left hemisphere only contains a map of the right visual field (Heilman and Van Den Abell, 1980). According to this model, if the left hemisphere were damaged, the right hemisphere would be able to compensate and code for the left and right visual fields, but if the right hemisphere were damaged, there would be no representational maps to code for the left visual field, resulting in hemispatial neglect. However, visuotopic mapping studies have identified symmetric maps within the intraparietal sulcus including at least five maps of the contralateral visual field (Serenio et al., 2001; Silver et al., 2005; Wandell et al., 2007; Swisher et al., 2007). Recent work has elucidated this paradox by showing that a hemispheric asymmetry emerges at high attention and short-term memory

loads (Szcepaniski et al., 2010; Sheremata et al., 2010; Sheremata and Silver, 2015), such that the left IPS continues to respond to targets in the contralateral visual field, while the right IPS switches its spatial responsivity to the full visual field. Results from this dissertation make an important replication of this finding by showing that during stimulus-guided attention in a change detection task on visual scenes, the right IPS responds to targets in the full visual field whereas the left IPS continues to have a strong contralateral bias. This finding also extends previous findings with the use of naturalistic images.

Furthermore, results presented in this dissertation show when subjects use memory to guide their attention, the left IPS also switches its spatial responsivity to the full visual field. These findings are consistent with the known left lateralized effects of long-term memory retrieval (e.g. Kahn et al., 2004; Wagner et al., 2005; Berryhill et al., 2007; Hutchinson et al., 2014). Together these findings point to complementary influences in the spatial responsivity of the right and left IPS indicating that the right IPS may contain non-spatiotopic attentional influences and the left IPS may contain non-spatiotopic mnemonic mechanisms.

### **6.3 Conclusions**

The results of these experiments help us understand the behavioral and neural mechanisms by which long-term memory guides spatial attention. The behavioral experiments presented here extend previous work exploring how humans divide spatial attention by showing that we can use long-term memory to

guide attention to more than one spatial location simultaneously. These experiments provided an important development to the field by using naturalistic scenes and offer evidence that in the real world, humans may combine the benefits of both long-term memory-guided attention and divided attention to enhance performance in complex visual environments. The fMRI experiments presented here provide an important bridge to understanding the neural mechanisms by which long-term memory and attention cooperate. Results in this dissertation indicate that a posterior subnetwork of the Cognitive Control Network, including the posterior precuneus, posterior callosal sulcus and lateral intraparietal sulcus are preferentially recruited during long-term memory-guided attention compared to stimulus-guided attention in a change detection task. This result was replicated in a separate experiment using a target detection task and further extended the finding by showing that these regions are specifically recruited for long-term memory-guided attention and are not supporting a general long-term memory retrieval function. Finally, work in this dissertation extends previous work showing that contralateral visuotopic maps in the parietal cortex dynamically change their spatial responsivity depending the attentional demands of the task, suggesting that the right parietal regions may be influenced by non-spatiotopic attentional mechanisms and left parietal regions may be influenced by non-spatiotopic mnemonic mechanisms. Taken together, these experiments provide an important contribution to understanding the neural and behavioral mechanisms by which long-term memory and attention interact.

## References

- Adamo, M., Pun, C., Pratt, J., & Ferber, S. (2008). Your divided attention, please! The maintenance of multiple attentional control sets over distinct regions in space. *Cognition*, *107*(1), 295–303. doi:10.1016/j.cognition.2007.07.003
- Ally, B. A., Simons, J. S., McKeever, J. D., Peers, P. V., & Budson, A. E. (2008). Parietal contributions to recollection: electrophysiological evidence from aging and patients with parietal lesions. *Neuropsychologia*, *46*(7), 1800–1812. doi:10.1016/j.neuropsychologia.2008.02.026
- Alvarez, G. A., & Franconeri, S. L. (2007). How many objects can you track? Evidence for a resource-limited attentive tracking mechanism. *Journal of Vision*, *7*(13), 14.1–10. doi:10.1167/7.13.14
- Andrews-Hanna, J. R., Reidler, J. S., Huang, C., & Buckner, R. L. (2010). Evidence for the default network's role in spontaneous cognition. *Journal of Neurophysiology*, *104*(1), 322–335. doi:10.1152/jn.00830.2009
- Awh, E., & Pashler, H. (2000). Evidence for split attentional foci. *Journal of Experimental Psychology. Human Perception and Performance*, *26*(2), 834–846.
- Baleydier, C., & Mauguière, F. (1987). Network organization of the connectivity between parietal area 7, posterior cingulate cortex and medial pulvinar nucleus: a double fluorescent tracer study in monkey. *Experimental Brain Research*, *66*(2), 385–393.
- Beckmann, M., Johansen-Berg, H., & Rushworth, M. F. S. (2009). Connectivity-based parcellation of human cingulate cortex and its relation to functional specialization. *The Journal of Neuroscience : the Official Journal of the Society for Neuroscience*, *29*(4), 1175–1190. doi:10.1523/JNEUROSCI.3328-08.2009
- Berryhill, M. E., Chein, J., & Olson, I. R. (2011). At the intersection of attention and memory: the mechanistic role of the posterior parietal lobe in working memory. *Neuropsychologia*, *49*(5), 1306–1315. doi:10.1016/j.neuropsychologia.2011.02.033
- Berryhill, M. E., Phuong, L., Picasso, L., Cabeza, R., & Olson, I. R. (2007). Parietal lobe and episodic memory: bilateral damage causes impaired free recall of autobiographical memory. *The Journal of Neuroscience : the Official Journal of the Society for Neuroscience*, *27*(52), 14415–14423. doi:10.1523/JNEUROSCI.4163-07.2007

- Bettencourt, K. C., & Somers, D. C. (2009). Effects of target enhancement and distractor suppression on multiple object tracking capacity. *Journal of Vision*, 9(7), 9–9. doi:10.1167/9.7.9
- Bisiach, E., & Luzzatti, C. (1978). Unilateral neglect of representational space. *Cortex; a Journal Devoted to the Study of the Nervous System and Behavior*, 14(1), 129–133.
- Brady, T. F., Konkle, T., Alvarez, G. A., & Oliva, A. (2008). Visual long-term memory has a massive storage capacity for object details. *Proceedings of the National Academy of Sciences of the United States of America*, 105(38), 14325–14329. doi:10.1073/pnas.0803390105
- Braver, T. S. (2012). The variable nature of cognitive control: a dual mechanisms framework. *Trends in Cognitive Sciences*, 16(2), 106–113. doi:10.1016/j.tics.2011.12.010
- Brockmole, J. R., & Henderson, J. M. (2006). Recognition and attention guidance during contextual cueing in real-world scenes: evidence from eye movements. *Quarterly Journal of Experimental Psychology (2006)*, 59(7), 1177–1187. doi:10.1080/17470210600665996
- Brown, T. I., Ross, R. S., Tobyne, S. M., & Stern, C. E. (2012). Cooperative interactions between hippocampal and striatal systems support flexible navigation. *NeuroImage*, 60(2), 1316–1330. doi:10.1016/j.neuroimage.2012.01.046
- Buckner, R. L., & Vincent, J. L. (2007). Unrest at rest: default activity and spontaneous network correlations. *NeuroImage*, 37(4), 1091–6– discussion 1097–9. doi:10.1016/j.neuroimage.2007.01.010
- Buckner, R. L., Andrews-Hanna, J. R., & Schacter, D. L. (2008). The brain's default network: anatomy, function, and relevance to disease. *Annals of the New York Academy of Sciences*, 1124(1), 1–38. doi:10.1196/annals.1440.011
- Buxbaum, L. J., Ferraro, M. K., Veramonti, T., Farne, A., Whyte, J., Ladavas, E., et al. (2004). Hemispatial neglect: Subtypes, neuroanatomy, and disability. *Neurology*, 62(5), 749–756.
- Cabeza, R. (2008). Role of parietal regions in episodic memory retrieval: the dual attentional processes hypothesis. *Neuropsychologia*, 46(7), 1813–1827. doi:10.1016/j.neuropsychologia.2008.03.019

- Cabeza, R., Ciaramelli, E., Olson, I. R., & Moscovitch, M. (2008). The parietal cortex and episodic memory: an attentional account. *Nature Reviews Neuroscience*, 9(8), 613–625. doi:10.1038/nrn2459
- Carp, J. (2013). Optimizing the order of operations for movement scrubbing: Comment on Power et al. *NeuroImage*, 76, 436–438. doi:10.1016/j.neuroimage.2011.12.061
- Cavanagh, P., & Alvarez, G. A. (2005). Tracking multiple targets with multifocal attention. *Trends in Cognitive Sciences*, 9(7), 349–354. doi:10.1016/j.tics.2005.05.009
- Cave, K. R., & Bichot, N. P. (1999). Visuospatial attention: beyond a spotlight model. *Psychonomic Bulletin & Review*, 6(2), 204–223.
- Cave, K. R., Bush, W. S., & Taylor, T. G. G. (2010). Split attention as part of a flexible attentional system for complex scenes: comment on Jans, Peters, and De Weerd (2010). *Psychological Review*, 117(2), 685–696. doi:10.1037/a0019083
- Chiu, Y.-C., & Yantis, S. (2009). A domain-independent source of cognitive control for task sets: shifting spatial attention and switching categorization rules. *The Journal of Neuroscience : the Official Journal of the Society for Neuroscience*, 29(12), 3930–3938. doi:10.1523/JNEUROSCI.5737-08.2009
- Chun, M. (2000). Contextual cueing of visual attention. *Trends in Cognitive Sciences*, 4(5), 170–178.
- Chun, M. M., & Jiang, Y. (1998). Contextual cueing: implicit learning and memory of visual context guides spatial attention. *Cognitive Psychology*, 36(1), 28–71. doi:10.1006/cogp.1998.0681
- Chun, M. M., & Jiang, Y. (2003). Implicit, long-term spatial contextual memory. *Journal of Experimental Psychology. Learning, Memory, and Cognition*, 29(2), 224–234.
- Chun, M. M., & Turk-Browne, N. B. (2007). Interactions between attention and memory. *Current Opinion in Neurobiology*, 17(2), 177–184. doi:10.1016/j.conb.2007.03.005
- Ciaramelli, E., Grady, C. L., & Moscovitch, M. (2008). Top-down and bottom-up attention to memory: a hypothesis (AtoM) on the role of the posterior parietal

- cortex in memory retrieval. *Neuropsychologia*, 46(7), 1828–1851.  
doi:10.1016/j.neuropsychologia.2008.03.022
- Ciaramelli, E., Grady, C., Levine, B., Ween, J., & Moscovitch, M. (2010). Top-down and bottom-up attention to memory are dissociated in posterior parietal cortex: neuroimaging and neuropsychological evidence. *The Journal of Neuroscience : the Official Journal of the Society for Neuroscience*, 30(14), 4943–4956. doi:10.1523/JNEUROSCI.1209-09.2010
- Cohen, J. D., Perlstein, W. M., Braver, T. S., Nystrom, L. E., Noll, D. C., Jonides, J., & Smith, E. E. (1997). Temporal dynamics of brain activation during a working memory task. *Nature*, 386(6625), 604–608. doi:10.1038/386604a0
- Cole, M. W., & Schneider, W. (2007). The cognitive control network: Integrated cortical regions with dissociable functions. *NeuroImage*, 37(1), 343–360. doi:10.1016/j.neuroimage.2007.03.071
- Conci, M., Zellin, M., & Müller, H. J. (2012). Whatever after next? Adaptive predictions based on short- and long-term memory in visual search. *Frontiers in Psychology*, 3, 409. doi:10.3389/fpsyg.2012.00409
- Corbetta, M., & Shulman, G. L. (2002). Control of goal-directed and stimulus-driven attention in the brain. *Nature Reviews. Neuroscience*, 3(3), 201–215. doi:10.1038/nrn755
- Corbetta, M., & Shulman, G. L. (2011). Spatial neglect and attention networks. *Annual Review of Neuroscience*, 34(1), 569–599. doi:10.1146/annurev-neuro-061010-113731
- Corbetta, M., Tansy, A. P., Stanley, C. M., Astafiev, S. V., Snyder, A. Z., & Shulman, G. L. (2005). A functional MRI study of preparatory signals for spatial location and objects. *Neuropsychologia*, 43(14), 2041–2056. doi:10.1016/j.neuropsychologia.2005.03.020
- Courtney S. M. (2004). Attention and cognitive control as emergent properties of information representation in working memory. *Cognitive, Affective, & Behavioral Neuroscience*. 4(4), 501-516.
- Cowan, N. (1998). Visual and auditory working memory capacity. *Trends in Cognitive Sciences*, 2(3), 77.
- Cowan, N. (2001). The magical number 4 in short-term memory: a reconsideration of mental storage capacity. *The Behavioral and Brain*

- Sciences*, 24(1), 87–114– discussion 114–85.
- Dale, A. M., Fischl, B., & Sereno, M. I. (1999). Cortical surface-based analysis. I. Segmentation and surface reconstruction. *NeuroImage*, 9(2), 179–194. doi:10.1006/nimg.1998.0395
- Dosenbach, N. U. F., Fair, D. A., Miezin, F. M., Cohen, A. L., Wenger, K. K., Dosenbach, R. A. T., et al. (2007). Distinct brain networks for adaptive and stable task control in humans. *Proceedings of the National Academy of Sciences of the United States of America*, 104(26), 11073–11078. doi:10.1073/pnas.0704320104
- Downing, P., & Dodds, C. (2010). Competition in visual working memory for control of search. *Visual Cognition*, 11(6), 689–703. doi:10.1080/13506280344000446
- Esterman, M., Chiu, Y.-C., Tamber-Rosenau, B. J., & Yantis, S. (2009). Decoding cognitive control in human parietal cortex. *Proceedings of the National Academy of Sciences of the United States of America*, 106(42), 17974–17979. doi:10.1073/pnas.0903593106
- Fischl, B. (2012). FreeSurfer. *NeuroImage*, 62(2), 774–781. doi:10.1016/j.neuroimage.2012.01.021
- Fischl, B., Sereno, M. I., & Dale, A. M. (1999a). Cortical surface-based analysis. II: Inflation, flattening, and a surface-based coordinate system. *NeuroImage*, 9(2), 195–207. doi:10.1006/nimg.1998.0396
- Fischl, B., Sereno, M. I., Tootell, R. B., & Dale, A. M. (1999b). High-resolution intersubject averaging and a coordinate system for the cortical surface. *Human Brain Mapping*, 8(4), 272–284. doi:10.1002/(SICI)1097-0193(1999)8:4<272::AID-HBM10>3.0.CO;2-4
- Forman, S. D., Cohen, J. D., Fitzgerald, M., Eddy, W. F., Mintun, M. A., & Noll, D. C. (1995). Improved assessment of significant activation in functional magnetic resonance imaging (fMRI): use of a cluster-size threshold. *Magnetic Resonance in Medicine : Official Journal of the Society of Magnetic Resonance in Medicine / Society of Magnetic Resonance in Medicine*, 33(5), 636–647.
- Fox, M. D., Snyder, A. Z., Zacks, J. M., & Raichle, M. E. (2006). Coherent spontaneous activity accounts for trial-to-trial variability in human evoked brain responses. *Nature Neuroscience*, 9(1), 23–25. doi:10.1038/nn1616
- Gilchrist, A. L., & Cowan, N. (2011). Can the focus of attention accommodate

- multiple, separate items? *Journal of Experimental Psychology. Learning, Memory, and Cognition*, 37(6), 1484–1502. doi:10.1037/a0024352
- Greicius, M. D., Supekar, K., Menon, V., & Dougherty, R. F. (2009). Resting-state functional connectivity reflects structural connectivity in the default mode network. *Cerebral Cortex (New York, N.Y. : 1991)*, 19(1), 72–78. doi:10.1093/cercor/bhn059
- Gundersen, H., Specht, K., Grüner, R., Ersland, L., & Hugdahl, K. (2008). Separating the effects of alcohol and expectancy on brain activation: an fMRI working memory study. *NeuroImage*, 42(4), 1587–1596. doi:10.1016/j.neuroimage.2008.05.037
- Hagler, D. J., & Sereno, M. I. (2006). Spatial maps in frontal and prefrontal cortex. *NeuroImage*, 29(2), 567–577. doi:10.1016/j.neuroimage.2005.08.058
- He, B. J., Snyder, A. Z., Vincent, J. L., Epstein, A., Shulman, G. L., & Corbetta, M. (2007). Breakdown of functional connectivity in frontoparietal networks underlies behavioral deficits in spatial neglect. *Neuron*, 53(6), 905–918. doi:10.1016/j.neuron.2007.02.013
- Heilman, K. M., & Van Den Abell, T. (1980). Right hemisphere dominance for attention: the mechanism underlying hemispheric asymmetries of inattention (neglect). *Neurology*, 30(3), 327–330.
- Henderson, J. M., & Hollingworth, A. (1999). High-level scene perception. *Annual Review of Psychology*, 50(1), 243–271. doi:10.1146/annurev.psych.50.1.243
- Hollingworth, A. (2004). Constructing visual representations of natural scenes: the roles of short- and long-term visual memory. *Journal of Experimental Psychology. Human Perception and Performance*, 30(3), 519–537. doi:10.1037/0096-1523.30.3.519
- Hollingworth, A. (2005). The relationship between online visual representation of a scene and long-term scene memory. *Journal of Experimental Psychology. Learning, Memory, and Cognition*, 31(3), 396–411. doi:10.1037/0278-7393.31.3.396
- Hollingworth, A., & Henderson, J. M. (2004). Sustained change blindness to incremental scene rotation: a dissociation between explicit change detection and visual memory. *Perception & Psychophysics*, 66(5), 800–807.
- Huijbers, W., Pennartz, C. M. A., Rubin, D. C., & Daselaar, S. M. (2011). Imagery

- and retrieval of auditory and visual information: neural correlates of successful and unsuccessful performance. *Neuropsychologia*, 49(7), 1730–1740. doi:10.1016/j.neuropsychologia.2011.02.051
- Hutchinson, J. B., & Turk-Browne, N. B. (2012). Memory-guided attention: control from multiple memory systems. *Trends in Cognitive Sciences*, 16(12), 576–579. doi:10.1016/j.tics.2012.10.003
- Hutchinson, J. B., Uncapher, M. R., & Wagner, A. D. (2009). Posterior parietal cortex and episodic retrieval: convergent and divergent effects of attention and memory. *Learning & Memory (Cold Spring Harbor, N.Y.)*, 16(6), 343–356. doi:10.1101/lm.919109
- Hutchinson, J. B., Uncapher, M. R., Weiner, K. S., Bressler, D. W., Silver, M. A., Preston, A. R., & Wagner, A. D. (2014). Functional heterogeneity in posterior parietal cortex across attention and episodic memory retrieval. *Cerebral Cortex (New York, N.Y. : 1991)*, 24(1), 49–66. doi:10.1093/cercor/bhs278
- Jaeger, A., Konkell, A., & Dobbins, I. G. (2013). Unexpected novelty and familiarity orienting responses in lateral parietal cortex during recognition judgment. *Neuropsychologia*, 51(6), 1061–1076. doi:10.1016/j.neuropsychologia.2013.02.018
- Jans, B., Peters, J. C., & De Weerd, P. (2010). Visual spatial attention to multiple locations at once: the jury is still out. *Psychological Review*, 117(2), 637–684. doi:10.1037/a0019082
- Jiang, Y. V., Swallow, K. M., & Rosenbaum, G. M. (2013). Guidance of spatial attention by incidental learning and endogenous cuing. *Psychological Review*, 120(1), 285–297. doi:10.1037/a0028022
- Kahn, I., Andrews-Hanna, J. R., Vincent, J. L., Snyder, A. Z., & Buckner, R. L. (2008). Distinct cortical anatomy linked to subregions of the medial temporal lobe revealed by intrinsic functional connectivity. *Journal of Neurophysiology*, 100(1), 129–139. doi:10.1152/jn.00077.2008
- Kahn, I., Davachi, L., & Wagner, A. D. (2004). Functional-neuroanatomic correlates of recollection: implications for models of recognition memory. *The Journal of Neuroscience : the Official Journal of the Society for Neuroscience*, 24(17), 4172–4180. doi:10.1523/JNEUROSCI.0624-04.2004
- Konen, C. S., & Kastner, S. (2008). Representation of eye movements and stimulus motion in topographically organized areas of human posterior

- parietal cortex. *The Journal of Neuroscience : the Official Journal of the Society for Neuroscience*, 28(33), 8361–8375.  
doi:10.1523/JNEUROSCI.1930-08.2008
- Leech, R., Kamourieh, S., Beckmann, C. F., & Sharp, D. J. (2011). Fractionating the default mode network: distinct contributions of the ventral and dorsal posterior cingulate cortex to cognitive control. *The Journal of Neuroscience : the Official Journal of the Society for Neuroscience*, 31(9), 3217–3224.  
doi:10.1523/JNEUROSCI.5626-10.2011
- Levin, D. T., & Simons, D. J. (1997). Failure to detect changes to attended objects in motion pictures. *Psychonomic Bulletin & Review*, 4(4), 501–506.  
doi:10.3758/BF03214339
- Lewis-Peacock, J. A., & Postle, B. R. (2008). Temporary activation of long-term memory supports working memory. *The Journal of Neuroscience : the Official Journal of the Society for Neuroscience*, 28(35), 8765–8771.  
doi:10.1523/JNEUROSCI.1953-08.2008
- Lewis-Peacock, J. A., & Postle, B. R. (2012). Decoding the internal focus of attention. *Neuropsychologia*, 50(4), 470–478.  
doi:10.1016/j.neuropsychologia.2011.11.006
- Luck, S. J., & Vogel, E. K. (1997). The capacity of visual working memory for features and conjunctions. *Nature*, 390(6657), 279–281. doi:10.1038/36846
- Maddock, R. J., Garrett, A. S., & Buonocore, M. H. (2001). Remembering familiar people: the posterior cingulate cortex and autobiographical memory retrieval. *Neuroscience*, 104(3), 667–676.
- McLaughlin, K. A., Sheridan, M. A., Winter, W., Fox, N. A., Zeanah, C. H., & Nelson, C. A. (2014). Widespread reductions in cortical thickness following severe early-life deprivation: a neurodevelopmental pathway to attention-deficit/hyperactivity disorder. *Biological Psychiatry*, 76(8), 629–638.  
doi:10.1016/j.biopsych.2013.08.016
- McMains, S. A., & Somers, D. C. (2004). Multiple spotlights of attentional selection in human visual cortex. *Neuron*, 42(4), 677–686.
- McMains, S. A., & Somers, D. C. (2005). Processing efficiency of divided spatial attention mechanisms in human visual cortex. *The Journal of Neuroscience : the Official Journal of the Society for Neuroscience*, 25(41), 9444–9448.  
doi:10.1523/JNEUROSCI.2647-05.2005

- Mesulam, M. M. (1981). A cortical network for directed attention and unilateral neglect. *Annals of Neurology*, *10*(4), 309–325. doi:10.1002/ana.410100402
- Moores, E., Laiti, L., & Chelazzi, L. (2003). Associative knowledge controls deployment of visual selective attention. *Nature Neuroscience*, *6*(2), 182–189. doi:10.1038/nn996
- Moreh, E., Malkinson, T. S., Zohary, E., & Soroker, N. (2014). Visual memory in unilateral spatial neglect: immediate recall versus delayed recognition. *Journal of Cognitive Neuroscience*, *26*(9), 2155–2170. doi:10.1162/jocn\_a\_00603
- Müller, M. M., Malinowski, P., Gruber, T., & Hillyard, S. A. (2003). Sustained division of the attentional spotlight. *Nature*, *424*(6946), 309–312. doi:10.1038/nature01812
- Narr, K. L., Woods, R. P., Lin, J., Kim, J., Phillips, O. R., Del'Homme, M., et al. (2009). Widespread cortical thinning is a robust anatomical marker for attention-deficit/hyperactivity disorder. *Journal of the American Academy of Child and Adolescent Psychiatry*, *48*(10), 1014–1022. doi:10.1097/CHI.0b013e3181b395c0
- Nelson, S. M., Arnold, K. M., Gilmore, A. W., & McDermott, K. B. (2013). Neural signatures of test-potentiated learning in parietal cortex. *The Journal of Neuroscience : the Official Journal of the Society for Neuroscience*, *33*(29), 11754–11762. doi:10.1523/JNEUROSCI.0960-13.2013
- Nelson, S. M., Cohen, A. L., Power, J. D., Wig, G. S., Miezin, F. M., Wheeler, M. E., et al. (2010). A parcellation scheme for human left lateral parietal cortex. *Neuron*, *67*(1), 156–170. doi:10.1016/j.neuron.2010.05.025
- Niebergall, R., Khayat, P. S., Treue, S., & Martinez-Trujillo, J. C. (2011). Multifocal attention filters targets from distracters within and beyond primate MT neurons' receptive field boundaries. *Neuron*, *72*(6), 1067–1079. doi:10.1016/j.neuron.2011.10.013
- Oberauer, K. (2002). Access to information in working memory: exploring the focus of attention. *Journal of Experimental Psychology. Learning, Memory, and Cognition*, *28*(3), 411–421.
- Oberauer, K. (2013). The focus of attention in working memory—from metaphors to mechanisms. *Frontiers in Human Neuroscience*, *7*, 673.

doi:10.3389/fnhum.2013.00673

- Oberauer, K., & Bialkova, S. (2009). Accessing information in working memory: can the focus of attention grasp two elements at the same time? *Journal of Experimental Psychology. General*, *138*(1), 64–87. doi:10.1037/a0014738
- Olivers, C. N. L. (2011). Long-term visual associations affect attentional guidance. *Acta Psychologica*, *137*(2), 243–247. doi:10.1016/j.actpsy.2010.07.001
- Pashler, H. (1988). Familiarity and visual change detection. *Perception & Psychophysics*, *44*(4), 369–378.
- Patai, E. Z., Doallo, S., & Nobre, A. C. (2012). Long-term memories bias sensitivity and target selection in complex scenes. *Journal of Cognitive Neuroscience*, *24*(12), 2281–2291. doi:10.1162/jocn\_a\_00294
- Posner, M. I., Walker, J. A., Friedrich, F. J., & Rafal, R. D. (1984). Effects of parietal injury on covert orienting of attention. *The Journal of Neuroscience : the Official Journal of the Society for Neuroscience*, *4*(7), 1863–1874.
- Postle, B. R., Stern, C. E., Rosen, B. R., & Corkin, S. (2000). An fMRI investigation of cortical contributions to spatial and nonspatial visual working memory. *NeuroImage*, *11*(5 Pt 1), 409–423. doi:10.1006/nimg.2000.0570
- Postle, B. R. (2006) Working memory as an emergent property of the mind and brain. *Neuroscience*, *139*. 23-38.
- Power, J. D., Barnes, K. A., Snyder, A. Z., Schlaggar, B. L., & Petersen, S. E. (2012). Spurious but systematic correlations in functional connectivity MRI networks arise from subject motion. *NeuroImage*, *59*(3), 2142–2154. doi:10.1016/j.neuroimage.2011.10.018
- Power, J. D., Cohen, A. L., Nelson, S. M., Wig, G. S., Barnes, K. A., Church, J. A., et al. (2011). Functional network organization of the human brain. *Neuron*, *72*(4), 665–678. doi:10.1016/j.neuron.2011.09.006
- Power, J. D., Schlaggar, B. L., & Petersen, S. E. (2014). Studying brain organization via spontaneous fMRI signal. *Neuron*, *84*(4), 681–696. doi:10.1016/j.neuron.2014.09.007
- Ptak, R., & Schnider, A. (2010). The dorsal attention network mediates orienting toward behaviorally relevant stimuli in spatial neglect. *The Journal of*

- Neuroscience : the Official Journal of the Society for Neuroscience*, 30(38), 12557–12565. doi:10.1523/JNEUROSCI.2722-10.2010
- Pylyshyn, Z. W., & Storm, R. W. (1988). Tracking multiple independent targets: evidence for a parallel tracking mechanism. *Spatial Vision*, 3(3), 179–197.
- Raichle, M. E., MacLeod, A. M., Snyder, A. Z., Powers, W. J., Gusnard, D. A., & Shulman, G. L. (2001). A default mode of brain function. *Proceedings of the National Academy of Sciences of the United States of America*, 98(2), 676–682. doi:10.1073/pnas.98.2.676
- Reeves, A., & Sperling, G. (1986). Attention gating in short-term visual memory. *Psychological Review*, 93(2), 180–206.
- Rensink, R. A., O'Regan, J. K., & Clark, J. J. (1997). To See or not to See: The Need for Attention to Perceive Changes in Scenes. *Psychological Science*, 8(5), 368–373. doi:10.1111/j.1467-9280.1997.tb00427.x
- Rosen, M. L., Stern, C. E., & Somers, D. C. (2014). Long-term memory guidance of visuospatial attention in a change-detection paradigm. *Frontiers in Psychology*, 5, 266. doi:10.3389/fpsyg.2014.00266
- Rosen, M. L., Stern, C. E., Michalka, S. W., Devaney, K. J., Somers, D. C. (2015). Cognitive Control Network Contributions to Memory-Guided Visual Attention. *Cerebral Cortex*. doi: 10.1093/cercor/bhv028
- Ross, R. S., Sherrill, K. R., & Stern, C. E. (2011). The hippocampus is functionally connected to the striatum and orbitofrontal cortex during context dependent decision making. *Brain Research*, 1423, 53–66. doi:10.1016/j.brainres.2011.09.038
- Ryan, J. D., Althoff, R. R., Whitlow, S., & Cohen, N. J. (2000). Amnesia is a deficit in relational memory. *Psychological Science*, 11(6), 454–461.
- Schon, K., Hasselmo, M. E., Lopresti, M. L., Tricarico, M. D., & Stern, C. E. (2004). Persistence of parahippocampal representation in the absence of stimulus input enhances long-term encoding: a functional magnetic resonance imaging study of subsequent memory after a delayed match-to-sample task. *The Journal of Neuroscience : the Official Journal of the Society for Neuroscience*, 24(49), 11088–11097. doi:10.1523/JNEUROSCI.3807-04.2004
- Schon, K., Quiroz, Y. T., Hasselmo, M. E., & Stern, C. E. (2009). Greater working memory load results in greater medial temporal activity at retrieval. *Cerebral*

*Cortex (New York, N.Y. : 1991)*, 19(11), 2561–2571.  
doi:10.1093/cercor/bhp006

Schoo, L. A., van Zandvoort, M. J. E., Biessels, G. J., Kappelle, L. J., Postma, A., & de Haan, E. H. F. (2011). The posterior parietal paradox: Why do functional magnetic resonance imaging and lesion studies on episodic memory produce conflicting results? *Journal of Neuropsychology*, 5(Pt 1), 15–38.  
doi:10.1348/174866410X504059

Sereno, M. I., Pitzalis, S., & Martinez, A. (2001). Mapping of contralateral space in retinotopic coordinates by a parietal cortical area in humans. *Science (New York, N.Y.)*, 294(5545), 1350–1354. doi:10.1126/science.1063695

Sestieri, C., Corbetta, M., Romani, G. L., & Shulman, G. L. (2011). Episodic memory retrieval, parietal cortex, and the default mode network: functional and topographic analyses. *The Journal of Neuroscience : the Official Journal of the Society for Neuroscience*, 31(12), 4407–4420.  
doi:10.1523/JNEUROSCI.3335-10.2011

Sestieri, C., Shulman, G. L., & Corbetta, M. (2010). Attention to memory and the environment: functional specialization and dynamic competition in human posterior parietal cortex. *The Journal of Neuroscience : the Official Journal of the Society for Neuroscience*, 30(25), 8445–8456.  
doi:10.1523/JNEUROSCI.4719-09.2010

Shaw, M. L., & Shaw, P. (1977). Optimal allocation of cognitive resources to spatial locations. *Journal of Experimental Psychology. Human Perception and Performance*, 3(2), 201–211.

Shaw, P., Lerch, J., Greenstein, D., Sharp, W., Clasen, L., Evans, A., et al. (2006). Longitudinal mapping of cortical thickness and clinical outcome in children and adolescents with attention-deficit/hyperactivity disorder. *Archives of General Psychiatry*, 63(5), 540–549. doi:10.1001/archpsyc.63.5.540

Sheremata, S. L., & Silver, M. A. (2015). Hemisphere-dependent attentional modulation of human parietal visual field representations. *The Journal of Neuroscience : the Official Journal of the Society for Neuroscience*, 35(2), 508–517. doi:10.1523/JNEUROSCI.2378-14.2015

Sheremata, S. L., Bettencourt, K. C., & Somers, D. C. (2010). Hemispheric asymmetry in visuotopic posterior parietal cortex emerges with visual short-term memory load. *The Journal of Neuroscience : the Official Journal of the Society for Neuroscience*, 30(38), 12581–12588.

doi:10.1523/JNEUROSCI.2689-10.2010

Shomstein, S., & Yantis, S. (2004). Control of attention shifts between vision and audition in human cortex. *The Journal of Neuroscience : the Official Journal of the Society for Neuroscience*, *24*(47), 10702–10706. doi:10.1523/JNEUROSCI.2939-04.2004

Shomstein, S., & Yantis, S. (2006). Parietal cortex mediates voluntary control of spatial and nonspatial auditory attention. *The Journal of Neuroscience : the Official Journal of the Society for Neuroscience*, *26*(2), 435–439. doi:10.1523/JNEUROSCI.4408-05.2006

Silver, M. A., & Kastner, S. (2009). Topographic maps in human frontal and parietal cortex. *Trends in Cognitive Sciences*, *13*(11), 488–495. doi:10.1016/j.tics.2009.08.005

Silver, M. A., Ress, D., & Heeger, D. J. (2005). Topographic maps of visual spatial attention in human parietal cortex. *Journal of Neurophysiology*, *94*(2), 1358–1371. doi:10.1152/jn.01316.2004

Simons, D. J. (2010). Current Approaches to Change Blindness. *Visual Cognition*, *7*(1-3), 1–15. doi:10.1080/135062800394658

Simons, D. J., & Chabris, C. F. (1999). Gorillas in our midst: sustained inattentive blindness for dynamic events. *Perception*, *28*(9), 1059–1074.

Simons, D. J., & Levin, D. T. (1997). Change blindness. *Trends in Cognitive Sciences*, *1*(7), 261–267. doi:10.1016/S1364-6613(97)01080-2

Soto, D., & Humphreys, G. W. (2007). Automatic guidance of visual attention from verbal working memory. *Journal of Experimental Psychology. Human Perception and Performance*, *33*(3), 730–737. doi:10.1037/0096-1523.33.3.730

Soto, D., & Humphreys, G. W. (2009). Automatic selection of irrelevant object features through working memory: evidence for top-down attentional capture. *Experimental Psychology*, *56*(3), 165–172. doi:10.1027/1618-3169.56.3.165

Sperling, G., & Weichselgartner, E. (1995). Episodic theory of the dynamics of spatial attention. *Psychological Review*, *102*(3), 503–532. doi:10.1037/0033-295X.102.3.503

Spreng, R. N., & Grady, C. L. (2010). Patterns of brain activity supporting autobiographical memory, prospection, and theory of mind, and their

- relationship to the default mode network. *Journal of Cognitive Neuroscience*, 22(6), 1112–1123. doi:10.1162/jocn.2009.21282
- Spreng, R. N., & Schacter, D. L. (2012). Default network modulation and large-scale network interactivity in healthy young and old adults. *Cerebral Cortex (New York, N.Y. : 1991)*, 22(11), 2610–2621. doi:10.1093/cercor/bhr339
- Spreng, R. N., Sepulcre, J., Turner, G. R., Stevens, W. D., & Schacter, D. L. (2013). Intrinsic architecture underlying the relations among the default, dorsal attention, and frontoparietal control networks of the human brain. *Journal of Cognitive Neuroscience*, 25(1), 74–86. doi:10.1162/jocn\_a\_00281
- Stern, C. E., Corkin, S., González, R. G., Guimaraes, A. R., Baker, J. R., Jennings, P. J., et al. (1996). The hippocampal formation participates in novel picture encoding: evidence from functional magnetic resonance imaging. *Proceedings of the National Academy of Sciences of the United States of America*, 93(16), 8660–8665.
- Stokes, M. G., Atherton, K., Patai, E. Z., & Nobre, A. C. (2012). Long-term memory prepares neural activity for perception. *Proceedings of the National Academy of Sciences of the United States of America*, 109(6), E360–7. doi:10.1073/pnas.1108555108
- Stone, S. P., Halligan, P. W., & Greenwood, R. J. (1993). The incidence of neglect phenomena and related disorders in patients with an acute right or left hemisphere stroke. *Age and Ageing*, 22(1), 46–52.
- Straw, A. D. (2008). Vision egg: an open-source library for realtime visual stimulus generation. *Frontiers in Neuroinformatics*, 2, 4. doi:10.3389/neuro.11.004.2008
- Summerfield, J. J., Hassabis, D., & Maguire, E. A. (2009). Cortical midline involvement in autobiographical memory. *NeuroImage*, 44(3), 1188–1200. doi:10.1016/j.neuroimage.2008.09.033
- Summerfield, J. J., Lepsien, J., Gitelman, D. R., Mesulam, M. M., & Nobre, A. C. (2006). Orienting attention based on long-term memory experience. *Neuron*, 49(6), 905–916. doi:10.1016/j.neuron.2006.01.021
- Summerfield, J. J., Rao, A., Garside, N., & Nobre, A. C. (2011). Biasing perception by spatial long-term memory. *The Journal of Neuroscience : the Official Journal of the Society for Neuroscience*, 31(42), 14952–14960. doi:10.1523/JNEUROSCI.5541-10.2011

- Swisher, J. D., Halko, M. A., Merabet, L. B., McMains, S. A., & Somers, D. C. (2007). Visual topography of human intraparietal sulcus. *The Journal of Neuroscience : the Official Journal of the Society for Neuroscience*, *27*(20), 5326–5337. doi:10.1523/JNEUROSCI.0991-07.2007
- Szczepanski, S. M., Konen, C. S., & Kastner, S. (2010). Mechanisms of spatial attention control in frontal and parietal cortex. *The Journal of Neuroscience : the Official Journal of the Society for Neuroscience*, *30*(1), 148–160. doi:10.1523/JNEUROSCI.3862-09.2010
- Tamm, L., Menon, V., Ringel, J., & Reiss, A. L. (2004). Event-related fMRI evidence of frontotemporal involvement in aberrant response inhibition and task switching in attention-deficit/hyperactivity disorder. *Journal of the American Academy of Child and Adolescent Psychiatry*, *43*(11), 1430–1440. doi:10.1097/01.chi.0000140452.51205.8d
- Todd, J. J., & Marois, R. (2004). Capacity limit of visual short-term memory in human posterior parietal cortex. *Nature*, *428*(6984), 751–754. doi:10.1038/nature02466
- Todd, J. J., Fougnie, D., & Marois, R. (2005). Visual short-term memory load suppresses temporo-parietal junction activity and induces inattention blindness. *Psychological Science*, *16*(12), 965–972. doi:10.1111/j.1467-9280.2005.01645.x
- Tsal, Y. (1983). Movements of attention across the visual field. *Journal of Experimental Psychology. Human Perception and Performance*, *9*(4), 523–530.
- Van Dijk, K. R. A., Hedden, T., Venkataraman, A., Evans, K. C., Lazar, S. W., & Buckner, R. L. (2010). Intrinsic functional connectivity as a tool for human connectomics: theory, properties, and optimization. *Journal of Neurophysiology*, *103*(1), 297–321. doi:10.1152/jn.00783.2009
- Verdon, V., Schwartz, S., Lovblad, K.-O., Hauert, C.-A., & Vuilleumier, P. (2010). Neuroanatomy of hemispatial neglect and its functional components: a study using voxel-based lesion-symptom mapping. *Brain : a Journal of Neurology*, *133*(Pt 3), 880–894. doi:10.1093/brain/awp305
- Vilberg, K. L., & Rugg, M. D. (2007). Dissociation of the neural correlates of recognition memory according to familiarity, recollection, and amount of recollected information. *Neuropsychologia*, *45*(10), 2216–2225.

doi:10.1016/j.neuropsychologia.2007.02.027

- Vilberg, K. L., & Rugg, M. D. (2008). Memory retrieval and the parietal cortex: a review of evidence from a dual-process perspective. *Neuropsychologia*, *46*(7), 1787–1799. doi:10.1016/j.neuropsychologia.2008.01.004
- Vilberg, K. L., & Rugg, M. D. (2009). Left parietal cortex is modulated by amount of recollected verbal information. *Neuroreport*, *20*(14), 1295–1299. doi:10.1097/WNR.0b013e3283306798
- Vincent, J. L., Kahn, I., Snyder, A. Z., Raichle, M. E., & Buckner, R. L. (2008). Evidence for a frontoparietal control system revealed by intrinsic functional connectivity. *Journal of Neurophysiology*, *100*(6), 3328–3342. doi:10.1152/jn.90355.2008
- Vincent, J. L., Snyder, A. Z., Fox, M. D., Shannon, B. J., Andrews, J. R., Raichle, M. E., & Buckner, R. L. (2006). Coherent spontaneous activity identifies a hippocampal-parietal memory network. *Journal of Neurophysiology*, *96*(6), 3517–3531. doi:10.1152/jn.00048.2006
- Vogt, B. A., Vogt, L., & Laureys, S. (2006). Cytology and functionally correlated circuits of human posterior cingulate areas. *NeuroImage*, *29*(2), 452–466. doi:10.1016/j.neuroimage.2005.07.048
- Wagner, A. D., Schacter, D. L., Rotte, M., Koutstaal, W., Maril, A., Dale, A. M., et al. (1998). Building memories: remembering and forgetting of verbal experiences as predicted by brain activity. *Science (New York, N.Y.)*, *281*(5380), 1188–1191.
- Wagner, A. D., Shannon, B. J., Kahn, I., & Buckner, R. L. (2005). Parietal lobe contributions to episodic memory retrieval. *Trends in Cognitive Sciences*, *9*(9), 445–453. doi:10.1016/j.tics.2005.07.001
- Wandell, B. A., Dumoulin, S. O., & Brewer, A. A. (2007). Visual field maps in human cortex. *Neuron*, *56*(2), 366–383. doi:10.1016/j.neuron.2007.10.012
- Werner, S., & Thies, B. (2010). Is “Change Blindness” Attenuated by Domain-specific Expertise? An Expert-Novices Comparison of Change Detection in Football Images. *Visual Cognition*, *7*(1-3), 163–173. doi:10.1080/135062800394748
- Wolfe, J. M., Alvarez, G. A., & Horowitz, T. S. (2000). Attention is fast but volition is slow. *Nature*, *406*(6797), 691–691. doi:10.1038/35021132

- Woodman, G. F., & Luck, S. J. (2007). Do the contents of visual working memory automatically influence attentional selection during visual search? *Journal of Experimental Psychology. Human Perception and Performance*, 33(2), 363–377. doi:10.1037/0096-1523.33.2.363
- Woodman, G. F., Carlisle, N. B., & Reinhart, R. M. G. (2013). Where do we store the memory representations that guide attention? *Journal of Vision*, 13(3), 1–1. doi:10.1167/13.3.1
- Xu, Y., & Chun, M. M. (2006). Dissociable neural mechanisms supporting visual short-term memory for objects. *Nature*, 440(7080), 91–95. doi:10.1038/nature04262
- Yantis, S. (1988). On analog movements of visual attention. *Perception & Psychophysics*, 43(2), 203–206.
- Yantis, S. (1992). Multielement visual tracking: attention and perceptual organization. *Cognitive Psychology*, 24(3), 295–340.
- Yee, L. T. S., Warren, D. E., Voss, J. L., Duff, M. C., Tranel, D., & Cohen, N. J. (2014). The hippocampus uses information just encountered to guide efficient ongoing behavior. *Hippocampus*, 24(2), 154–164. doi:10.1002/hipo.22211
- Yeo, B. T. T., Krienen, F. M., Sepulcre, J., Sabuncu, M. R., Lashkari, D., Hollinshead, M., et al. (2011). The organization of the human cerebral cortex estimated by intrinsic functional connectivity. *Journal of Neurophysiology*, 106(3), 1125–1165. doi:10.1152/jn.00338.2011

**CURRICULUM VITAE**

